Spring 1975

AN INTERACTIVE COMPUTER ANALYSIS OF PHONOCARDIOGRAMS

ANTAL ANDRAS SARKADY

76-2523

SARKADY, Antal Andras, 1937-
AN INTERACTIVE COMPUTER ANALYSIS OF PHONOCARDIOGRAMS.

University of New Hampshire, Ph.D., 1975
Engineering, electronics and electrical

Xerox University Microfilms, Ann Arbor, Michigan 48106

AN INTERACTIVE COMPUTER ANALYSIS OF PHONOCARDIOGRAMS

by

ANTAL A. SARKADY

B.S., University of New Hampshire, 1965

M.S., University of New Hampshire, 1967

A DISSERTATION

Submitted to the University of New Hampshire

In Partial Fulfillment of

The Requirements for the Degree of

Doctor of Philosophy

In Engineering

Graduate School

June, 1975

This dissertation has been examined and approved.

Dissertation Adviser
Ronald R. Clark, Professor, Electrical Engineering
Signal Processing Area, Engineering Ph.D. Program

Donald W. Melvin, Associate Professor, Electrical Engineering
Signal Processing Area, Engineering Ph.D. Program

Filson H. Glanz, Associate Professor, Electrical Engineering
Signal Processing Area, Engineering Ph.D. Program

John E. Mulhern, Jr., Professor, Physics

Leonard G. Christie, Jr., M.D., Cardiologist
Dartmouth-Hitchcock Medical Center

June 24, 1975
Date

ACKNOWLEDGMENTS

As is usually the case in research of this type, many people have made significant contributions to make this work possible. Foremost among these is my wife, Joyce and my children, Lynne and Kenneth, who made many personal sacrifices during the course of this study. In addition, I would like to thank Dr. Roberta Williams of Children's Hospital, Boston, Massachusetts for suggesting and supporting the aortic stenosis study, Ms. Judith Keymont for her assistance in selecting and recording phonocardiogram data, Dr. Ronald R. Clark, University of New Hampshire, for his advice and guidance throughout the study, Dr. Edward L. Chupp for making the University of New Hampshire Space Science Center computer facilities available for this project, and Mr. Ernie Nichols for helpful suggestions and aid in the development of the FFT subroutine.

TABLE OF CONTENTS

TABLE OF CONTENTS (Continued)

TABLE OF CONTENTS (Continued)

TABLE OF CONTENTS (Continued)

LIST OF TABLES

LIST OF TABLES (Continued)

LIST OF ILLUSTRATIONS

LIST OF ILLUSTRATIONS (Continued)

ABSTRACT

AN INTERACTIVE COMPUTER ANALYSIS
OF PHONOCARDIOGRAMS

by

Antal A. Sarkady

Computerized phonocardiogram analysis techniques were developed to aid in the positive diagnosis of systolic heart diseases and these techniques were applied to noninvasively assess the severity of valvar aortic stenosis. Signal processing algorithms were incorporated into an interactive analysis program used to study heart sounds and murmurs in the time and frequency domains. The algorithms are applicable to several heart diseases, but this study was conducted on six normal patients, thirteen catheterized, and four clinically-diagnosed valvar aortic stenosis patients.

For each patient, phonocardiogram data (30-1200Hz range) from four listening sites, along with an ECG, respiration, and carotid pulse, were recorded for approximately 100 seconds. A typical patient data set consists of seven data files; two mid-inspiration, two mid-expiration, two carotid and one calibration file.

As a starting point of the interactive analysis branch, a normalized ensemble-averaged envelogram is

computed and plotted for each file. From these plots, maximum precardium intensity areas, respiration affects, murmur shape, and the timing of clicks, murmurs and sounds are identified or measured. Using the measured onset times and durations, murmur, click, and heart sound signals are gated and separately studied in the time and frequency domains.

The severity of valvar aortic stenosis is estimated noninvasively from a gated and ensemble-averaged phonocardiogram murmur power spectrum. The averaged spectrum is computed from several cardiocycles (typically 40-50 records) recorded from the second right intercostal space. Ensemble averaging is essential in this analysis to reduce spectrum variance and to obtain consistent results. A high degree of correlation exists (correlation coefficient = 0.96) between the peak systolic ejection gradient measured by cardiac catheterization, and the calculated first moment of the mean murmur spectrum.

A Varian 620/I 16 bits/word minicomputer was used for this study. The computer was equipped with a 12K word memory, two seven-track digital tape recorders, a graphics terminal, an analog multiplexer, and an analog-to-digital converter.

INTRODUCTION

The computerized phonocardiogram analysis techniques presented in this dissertation are applicable to many systolic heart diseases found in a wide age group. However, children and adolescents four to twenty years of age were selected for this study for the following reasons. A large portion of heart diseases are congenital or can be traced to a minor cardiac disorder occurring in early life; consequently, early detection and correction are necessary for a long and active adult life. In addition, innocent murmurs are extremely common in children and adolescents, occurring in approximately 50 percent of these subjects [36]. Therefore, a need exists for an accurate and rapid screening instrument. The analysis techniques presented here can be adapted in the design of such an instrument. Finally, children are relatively free from arterial diseases such as arteriosclerosis and may serve as a ready standard for a large number of heart diseases.

In order to assess the merits of the computerized phonocardiogram analysis techniques, the study of valvar aortic stenosis was suggested by Dr. Roberta Williams of Children's Hospital, Boston, Massachusetts. Her proposal was an excellent and challenging choice for several reasons.

Valvar aortic stenosis is a frequently detected disease representing approximately three to six percent of the total heart diseases found in children [10]. Severity of the disease requires frequent assessment, particularly in moderate and severe cases, since for these patients sudden death is a distinct possibility. Accurate assessment of the severity of this disease is presently possible only by catheterization, an invasive surgical procedure requiring three days of hospital care. It is clear that a definite need exists for an accurate, noninvasive technique to assess the severity of valvar aortic stenosis; such a technique is presented in this dissertation. Finally, the valvar aortic stenosis murmur is produced by a "turbulent jet" [1] where similar jets are found in several other heart diseases (pulmonary stenosis, ventricular septal defect, atrial septal defect, etc.). Consequently, this anomaly can be considered as a representative prototype of several "noisy systolic murmurs" and it may be possible for this analysis technique to be extended to these heart diseases as well.

CHAPTER I

PHYSIOLOGY OF THE NORMAL AND ABNORMAL HEART

FUNCTION AND OPERATION OF THE HEART

The function of the heart is to pump oxygenated blood to all parts of the body. It is readily visualized as two serially-connected dual-chamber pumps, activated by a common electrical pacemaker through conduction bands [28]. The two pumps are similar in size but the left side is a considerably higher-pressured system than the right side. A full scale drawing of a normal child's heart and the connecting great vessels is shown in Fig. 1. Pumping action of the heart is described with the aid of this diagram.

Oxygen-poor blood (blue blood) is pooled in the right atrium (RA) and enters the right ventricle (RV) through the tricuspid valve (TV). The right ventricle pumps the blood through the pulmonary valve (PV) into the small capillaries of the lungs where it becomes enriched with oxygen. The oxygenated blood (red blood) is pooled in the left atrium and enters the left ventricle (LV) through the mitral valve (MV).

The left ventricle pumps the red blood through the aortic valve (AV) to the aorta (AO) where it is distributed by smaller arteries to the rest of the body. The circulation path is completed when the blue blood is returned to the

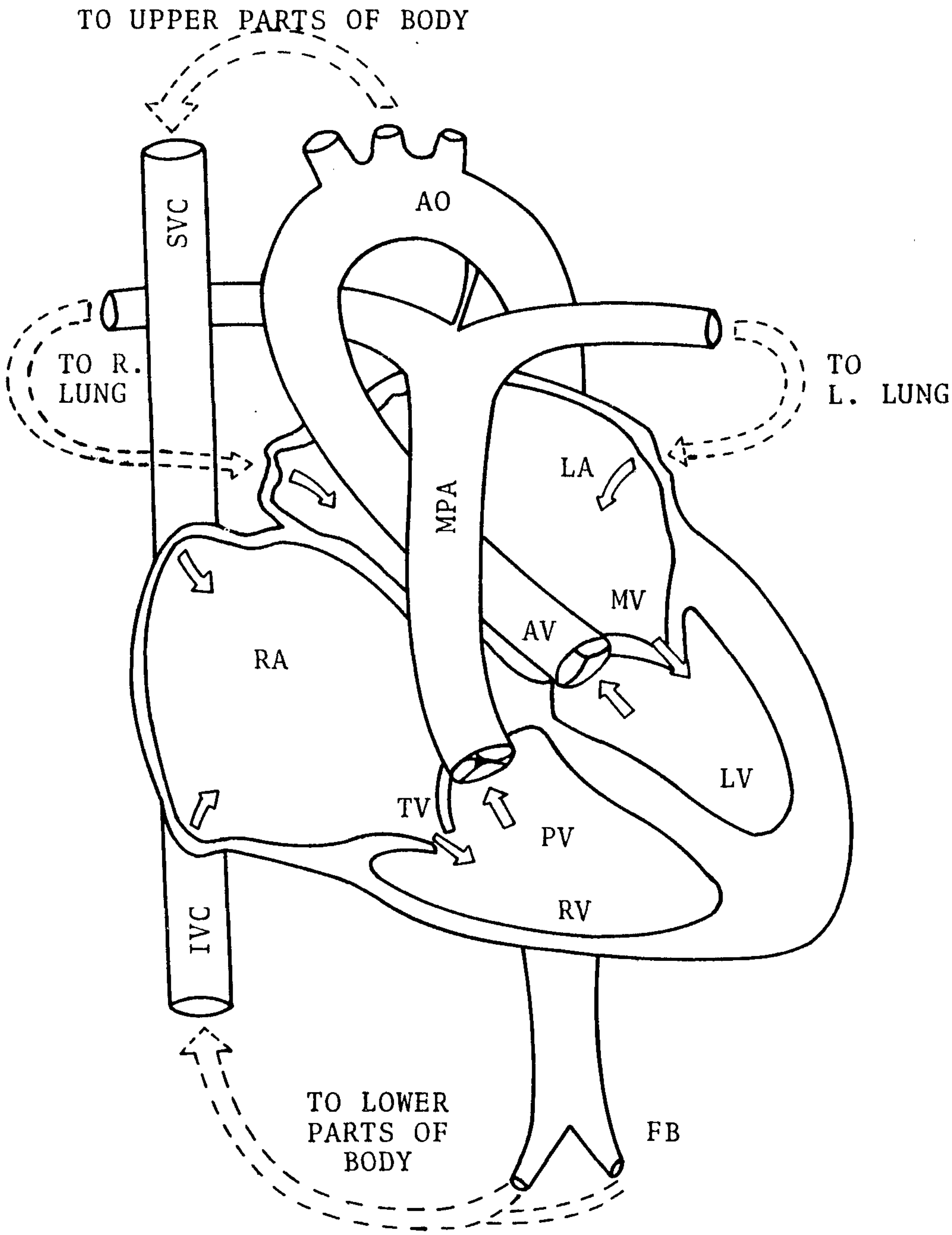

AO-aorta, AV-aortic valve, IVC-inferior vena cava
LA-left atrim, LV-left ventricle, MPA, main pulmonary artery
MV-mitral valve, PV-pulmonary valve, RV-right atrium
RV-right ventricle, SVC-superior vena cava
TR-tricuspid valve, FB-femoral bifurcation

Fig. 1. Normal heart of a child

right atrium via the inferior vena cava (IVC) and the superior vena cava (SVC).

The pumping cycles of the two sides of the heart are nearly synchronous. A cardiocycle is divided into systolic and diastolic phases, at which times the ventricular muscles are contracted and relaxed respectively. In the early part of the systole, the ventricle is at a constant volume, while during the latter part, blood is being pumped from it. In the early part of the diastole, the ventricle is at a constant volume, while during the latter part, blood is being pooled in it.

Functions of the atria are to assure an adequate blood supply to the ventricle during the filling phase and to assist in the filling by contracting at the end of the diastolic phase. This is often referred to as "topping off" the ventricle.

All of the heart valves are operated by the blood flow; nearly zero pressure drop occurs across the valves during forward flow and they are closed by reverse flow.

STRUCTURE OF THE HEART

A dense connective tissue forms a fibrous "skeleton" of the heart surrounding the valves. The atria, ventricles and arterial trunks are firmly attached to this "skeleton" [1].

The ventricles are composed of sheets of spiralling, tightly-bound, myocardial fibers which thicken near the apex. The wall of the left ventricle is considerably thicker than that of the right ventricle. Capillaries connected to the coronary arteries supply blood to the heart muscle at a rate ten to twenty times higher than to the skeletal muscle. This high nourishment rate is required to support the mechanical work performed by the ventricles.

ARTERIAL BLOOD FLOW

The outstanding feature of arterial blood flow is its pulsatile character. During the early systole, blood is suddenly ejected into the ascending aorta. The ventricle has insufficient energy to overcome the inertia of the long column of blood in the arteries; consequently, the blood tends to pile up in the distended ascending aorta, producing a sudden, local pressure increase. A pressure wave propagates down the descending aorta with a velocity of 4-5 m/sec. [1]. This velocity is ten to twenty times greater than the flow velocity of the blood [2] and is a function of the physical properties of the vessel wall and the blood.

The advancing pressure wave is reflected by the peripheral structures (primarily at the femoral bifurcation) producing a reflected wave traveling back toward the heart. The observed pressure wave at any point in the aorta is the superposition of the forward pressure wave and the reflected wave. As the aortic valve closes at the end of the systole, drainage from the aorta and arteries into the arterioles continues, transforming the highly pulsatile flow into a more continuous, steady flow. Dispersion of the pulse waveform during its travel is one of the characteristics of the vascular system.

A detailed analysis of pulsatile blood flow in distensible arteries is given in a book edited by Attinger [3]. A recent computer model of the left ventricle and the aorta is presented by Watts [4]. He models the aorta as a tapered, electrical delay line and studies the pressure pulse propagation produced by an impaired left ventricle. Watt's model, however, is valid only in the 0-20 Hz frequency range.

MECHANISM OF THE NORMAL AORTIC VALVE

The aortic valve is composed of three cusps of equal size attached around the circumference of the valve orifice. In children and adolescents, the cusps are thin, elastic membranes which thicken later in life. A considerable overlap in the cusps' area assures a tight closure; when open, it forms a triangular orifice which has a smaller cross-sectional area than the aorta. This opening however, is sufficiently large to have a negligibly small pressure drop across the open valve and to have laminar blood flow through the valve. Behind the aortic valve cusps are three cavities, the sinuses of valsalva [29], shown in Fig. 2. Left and right coronary circulation originates from two of these sinuses through small openings called coronary ostia. The sinuses perform an important role in the closing mechanism of the valve. If a valve leaflet comes in contact with the coronary ostia, the rapidly falling coronary pressure and

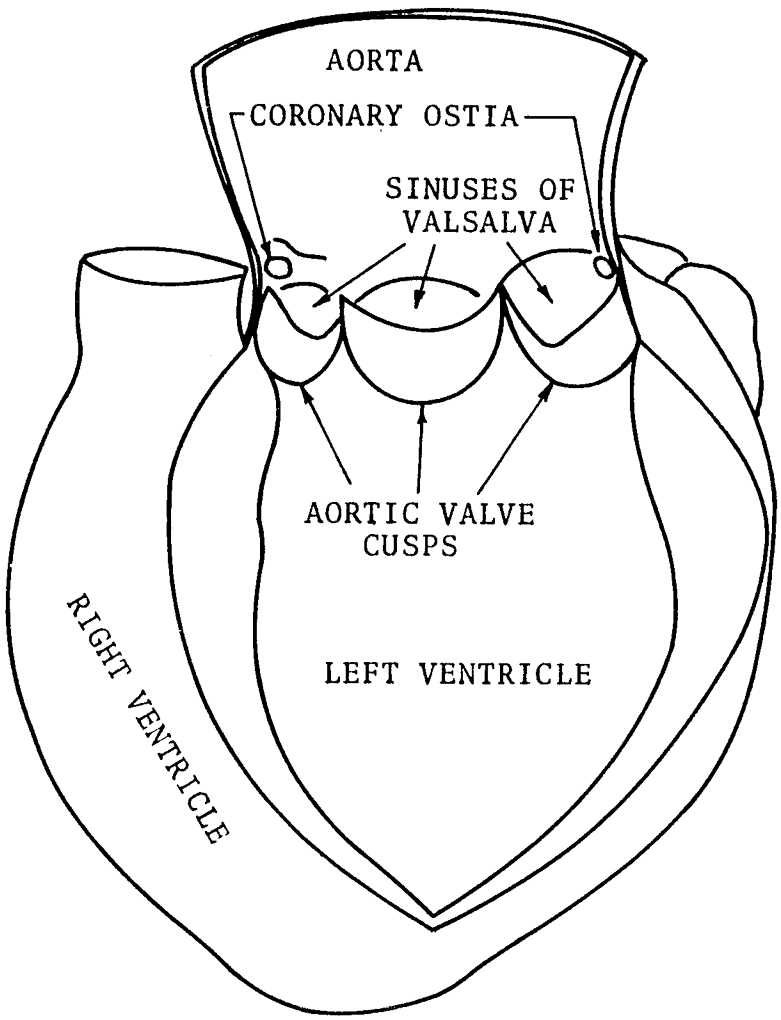

Fig. 2. The normal aortic valve

the increasing aortic pressure would seal the cusp against the wall of the aorta; space provided by the sinus prevents this from happening.

Bellhouse's [5,6,7] experiments with leaflet-type model valves demonstrated that vortices trapped in the sinuses provided a fluid mechanical valve control and aided systolic coronary circulation. In the model valve, the cusps presented negligible obstruction to the accelerating fluid flow during the opening phase. Thrown open, the cusps aligned themselves with the flow, and stagnation points were formed at the sinus ridges along with intense vortices inside the sinuses. During the early and mid-systole, the cusps were positioned so that their tips were slightly projected in the sinuses. The stagnation points, acting as high pressure sources, contributed to the systolic coronary circulation. During the end of the systole in the de-acceleration phase, the ventricular pressure fell below the sinus pressure and the cusps started to close. Streamlines were spread downstream and the cusps drifted to a three-quarter closed position; the valve was fully closed by a small amount of reverse flow. Bellhouse, et al. [7] measured four percent regurgitation in the model valves during the closing phase. During the entire systole the flow was laminar and no sign of turbulence was reported.

AORTIC STENOSIS

Aortic stenosis is defined as an obstruction to blood flow between the aorta and the left ventricle. Depending upon the location of the obstruction, it is divided into three major classes. Obstruction produced by an impaired valve is called valvar aortic stenosis, while obstruction above or below the valve is referred to as supravalvar aortic stenosis or subvalvar aortic stenosis respectively. Subaortic stenosis is usually further subdivided into discrete and idiopathic classes. The four types of stenosis, along with a normal heart, are shown in Fig. 3. Note that discrete subvalvar obstruction is produced by a fibrous band located below the valve, whereas supravalvar and idiopathic subaortic stenoses are produced by deformation of the aorta and ventricle respectively. Sub- and supravalvar stenoses are infrequent, while valvar stenosis is a common anomaly occurring in three to six percent of patients with congenital cardiovascular defects [10].

Valvar aortic stenosis may be acquired during the course of a disease, but in children it is most often due to congenital fusion of the cusps [12]. When all three cusps are fused near the valve root, valve motion is impaired, but the cusps can function as three independent units. This valve anomaly is called tricuspid valvar aortic stenosis. When the cusps are fused in such a way that they

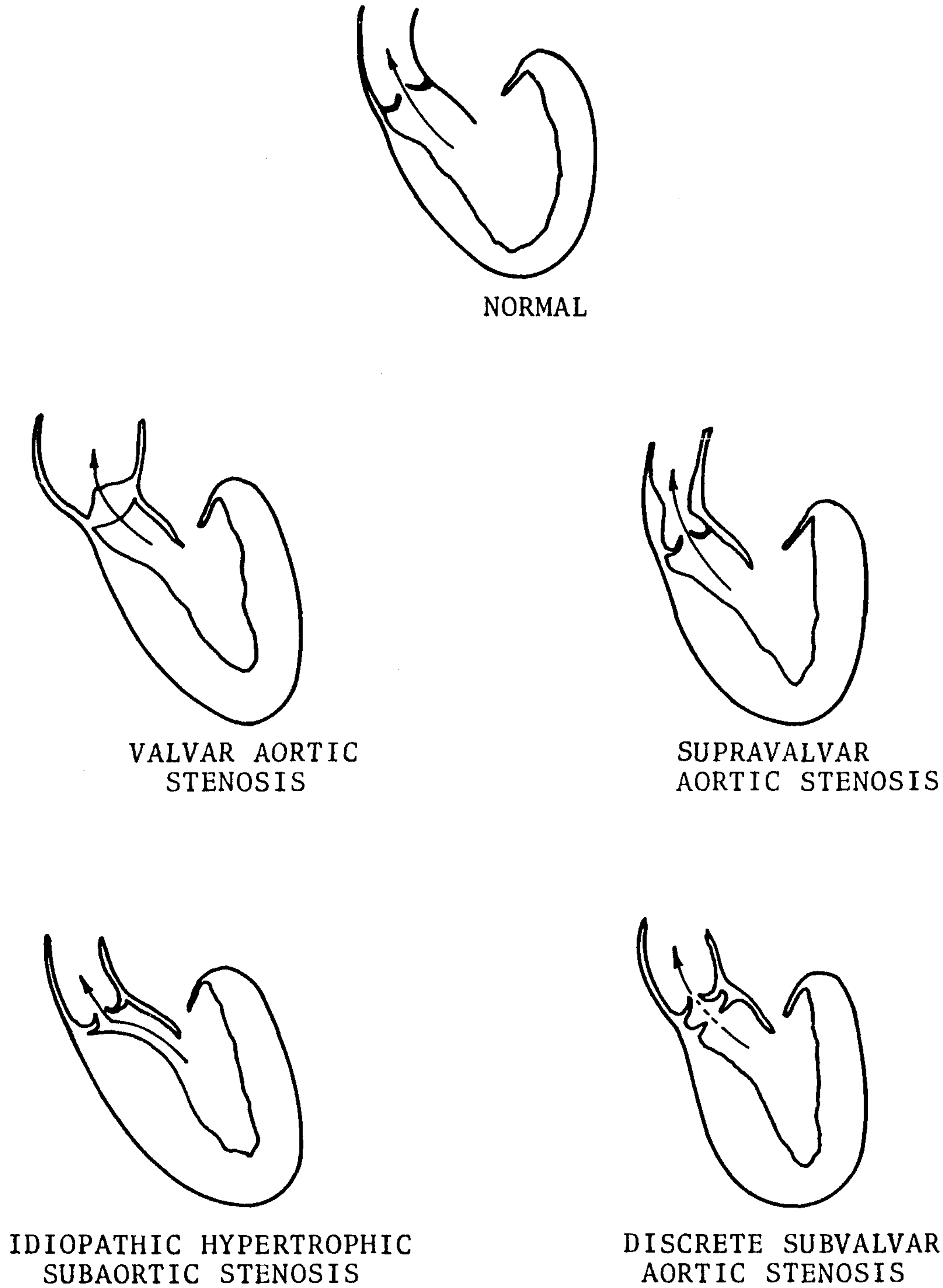

Fig. 3. Normal and aortic stenosed hearts

function as two independent units, the term bicuspid valvar aortic stenosis is used. Occasionally, in congenital deformation, the valve may become a single, semi-rigid perforated membrane acting as an obstruction rather than as a valve, presenting the same cross-sectional area for both flow directions. This anomaly is rare and its auscultatory features are distinct from tricuspid and bicuspid aortic stenoses [11]. Cross-sectional views of the three valve anomalies and of a normal valve for open and closed conditions are shown in Fig. 4.

The most common forms of aortic stenosis in children are the bicuspid and tricuspid types; the valves are seldom if ever calcified [10]. Calcification in humans begins at age 13-14 and damaged valves tend to accumulate calcium past this age. Consequently, even mild early valve impairment may lead to calcified aortic stenosis in adult life [12].

MECHANISM OF THE STENOSED AORTIC VALVE

A marked change in fluid flow occurs when the aortic valve area is reduced to approximately less than fifty percent of normal size. At the onset of the ejection phase a turbulent jet is formed in the ascending aorta and persists throughout the systole. Presence of the jet in the aorta is routinely observed in angiocardiographic studies [9,13, 31] and is considered to be a prime distinguishing feature in discriminating between valvar and subvalvar aortic

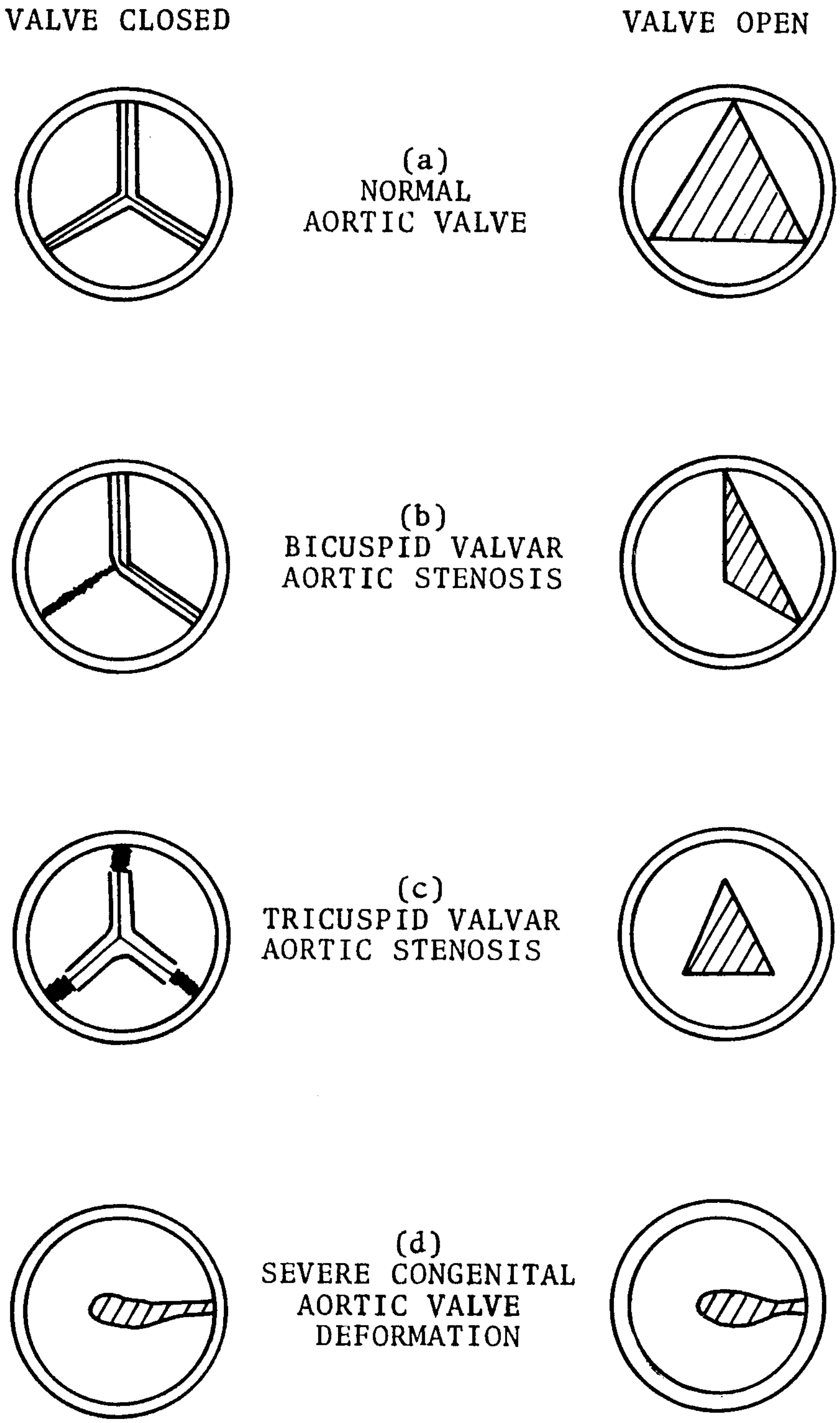

Fig. 4. Cross-sectional views of normal and stenosed valves

stenosis [11]. In the laboratory, turbulent flow of fluids in tubes and vessels is observed when the Reynolds number exceeds a critical value of 970 ± 80 [1].

Bellhouse, et al. [8] simulated valvar aortic stenosis by glueing the leaflets of the model valve together, reducing the valvar area by fifty percent. Under these conditions, instead of laminar flow in the systole, a turbulent jet formed at the valve and no vortices were observed in the sinuses. Pressure at the coronary ostia was slightly lower, indicating mild impairment of systolic coronary circulation and becoming more significant at a higher degree of stenosis. During the closing phase, the amount of reverse flow was only slightly more than that for the normal valve since the stenosed valve was never fully open.

PATHOPHYSIOLOGICAL DESCRIPTION OF VALVAR AORTIC STENOSIS

When the aortic valve area is reduced from the normal range of 2.5-3.5 cm^2 to a critical range of 0.5-1.0 cm^2, compensatory mechanisms fail and the following physiological symptoms develop: a marked increase in flow impedence [30], a marked left ventricle pressure increase accompanied by a slow rise in the aortic pressure wave, and a pressure drop across the valve. Peak pressure drop across the valve may exceed 100 mm. Hg in severe stenosis. Cardiac output remains nearly the same at rest but is reduced during exercise, indicating that the left ventricle relies on cardiac reserve to handle the overload. The overstressed ventricle responds by gradually increasing muscle mass [10], commonly observed in angiocardiography [31]. The increased muscle mass and wall tension greatly increase oxygen consumption of the ventricle at the time when coronary circulation is seriously impaired. Impairment is produced partially by the increased and prolonged intramural blood pressure and partially by the reduced systolic sinus pressure [12]. When oxygen demand exceeds the ability of the coronary blood flow to provide oxygen, myocardial ischemia and angina pectoris result [10,12]. Contractibility of the oxygen-starved cardiac muscle is reduced and congestive heart failure, syncope, or angina pectoris develops. At this stage the history of patient survival averages two, three, and five years, depending on the symptoms, where ten to fifteen percent die suddenly [32] if corrective surgery is not performed. In most instances the surgery is a valvarlaremy, but in some cases, particularly in older individuals, replacement of the impaired valve with a prosthetic valve is involved.

It is important to emphasize that the human heart tolerates mild aortic stenosis well, and not until the aortic valve area is reduced to less than fifty percent of normal, do clinical symptoms develop [12]. Surgery is required only in severe cases.

ESTIMATING THE SEVERITY OF AORTIC STENOSIS

Vector ECG and phonocardiography are considered to be adequate noninvasive diagnostic techniques for the identification of aortic stenosis; however, estimating the degree of stenosis has been poor with these techniques.

The most reliable invasive techniques for assessing the degree of stenosis are considered to be internal pressure measurements by cardiac catheterization, and simultaneous blood flow studies of X-ray motion pictures, known as angiocardiography. In these methods, access to the left ventricle is gained through hazardous routes, either by a transseptal needle [14] or by a retrograde arterial route past the aortic valve [15]. If the transseptal needle (catheter with a needle tip) is used, it is inserted into the femoral vein and advanced into the right atrium. The interatrial septum is punctured and the catheter is advanced into the left atrium and left ventricle. Proper positioning of the needle prior to puncturing is one of the more hazardous aspects of this procedure.

Retrograde arterial catheterization is usually performed through the femoral artery or the bronchial artery. This procedure often involves some degree of arterial trauma and is occasionally difficult to perform in children.

After the catheter is placed irto the left ventricle by one of the foregoing routes, oxygen saturation and pressure measurements are taken. An X-ray absorbing dye is injected and angiocardiographic studies are performed. Next, the catheter is withdrawn and pressure measurements are performed in the ascending aorta. The peak systolic pressure drop (referred to as peak systolic ejection gradient, P.S.E.G.) across the aortic valve is determined and the valve area is calculated from Gorlin's formula [16]. The degree of stenosis is determined on the basis of these measurements and is classified as mild, moderate, or severe according to the limits [11] listed in Table 1.

It is clear that cardiac catheterization is an accurate diagnostic technique; however, it is a surgical procedure requiring three days of hospitalization and is not a clinical diagnostic tool.

TABLE 1

LIMITS OF P.S.E.G. AND AORTIC VALVE AREA IN V.A.S.

Degree of Stenosis	Peak Valvar Pressure Drop P.S.E.G. in mm. Hg	Value Area cm^2
Mild	10 - 40	1.5 - 0.8
Moderate	40 - 80	0.9 - 0.6
Severe	> 80	< 0.6
Surgery Recommended	> 110	< 0.5

CHAPTER II

THE PHONOCARDIOGRAM SIGNAL

In this chapter the normal and abnormal phonocardiogram signal waveforms are discussed and the various signal components are correlated with hemodynamic events. In addition, production and transmission of vibrational energy is described. Finally, diagnostic signal features of aortic stenosis are tabulated and the differential diagnosis of the disease is presented.

STETHOSCOPIC AUSCULTATION

Vibrations in the 1-750 Hz frequency range are commonly observed on the surface of the human chest. A representative power spectrum of the vibrations measured in normal subjects, along with the mean threshold of hearing, are given by [17] and shown in Fig. 5. Note that stethoscopic auscultation is limited to the 40-750 Hz range and that most of the vibration energy is below this range.

In the audible range, the human ear and stethoscope is an extremely sensitive detector and assisted by the brain, forms an adaptive filter; however, it is a time variant, nonquantitative, ausculatory system. Perhaps the most serious problem with stethoscopic auscultation is the lack of data storage and retrieval features which often leads to

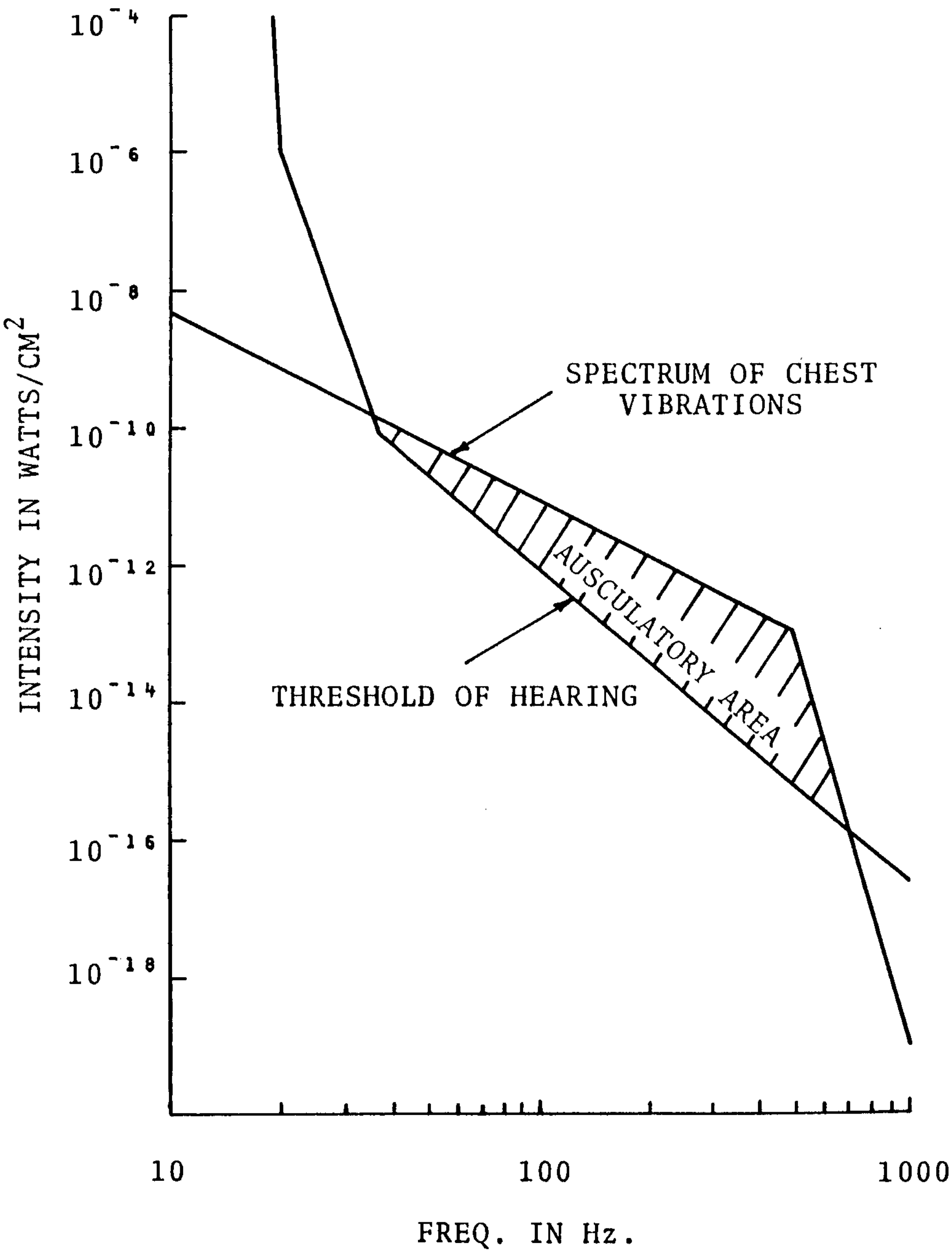

Fig. 5. Spectrum of chest vibrations and threshold of hearing.

subjective diagnosis. These shortcomings were demonstrated by recent tests performed on physicians [18].

THE PHONOCARDIOGRAM

The phonocardiogram is an intensity versus time display by a high-frequency chart recorder of the audible vibrations observed on the human chest by a microphone. In principle, phonocardiography is a clinically-quantitative diagnostic technique; however, lack of amplitude calibration and nonstandardization of the recording equipment render this technique semi-quantitative; direct waveform comparison among clinical recordings is difficult. Still, a great deal of quantitative timing information has been gained by phonocardiography and it offers permanent data storage and display features.

The crystal microphones which are most often used in clinical phonocardiography have a relatively flat, frequency response curve in the 40-750 Hz range. Within these bounds the acoustical frequency region of interest can be selected by a band-pass filter. The filter characteristics are not standardized in phonocardiography, but most clinics use "mid-frequency filtration" [21] or "stethoscopic filtration" [33,34]. "Mid-frequency filtration" is produced by a filter with a flat frequency response function in the approximate band-pass range of 120-500 Hz and a roll-off of 6 db/octave outside this range. "Stethoscopic filtration" is similar to "mid-frequency filtration" with the notable exception that the band-pass is modified to produce a response at the filter output in the 120-500 Hz range which resembles the acoustical response of the human ear (see Fig. 5).

In this experiment "stethoscopic filtration" is employed with a slight low-frequency accentuation. This filter setting produces good sensitivity over a wide frequency range while essential identification features of the time series are preserved.

HEART SOUNDS IN THE PHONOCARDIOGRAM SIGNAL

Typical normal phonocardiogram (PCG) findings in time correlation with ECG, aortic pressure, left ventricular pressure, and left atrial pressure waves are shown in Fig. 6. Note the presence of four distinct groups of vibrations (marked $S_1,......,S_4$) in the phonocardiogram record. These are called heart sounds. Characteristics of these sounds will now be described and correlated with hemodynamic events.

Duration of the systole on a phonocardiogram is defined as the period from the onset of S_1 to the onset of S_2, and duration of the diastole is from the onset of S_2 to the onset of the next S_1.

HEMODYNAMIC CORRELATION OF HEART SOUNDS

First Heart Sound - S_1. Onset of the first heart sound occurs at the beginning of the systole following the ECG Q wave by approximately 10-20 ms. The entire event lasts for an average of 100-120 ms. It is generally

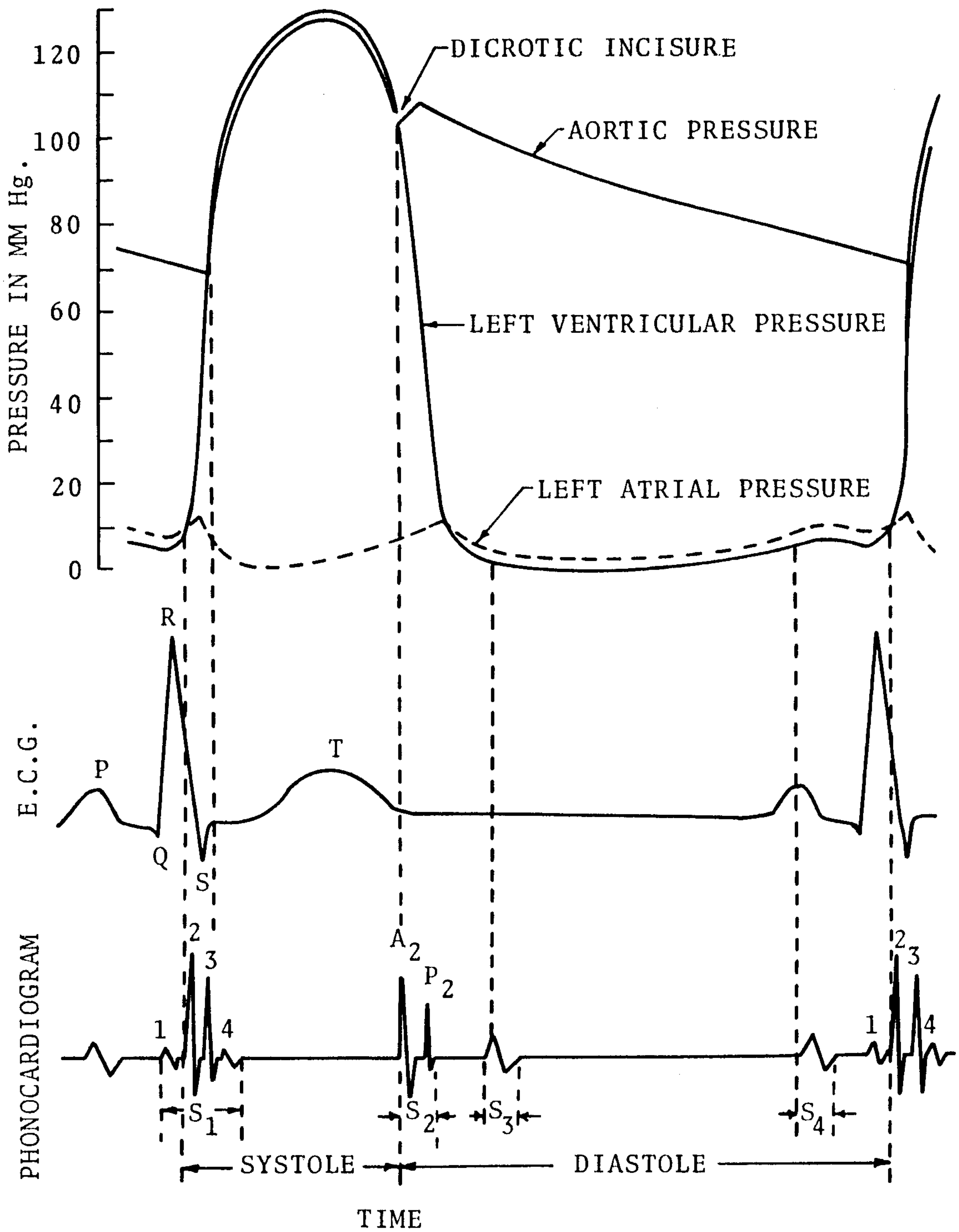

Fig. 6 . A typical normal cardiac cycle

recognized that the first heart sound has four components [20,21] as shown in Fig. 6. The chronological order of these is as follows: The first component is a small, low-frequency (≈ 30-50 Hz) initial vibration which coincides with and is produced by contraction of the left ventricular muscle. The second component consists of a large, high-frequency (80-200 Hz) vibration and is caused by abrupt closure of the mitral valve. The third component follows mitral valve closure by 30 ms. and is also a high-frequency (≈ 80-200 Hz) vibration. It is suspected that this component is produced by rapid ejection of blood into the great vessels, but some investigators contribute it to closure of the tricuspid valve [21]. The fourth component is a small, low-frequency (40-80 Hz) vibration produced by acceleration of blood in the great vessels.

Second Heart Sound - S_2. There is general agreement that the second heart sound is caused by closure of the aortic and pulmonic valves. The vibration produced is in the 70-200 Hz range and persists for about 100 ms. This sound is often "split" into aortic (A_2) and pulmonic (P_2) components (see Fig. 6). In normal subjects the splitting sequence is such that A_2 precedes P_2 by 10-20 ms. upon expiration. For any one individual the splitting is not constant, but increases by 6-10 ms. from expiration to inspiration.

The physiologic reasons for increased inspiratory splitting described by Tavel [21] are as follows: During inspiration the blood is pooled in the lungs causing a pressure decrease in the main pulmonary artery and incomplete filling of the left ventricle. The reduced pressure delays pulmonary valve closure, P_2, and incomplete filling causes aortic valve closure, A_2, to occur early. Thus, both events contribute to inspiratory widening, a respiratory effect which is an important discriminatory feature used to identify A_2 and P_2.

The onset of A_2 was believed to be correlated with the left ventricular pressure change, called the dicrotic notch or dicrotic incisure, (see Fig. 6). More recently, Piemme, et al. [23] demonstrated that the closing sound was delayed from the dicrotic notch by 20-30 ms. occurring in coincidence with maximum reverse blood flow. In addition, the presence of a low-frequency (30-40 Hz) component preceding the closing sound was observed. Its onset occurred in coincidence with the dicrotic notch and with the abrupt slope change of the forward blood flow curve. Piemme attributed this early component to vibration of the cardiohemic system, produced by rapid relaxation of the left ventricle and consequent deacceleration of the blood. These experiments were performed on dogs with implanted transducers of limited frequency response (0-40 Hz), and were significant in providing accurate measurements in vivo of the aortic valve closing time.

Third Heart Sound - S_3. The third heart sound is often observed, particularly in children, during the early rapid ventricular filling phase. This low-frequency (20-70 Hz) vibration occurs on the average of 150 ms. after A_2 and has a duration of 40-50 ms. Its origin remains evasive, but most investigators believe that it is caused by vibration of the rapidly elongating left ventricular walls excited by the incoming blood flow. Since the third heart sound is not produced by valve closure its presence is not considered to be clinically significant in children.

Fourth Heart Sound - S_4. The fourth heart sound has frequency characteristics similar to the third sound and may occur during the late diastolic filling phase. If observed, it usually precedes S_1 by 70-100 ms. and has a duration of 30-50 ms. This sound is most likely produced by vibration of the ventricle walls excited by rapid inflow of blood produced by atrial contractions. During this cardiac phase the atrium acts as a secondary pump "topping off" the ventricles [1].

The fourth heart sound is often observed in children and is considered to be a normal phonocardiographic finding, disappearing in young adult life. Therefore its presence is not considered to be clinically significant.

ABNORMALITIES OF HEART SOUNDS IN VALVAR AORTIC STENOSIS

Intensity Changes of S_2. Comparison of the intensity and tonal qualities of heart sounds taken at the same listening area are affected by extracardiac as well as by cardiac factors. Some prime examples of the former are thickness of the chest wall, pulmonary emphysema, fever, chest deformity and pericardial fluid. Examples of cardiac factors causing an intensity increase of S_2 are increased rate of valve closure [24] and stiffening of the valve cusps. An intensity decrease of S_2 is commonly caused by a reduced force of closure (reduced pressure gradient) across the aortic or pulmonic valve, and by calcification of valves (calcified aortic or pulmonic stenosis). Children's cusps are supple and noncalcified and thus, highly mobile [11]. Therefore, in children with congenital valvar aortic stenosis A_2 is of normal intensity.

Variations in the Splitting Interval of S_2. An abnormally wide splitting on expiration, but otherwise normal (A_2,P_2) sequence, is caused by delayed pulmonic or early aortic valve closure. This anomaly is often observed in pulmonic stenosis, mitral stenosis and ventricular septal defects.

The reversed or paradoxical splitting sequence (P_2,A_2) occurs when aortic valve closure is delayed, causing a splitting interval which decreases from expiration to inspiration. This condition is caused by left branch block, patent ductus arteriosis and severe aortic stenosis [19]. While paradoxical splitting occurs in severe aortic stenosis, it has not been found to be useful in estimating the degree of stenosis. Bache, et al. [35] reported that a prolonged left ventricular ejection time (LVET) existed in valvar aortic stenosis, but poor correlation was observed between LVET and the calculated valve area.

Ejection Clicks. A short, high-frequency (80-200 Hz) vibration may follow S_1; this extra sound may originate from the right or left side of the heart. The former is referred to as pulmonic click [21] and is associated with pulmonary valvar stenosis, pulmonary hypertension and conditions which increase the right ventricular output (e.g., A.S.D. and V.S.D.). When origin of the sound is from the left side, it is referred to as aortic click and is observed in almost all cases of congenital valvar aortic stenosis [11,21]. Since this form of stenosis is common, and other heart diseases seldom if ever produce an aortic click, its presence in children is considered a prime diagnostic feature of congenital valvar aortic stenosis [11,21]. Later in life, with gradual calcification of the valve, intensity of the click is reduced and its absence signifies severe calcified aortic stenosis. A typical phonocardiogram cycle (i.e., ECG Q-Q interval) containing an aortic ejection click is shown in Fig. 7. This cycle was acquired from a valvar

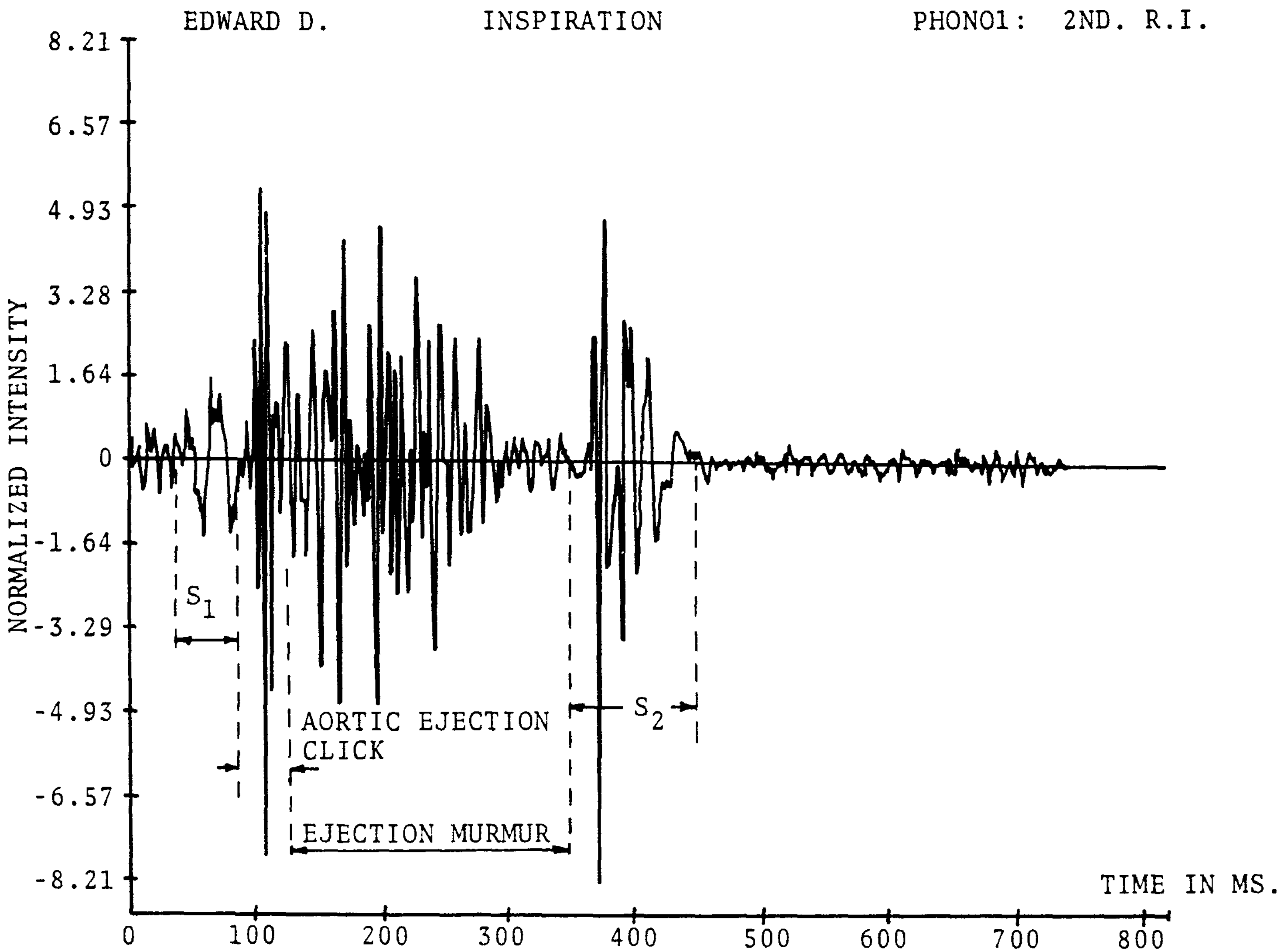

Fig. 7. A typical V.A.S. phonocardiogram cycle

aortic stenosis patient (Edward D.) at the second right intercostal space (2nd R.I.) during inspiration.

In pulmonary valvar stenosis, the pulmonic ejection click is of decreasing intensity or even disappears during inspiration and occurs earlier than normal [26]. The degree of prematurity has been found to be correlated with the severity of pulmonary stenosis [21]. In comparison, intensity and onset of the aortic click are independent of respiration, and onset time is not related to severity. While the onset time is not clinically useful, constant intensity of this click is an important feature and is used to identify aortic and pulmonic clicks.

Opinion on the origin of the aortic ejection click has been divided. Some investigators [21] state that it is a root event produced by acceleration of blood into the aorta and occurs at the onset of the pressure rise in the indirect carotid pulse. (Thus, more appropriately, it can be called an accentuated component of S_1). Others report that the click is independent of S_1, valvar in origin and is produced when the valve is fully domed and stressed by the ejected blood. Recent detailed intracardiac sound and angiogram studies on normal and valvar aortic stenosis subjects demonstrated, that while both mechanisms could produce sound [27,13], the aortic click is valvar in origin. The click produced by the stenosed valve always occurred in coincidence with the anacrotic notch. The time interval from the click to the rise of the aortic pressure pulse is approximately 24 ms. This time interval is defined as valve mobility and correlates poorly with the degree of stenosis in the wide age group of patients in Epstein's studies [27].

HEART MURMURS

Heart murmurs are relatively long-duration vibrations which may occur in any part of the cardiac cycle. Murmurs are classified into several, not necessarily mutually exclusive, groups. The most important classifications are listed below and are described according to:

1. their physiological properties; innocent or organic.
2. their frequency content; high-pitched, low-pitched, musical or harsh.
3. their intensity envelope; diamond-shaped, crescendo, or descrescendo.
4. their time of occurrence in the cardiac cycle; systolic, diastolic, or continuous.

To further define the time of a murmur's occurrence, the prefixes early, mid, late and holo are often used.

A typical cardiocycle containing a diamond-shaped systolic murmur is shown in Fig. 7. This type of murmur is commonly observed in valvar aortic stenosis. During auscultation, intensity of a murmur is graded on a subjective scale of 1 (very faint) to 6 (loudest possible).

The mere presence of a murmur does not imply the presence of heart disease or a heart disorder. Innocent murmurs (those not associated with significant heart disease) are common ausculatory findings and occur in approximately fifty percent of normal children [36]. The timing, location, intensity pattern shape and most importantly, the accompanying heart sound abnormalities, determine the presence and type of significant heart disease [18,21,36,37].

THE ORIGIN OF CARDIOVASCULAR VIBRATION ENERGY

A thorough study of the origin of cardiovascular vibration energy can be divided into three parts:

1. Study of the hemodynamic event which causes the heart to vibrate.
2. Modeling of the vibrating system and study of the production of vibrational energy.
3. Study of the propagation modes of vibrational energy and transmission properties of the human thorax.

There has been general agreement among physicians for many decades that S_1 and S_2 are caused by closing of the valves. Time correlation of heart sounds with major hemodynamic events are well established and well reported in literature [20,22,23,24,25].

It is generally accepted that harsh non-musical murmurs are produced by a turbulent jet of blood flowing through a small orifice [1,18,37]. Examples of such murmurs are aortic stenosis, pulmonic stenosis, ventricular septal defects, etc. Musical murmurs, those with tonal qualities, are produced by other processes. Vortex shedding, periodic wake, and flitter are the mechanisms proposed by Bruns [39] and Rushmer [18] to explain the origin of musical murmurs.

Detailed theories concerning the production mechanisms of cardiovascular vibration energy have been studied by many [38,39,40,41,42] and the turbulent murmur problem is extensively modeled by Yellin and Bellhouse [43,7,8].

A highly intuitive cardiac model is described by Rushmer [1]. In this model the blood, heart walls, and heart valves are considered as one vibrating "cardiohemic" system, where heart sounds are caused by acceleration or deacceleration of the blood. This non-mathematical model is quite successful in predicting the time of occurrence of normal heart sounds, but fails to account for the wave shapes of the sounds.

AREAS OF AUSCULTATION

Murmurs produced by various anomalies and heart diseases have definite, well established intensity radiation patterns on the chest. The point of maximum intensity and the radiation pattern are two important discriminatory diagnostic features in cardiology.

Conventionally, the chest is divided into four areas, referred to as the aortic (A), pulmonic (P), right ventricular or tricuspid (T), and left ventricular or mitral (M) auscultation areas. The locations of these areas are shown in Fig. 8. The areas are named after the heart sounds and murmurs which are best observed at these locations [51].

Vibrations originating from the aorta (i.e., aortic stenosis murmur, aortic ejection click, and the aortic component of the second heart sound) are usually best observed at the aortic area, or more specifically, at the second right intercostal space near the sternum border (2nd R.I.S.). Vibrations originating from the main pulmonary artery (i.e., pulmonic ejection click, pulmonary stenosis murmur, and pulmonary component of the second heart sound) are well transmitted to the pulmonary listening area at the second left intercostal space near the sternum border (2nd L.I.S.). While the aortic component of the second heart sound and the aortic ejection click tend to be maximum at the aortic area, they are well transmitted to other listening areas, particularly to the left ventricular area or apex. In contrast, the pulmonary component of the second heart sound is highly localized to the pulmonary area and seldom if ever is observed at the 2nd R.I.S. and apex. Predictable transmission characteristics of the second heart sound are most useful in identifying aortic and pulmonic components of the second heart sound.

Vibrations originating from the left ventricle (i.e., mitral closing sounds, third heart sounds, mitral stenosis murmur, etc.) are best observed at the mitral area or apex, whereas vibrations from the right heart (tricuspid closing

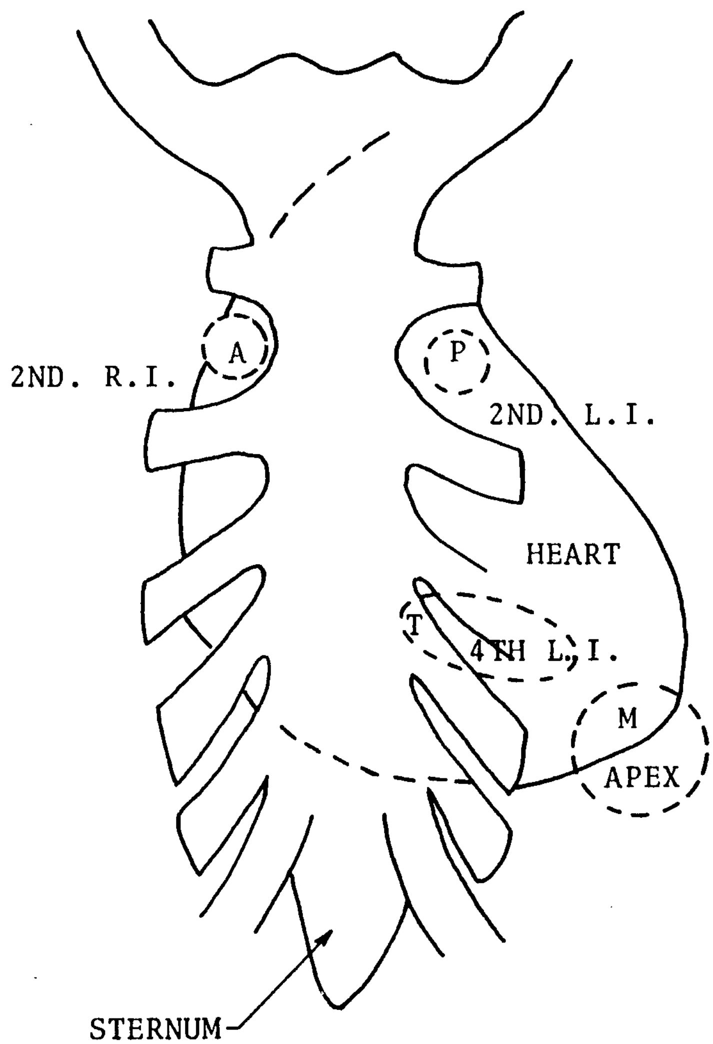

Fig. 8. Primary auscultation areas

sound, tricuspid stenosis murmur, etc.) are generally loudest at the tricuspid area.

As expected, these primary auscultation sites are located on the chest where the left and right ventricles and great vessels are closest to the surface.

TRANSMISSION CHARACTERISTICS OF THE HUMAN THORAX

The human body is an anisotropic, nonhomogeneous, acoustical medium where vibration energy propagates in several modes [45,46].

In the heart and arterial walls vibration energy propagates as shear waves [46] with a velocity of 4-5 m/sec. [45]. Shear waves are attenuated at 20 db/10cm. at 100 Hz. Additional relevant data obtained in vivo measurements are given in [45,46,50,53].

Energy is conducted as compressional waves in bone and tissue with velocities of 3400 m/sec. and 1490 m/sec. [45,53] respectively. Bone conducts sound energy well in a wide frequency range, where in tissue it is attenuated at an approximate rate of 10 db/10cm. at 90 Hz [45,52]. Additional relevant data is available in the literature [44,45, 47,48,49].

Faber, et al. [47] suggested that vibrational energy emerges at the primary auscultation sites and spreads to nearby locations as surface waves. Surface wave velocity on the human chest is approximately 15 m/sec. at 100 Hz and increases approximately with the square root of the frequency [47]. However, these waves are localized since they are attenuated at a rate of 27 db/10 cm. at 100 Hz [45].

From the above discussion we may conclude that the microphones must be located between the ribs and as close to the sources as possible. This choice minimizes the affect of multiple conduction paths and produces maximum signal intensities. In valvar aortic stenosis the murmur, ejection click, and A_2 are observed with maximum intensity at the 2nd R.I.S. The arch of the aorta is only 2-3 cm. away from this site as shown in Fig. 8. For the above reasons, the 2nd R.I.S. is chosen for the study of this disease.

INDIRECT CAROTID PULSE RECORDING

The carotid arteries are major vessels directly connected to the aorta and easily accessible at the neck. The recording of the carotid artery wall displacement versus time in the 0.2-20 Hz frequency band is referred to as the indirect carotid pulse recording, or in short, the carotid pulse [21]. This pulse shape closely resembles the waveshape measured in the ascending aorta, but is delayed by 20-30 ms. In addition, the high-frequency components (dicrotic notch) are considerably attenuated. When the proper time delay correction is applied, the upstroke of the carotid pulse and the dicrotic notch occur in coincidence with the onset of the ventricular ejection and aortic valve closure. Consequently, the carotid pulse is useful in identifying the aortic ejection click and the closing sound in the phonocardiogram tracings.

In valvar aortic stenosis the carotid pulse may show a "slow" upstroke, a prolonged left ventricular ejection time, and pressure fluctuation or trill. While these signs are usually present in patients with an aortic valve pressure gradient greater than 40-50 mm. Hg, a more precise classification with this method has not been possible [21].

PHONOCARDIOGRAM SIGNAL FEATURES

Phonocardiographic diagnosis of heart diseases must be based on rugged signal features which are statistically reliable and are defined by Levine [54] as features "whose presence are not changed and whose character are not greatly altered by normal variation in the image of a character in a given category".

Selection of general and rugged signal features is highly empirical and requires access to a complete data set, that is, a data set that contains all heart diseases. Cardiologists through years of experience have found the following rugged phonocardiogram signal features relevant to the diagnosis of heart diseases [1,18,21,36].

1. Presence of murmurs.
2. Presence of systolic click or other abnormal sounds.
3. Timing of murmurs and sounds.

4. Location of maximum intensity points and transmission paths of murmurs, clicks, and sounds on the chest.
5. Shape of murmur envelope.
6. Peak intensity of sounds, clicks, and murmurs.
7. Frequency content of murmurs.

It is important to note that correct diagnosis is not reached by considering features from one of the categories listed above. Rather, a combination of features from the entire group must be jointly interpreted; a weighted sum of the features leads to proper diagnosis.

PHONOCARDIOGRAM IDENTIFICATION FEATURES OF VALVAR AORTIC STENOSIS

The following phonocardiogram features are considered to be the rugged identification features of congenital valvar aortic stenosis in children [21].

1. A diamond-shaped, systolic ejection murmur is present and is usually loudest at the aortic listening area. The murmur must end before onset of the aortic component of the second heart sound.
2. The murmur is introduced by a constant intensity, aortic ejection click which is usually loudest at the aortic listening area or at the apex.

In addition, the following features are often observed in valvar aortic stenosis, particularly in moderate and severe cases.

3. The left ventricular ejection period is prolonged, producing a paradoxically-split second heart sound.
4. The carotid pulse may show a slow upstroke, prolonged peak time, a flattening of the dicrotic notch, and superimposed vibrations or a trill in the systole.

DIFFERENTIAL DIAGNOSIS OF VALVAR AORTIC STENOSIS

The following innocent systolic murmurs have one or more signal features similar to valvar aortic stenosis [36].

1. Still's murmur.
2. Innocent pulmonic murmur.
3. Supraclavicular atrial bruit.
4. Innocent late systolic murmur.
5. Innocent cardio-respiratory murmur.

These innocent systolic murmurs have typical diamond-shaped envelopes but are never introduced by an ejection click. Consequently, the presence of the aortic ejection click can be used to discriminate between valvar aortic stenosis and innocent systolic murmurs.

In children the following common heart anomalies have phonocardiogram signal features similar to valvar aortic stenosis [21,36].

1. Pulmonic stenosis.
2. Mild ventricular septal defect.
3. Moderate to severe atrial septal defect.
4. Tetrology of Fallot.

All of these anomalies have typical diamond-shaped, ejection-type systolic murmurs which may be introduced by an ejection click. However, they can be differentiated from valvar aortic stenosis by observing the following basic differences:

In pulmonic stenosis:

a. The pulmonary ejection click is variable; that is, intensity and onset of the click are functions of respiration.
b. The pulmonic ejection murmur is generally loudest at the pulmonic listening area. Its intensity is often a function of respiration, and it may continue to the onset of the pulmonic component of the second heart sound.

In mild ventricular septal defect:

a. The murmur is a harsh, short-duration, ejection-type, where the location of the maximum intensity point on the chest overlaps the location of the intracardiac location of the shunt, generally at the third left intercostal area or lower.

In moderate to severe atrial septal defect:

a. Abnormal first and second heart sounds are present.

b. A pulmonic-systolic ejection murmur is present related to the large pulmonary blood flow.

In Tetrology of Fallot:

a. The ejection-type murmur in mild to moderate cases is not introduced by an ejection click and consequently, can be easily discriminated.

b. In severe cases the short-duration ejection murmur is introduced by an ejection click making discrimination difficult on the basis of phonocardiogram features alone, but is easily identified by other clinical observations such as cyanosis and low oxygen content of the blood.

MAJOR PHONOCARDIOGRAM SIGNAL PROCESSING WORK DONE BY OTHERS

The following investigators have recently made significant contributions in the field of phonocardiogram signal processing:

Cambron [82] studies 111 patients with mitral stenosis, mitral insufficiency or normal phonocardiograms and uses pattern recognition techniques, such as the nearest-neighbor method, to identify these conditions in the frequency domain.

Vocker [83] employs an adaptive filter to select the epoch of the first and second heart sounds. He was able to update the filter to follow the epoch variation of the second sound caused by breathing.

Stephens [84] analyzes the first heart sound with bandpass filters and establishes frequency patterns useful in the identification of myocardial infarction.

In the work of Perry, et al. [85], analog as well as digital techniques are considered. In the digital analysis, 2.5 sec. recordings are made from four listening areas and successive threshold levels are used to identify sounds and murmurs. A band of filters is used to obtain the cardiogram energy spectra. A diagnostic decision process is employed to identify common heart diseases.

Frome and Frederickson [86] select several first and second heart sound waveforms, convert them into discrete data segments, and compute averaged first and second heart sound power spectra using the FFT algorithm. The authors suggest that the intensity of the computed spectra can be used to monitor the depth of anesthesia during surgery.

Gerbarg, et al. [87] make an indepth study on the use of computers to identify innocent heart murmurs. Identification is based primarily on timing of the innocent systolic murmur.

Townes, et al. [88] compare the signal features of several cycles of innocent and stenosed bruits using zero crossing, statistical, and power spectrum analysis techniques. The investigators conclude that the number of major peaks in the power spectra of stenosed bruits exceeds the number found in innocent bruits, and use this signal feature to differentiate the two kinds.

CHAPTER III

DESCRIPTION OF THE EXPERIMENT

APPROACH TO THE PROBLEM

A brief examination of abnormal phonocardiogram records reveals that the time series consists of repetitive cardiocycles. Each cycle is composed of deterministic wavelets (heart sounds) and amplitude-modulated, bandwidth-limited, random signals (murmurs). The term wavelet is used here to indicate a portion of the phonocardiogram time series which is associated with a single hemodynamic event, such as aortic ejection click.

The cardiologist examining a phonocardiogram time series selects a typical inspiration cardiocycle and an expiration cardiocycle free of artifacts, measures the diagnostic signal parameters, and derives a partial diagnosis on the basis of these two cycles [11]. The measured parameters obtained from a single cardiocycle are often statistically unreliable due to added noise and other random artifacts. The statistical errors cannot be reduced since the data is in an unsuitable form. Thus, the single, biggest disadvantage of this type of time series display is that it is unsuited for computer processing, particularly for power spectrum analysis.

The need for frequency information prompted some investigators [55,56] to complement the time series display with online power spectrum analysis display. While online spectrum analysis is useful in identifying and describing musical murmurs, such as the "sea gull" murmur, on the basis of a single estimate [55], high statistical variance prevents accurate descriptions of noiselike murmurs. Since most organic murmurs are of this type, the above statement applies to the majority of heart diseases.

At the start of this research it was felt that by properly averaging equivalent cardiocycles (those which are produced under identical hemodynamic conditions) in the time, envelope and frequency domains, statistically reliable decision parameters could be obtained. With the use of these reliable parameters, the diagnosis of systolic heart diseases can become more accurate, and assessment of the severity of valvar aortic stenosis by computer analysis may now become possible.

This study was conducted on fourteen catheterized and four clinically diagnosed valvar aortic stenosis patients. In addition, six normal patients were included in the study to facilitate the identification of valvar aortic stenosis signal features. The complete patient set is described in Chapter V.

A small 16 bits/word mini-computer with approximately 12-16K words memory capacity, equipped with digital tape recorders, a multiplexer, an analog-to-digital converter, and a graphics terminal, was used for this study. The multichannel time series was digitized and the large volume of data required was stored on digital magnetic tapes. With the aid of the graphics terminal the operator could interact with the computer, quickly reviewing and interpreting the processed data. In questionable cases, additional analysis could be requested. Quick turn-around time is of course the most essential characteristic of such an interactive analysis system.

SELECTION OF RECORDING SITES AND TIMING DATA

In this study phonocardiogram data from all four classical listening sites (2nd R.I.S., 2nd L.I.S., 4th L.I.S. and apex) were acquired. With this choice of listening sites, an adequate transmission pattern can be obtained and all heart diseases that can be diagnosed by phonocardiography can be adequately analyzed. Additionally, ECG, carotid pulse and respiration were recorded to facilitate the timing and identification of heart sounds and ejection clicks, and to observe changes in the phonocardiogram signal induced by respiration.

ESTIMATION OF THE RECORDING TIME DURATION

Clearly, the confidence limits of each analyzed point will be determined by the type of analysis, smoothing, and number of cardiocycles included in the analysis. The effects of this will be discussed in Chapter IV. Prior to analysis, the recording time interval must be selected to be consistent with the goals of the analysis, as well as with other considerations. An example of the latter is: can a young child maintain quiet and steady respiration for the duration of the recording interval? Another relevant question may be asked: how reproducible is the measurement on a weekly or monthly basis? It is useless to reduce the short range statistical errors to 1 percent when the unexplainable human variables limit the monthly reproducibility of the measurement to 100 percent.

The repetitive nature of the phonocardiogram makes it possible to estimate the number of cardiocycles required to obtain a desired short range statistical error. Each cardiocycle can be represented as a sample function of a finite population. The task is to estimate the population mean with a desired error d, on the basis of N samples and with a particular confidence level. Assuming that the population is approximately normally distributed with a mean of η and a standard deviation of σ, the number of samples required is given by the equation below [57],

$$N = \frac{Z^2 \sigma^2}{d^2}$$

where Z is the confidence constant; for a 95 percent confidence level Z = 1.96. Selecting a 10 percent short range measurement error as a realistic goal with a 95 percent confidence level, and assuming that the population variance is approximately one-half the population mean, these assumptions give

$$d = \eta/10$$

$$\sigma = \eta/2$$

$$Z = 1.96$$

and the corresponding sample size is N = 100 cardiocycles. Assuming that 0.9 sec. equals the average cardiocycle period, this yields a recording time duration T = 90 seconds. During data recording, it was observed that a patient could be maintained in a statistical equilibrium for these time durations, and repeated measurements taken on the same patient indicated that an acceptable 10 percent monthly reproducibility was possible.

EXPERIMENT ORGANIZATION AND BLOCK DIAGRAM

In this study the data "handling" was conveniently divided into four steps: analog data acquisition, analog-to-digital conversion, data selection, and data analysis. During the first step, four channels of analog data were acquired and recorded by an analog tape recorder. In the second step, analog data was converted into a continuous stream of digital records. During the third step, equivalent cardiocycles were selected and arranged in equivalent data files. In the final step, files were analyzed, diagnosis signal features were identified, and the severity of aortic stenosis was assessed.

A complete block diagram of the experiment is shown in Fig. 9.

The first three procedures will be described in this chapter while the next two chapters will be devoted to data analysis.

ANALOG DATA ACQUISITION AND RECORDING EQUIPMENT

The analog data acquisition and recording equipment, as shown in Fig. 9, was located in the Cardiology Department at Children's hospital and an analog tape recorder was used for data storage.

The transducer-amplifier display equipment used in the study was a commercial heart sound monitoring system manufactured by Cambridge Instrument Company, Inc. The crystal microphones were Cambridge type 53616 "adult size" and were secured to the chest by suction as shown in Fig. 1,AI (Appendix I). The manufacturer's acoustical calibration curve is shown in Fig. 2,AI and the measured differential error between the two microphones is given in Table 1,AI. The phonocardiogram amplifier-filters were Cambridge type 72352 with the filter switch set to the "L" position.

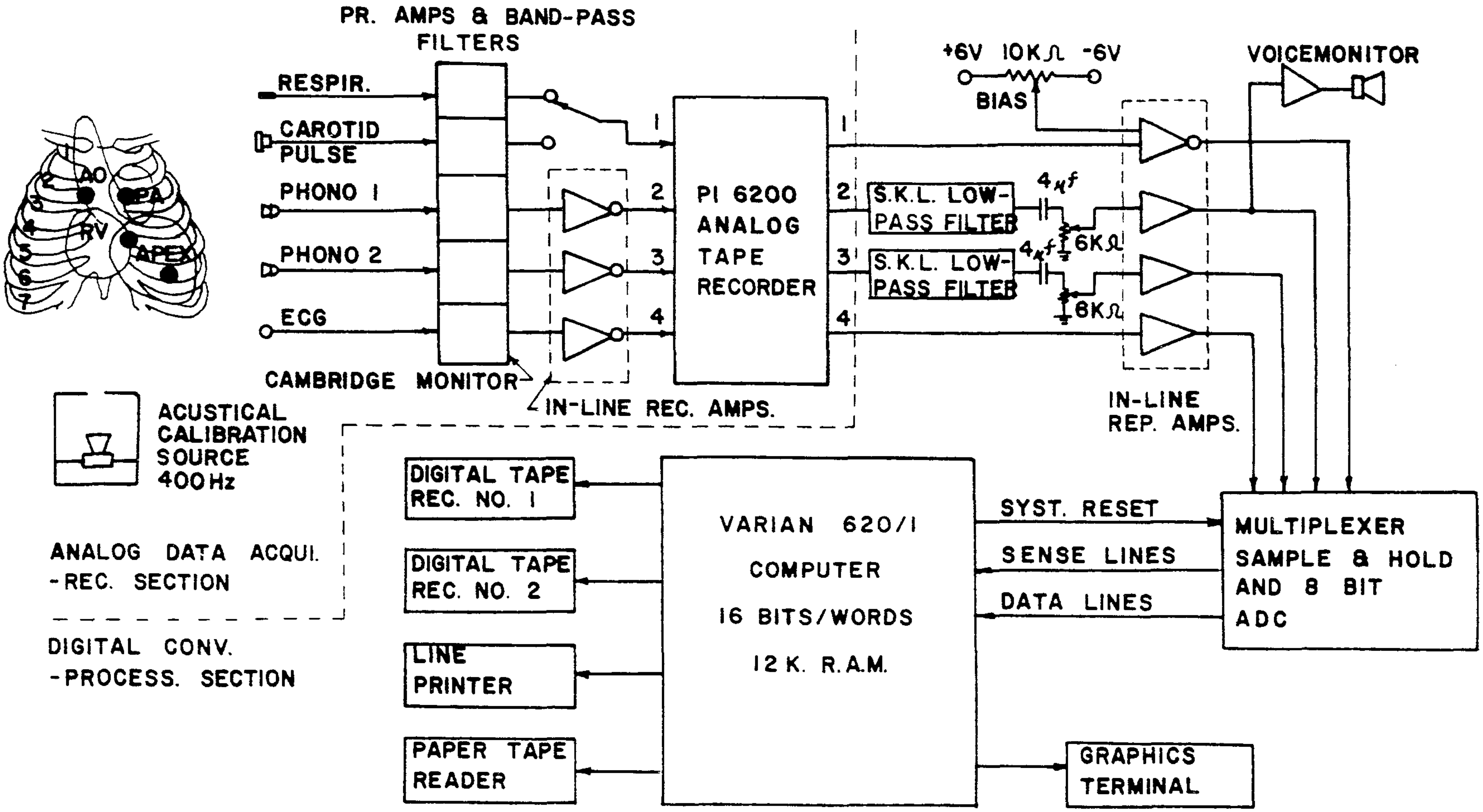

Fig. 9. Block diagram of the experiment

At the start of this project the exact phonocardiogram bandwidth was unknown. To obtain good frequency response above 1KHz, the first group of clinically-diagnosed patients (Analog Tapes No. 1 and No. 2) were AM recorded. During the data conversion and initial power spectrum analysis it became obvious that, even for the severe aortic stenosis case, 95 percent of the phonocardiogram signal energy is concentrated below 400 Hz, and therefore high-frequency response was not required. To improve the low-frequency response and the signal-to-noise ratio, subsequent analog tapes were recorded in the FM mode. With the exception of one valvar aortic stenosis patient, all catheterized patients were recorded in the FM mode. The measured frequency response curves of the two phono-channels are shown in Figs. 10 and 11. Here the Cambridge amplifier inputs were taken as the system input and the multiplexer input was taken as the system output. Measurements were performed with a constant-intensity sinusoidal source. Note that the two recording modes have almost identical "frequency response curves" in the 50-1000Hz range, but that below 50Hz the AM recording provides more attenuation.

RECORDING AND CALIBRATION PROCEDURES

Prior to data recording the patient was introduced to the equipment and was assured that no physical pain would be involved with this test. Since emotional strain affects the heart and blood flow rates, this step was

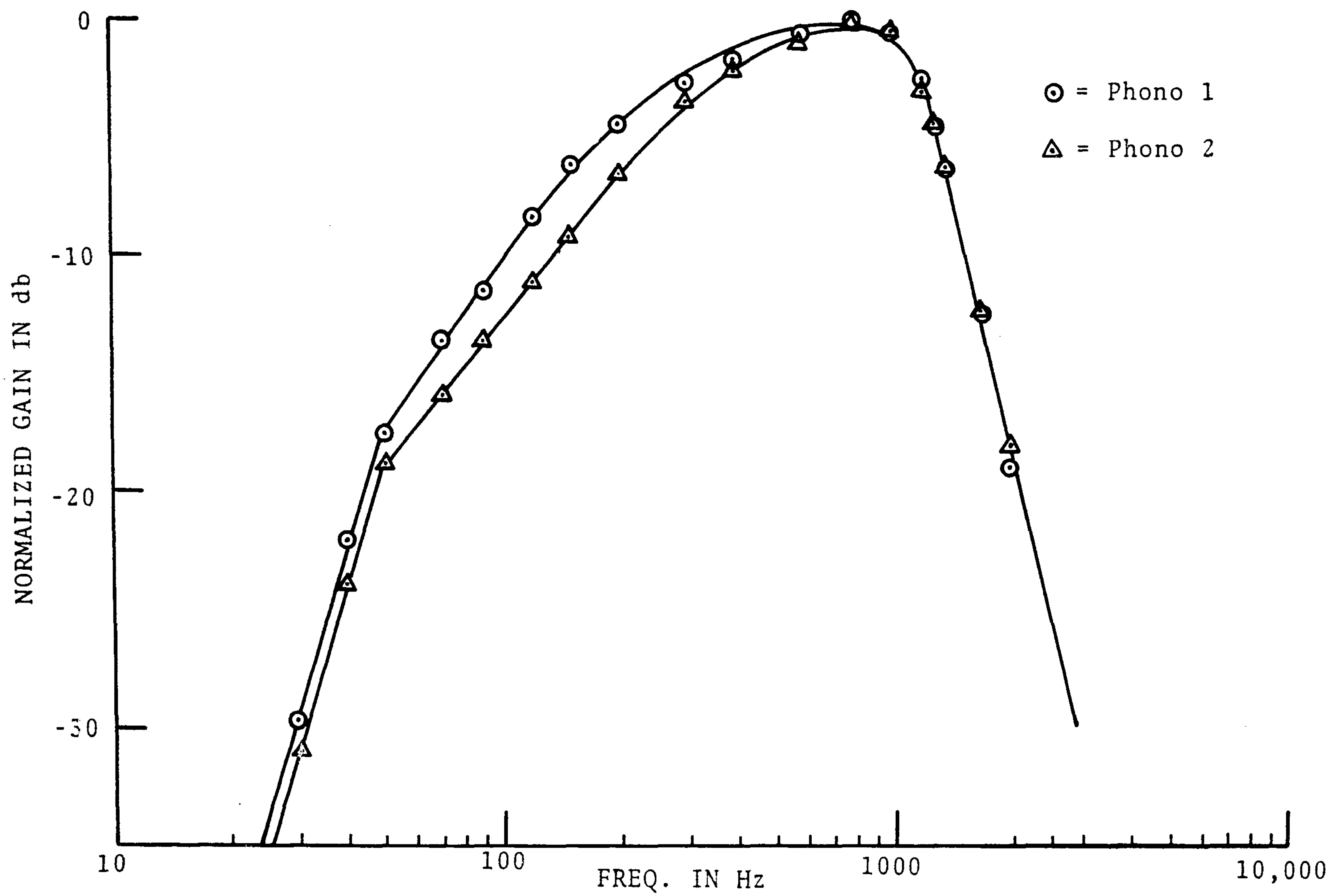

Fig. 10. Measured frequency response of electronics system with A.M. recording mode

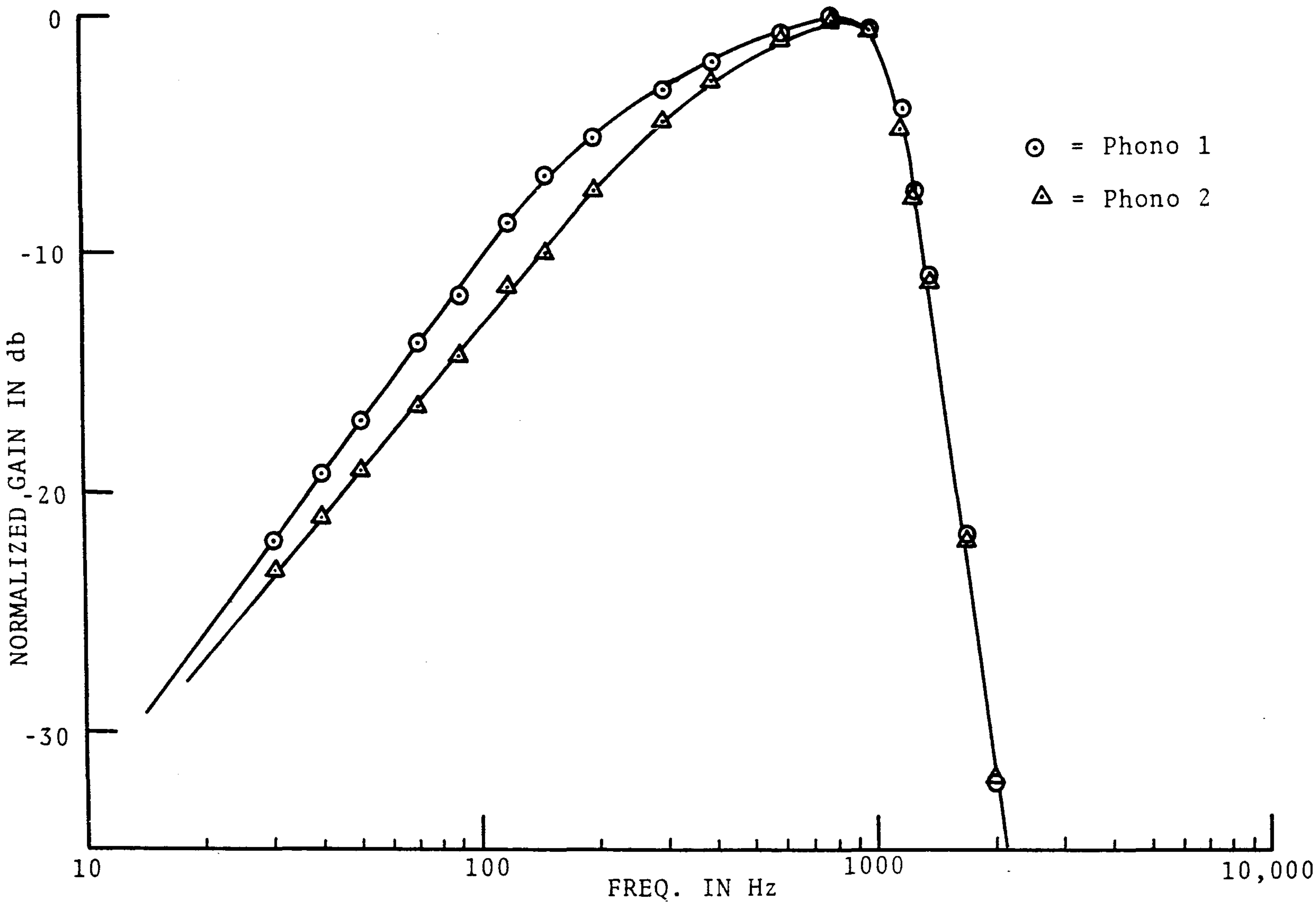

Fig. 11. Measured frequency response of electronic system with F.M. recording mode

required to obtain consistent phonocardiogram recordings and assured that the data was recorded under steady-state conditions. Before the actual recording was begun the four listening sites were briefly tested and the recorder gains were set to the maximum allowable levels (i.e. no limiting) at the maximum intensity sites. These settings were maintained throughout the recording. While being recorded the patients were in a supine position and respiration was at a normal, steady rhythm. A typical analog patient recording sequency is shown in Table 2.

TABLE 2

A TYPICAL ANALOG RECORD SEQUENCE

Recording Time in sec.	Channel 1	Channel 2	Channel 3	Channel 4
20	Phono 1 2nd L.I.	Phono 2 Apex	Carotid Pulse	ECG Lead 2
90	Phono 1 2nd L.I.	Phono 2 Apex	Respiration	ECG Lead 2
20	Phono 1 2nd R.I.	Phono 2 4th L.I.	Carotid Pulse	ECG Lead 2
90	Phono 1 2nd R.I.	Phono 2 4th L.I.	Respiration	ECG Lead 2
10	400 Hz Tone Cal.	Background Noise	---	---
10	Background Noise	400 Hz Tone Cal.	---	---

Note that the phonocardiogram channels were calibrated following each patient's recording by a 400 Hz constant-intensity acoustical source. The sound intensity at the calibrator aperture was approximately 10^{-14} watts/cm^2. This calibration signal was used later in the data analysis for normalization and made possible the direct comparison of processed data among the patients.

Differential Phono-Channel Delay. The total differential system delay between the two phono-channels was measured by on-off keying a common acoustical source placed an equal distance from the two microphones, and by observing the corresponding differential time delay at the graphics terminal. The measured differential time delay was less than 400 μsec. or less than one sample time increment.

Push Down Test. The phonocardiogram "signal sense" (sign relation between signal polarity and chest displacement) was determined by placing a rubber sheet over the microphone and applying a downward displacement with a rubber tipped pencil.

This test indicates that an outward chest displacement corresponds to a negative signal level, whereas an inward displacement corresponds to a positive signal level in the phonocardiogram time series as observed on the graphics terminal.

ANALOG-TO-DIGITAL CONVERSION

During analog-to-digital conversion, the four channels of analog data were time multiplexed and digitized by an 8-bit analog-to-digital converter. The choice of an 8-bit converter offers better than 1 percent quantitization accuracy (considered adequate for clinical measurements) and an efficient digital data format (i.e., with a 16 bits/word computer and an 8 bits/sample, two samples/word can be stored). The phonocardiogram signal was sampled at a 2.5 KHz rate, whereas the ECG, carotid pulse and respiration signals were sampled at a 625 Hz rate. The phonocardiogram and timing signals are bandwidth-limited functions with highest significant frequency components of 400 Hz and 60 Hz respectively. It is clear from the above that the selected sampling rates are more than three times the Nyquist sampling rates, and consequently the analog signals are completely defined by their digital sample sequence. A detailed mathematical description of the sampling process is presented in Chapter IV.

Continuous data storage was accomplished by the use of two 4K word computer memory buffers. The digital samples were sequentially stored in one of the buffers; when this buffer was full, data continued to be stored in the second buffer while the contents of the full buffer was transferred to digital magnetic tape by way of the DMA data path. Repetitive use of this process allowed continuous conversion.

The converted data is free of gaps because the read-out time is shorter than the read-in time, and the buffers can be switched within one sample time. During conversion, the high degree of time correlation between data channels was maintained. The computer subroutine used for sampling is given in Appendix I.

Each buffered data block stored on the magnetic tape comprised a data record and records were separated by inter-record gaps. Digital data processed in this manner is referred to as Pass 1 data and the record format is shown in Table 3. Digital data of each patient is arranged into five data files and each data file is preceded by an alpha-numeric header file describing it. Each header contains the patient's name, hospital number, and transducer locations. In addition, the first header contains other essential patient parameters and diagnostic information. The digital tape file format is shown in Table 4, and typical patient header files are shown in Tables 2,AI and 3,AI.

SELECTION OF EQUIVALENT CARDIOCYCLES

A detailed examination of the Pass 1 time series revealed that wavelets in the systole for properly selected phonocardiogram cardiocycles exhibited remarkable time coherence. This coherence existed within a Pass 1 data file for cardiocycles of the same respiration phase whose Q-Q interval variations were within 10 percent. For these selected cardiocycles, the ejection click and first and second heart sounds were very reproducible in both onset time and waveshape, with almost all of the Q-Q time deviation occurring in the diastole. The onset jitter (epoch

TABLE 3

PASS 1 DIGITAL DATA TAPE RECORD FORMAT

Pulse/Resp.	ECG

RECORD GAP

Sample Index	15	8 0 BIT No.
	PASS 1	RECORD NO.
1	Phono 1	Phono 2
2	Phono 1	Phono 2
3200	Phono 1	Phono 2
1	Car. or Resp.	ECG
4	Car. or Resp.	ECG
3200	Car. or Resp.	ECG

RECORD GAP

PASS 1	RECORD NO.
Phono 1	Phono 2

TABLE 4

PASS 1 DIGITAL DATA TAPE FILE FORMAT

File No.	Contents	
	ALPHA-NUMERIC PATIENT HEADER	
1		F.G.
	Phono 1/Phono 2 Tone Cal Binary Data Recs.	(FILE GAP)
2		F.G.
	ALPHA-NUM. HEADER FOR NEXT FILE	
3		F.G.
	Phono 1 = 2L.I. Phono 2 = Apex Pulse = Car. ECG = Lead 2 Binary Data Recs.	
4		F.G.
	ALPHA-NUM. HEADER FOR NEXT FILE	One Patient Data Block
5		F.G.
	Phono 1 = 2L.I. Phono 2 = Apex Respiration ECG = Lead 2 Binary Data Recs.	
6		F.G.
	ALPHA-NUM. HEADER FOR NEXT FILE	
7		F.G.
	Phono 1 = 2R.I. Phono 2 = 4L.I. Pulse = Car. ECG = Lead 2 Binary Data Recs.	
8		F.G.
	ALPHA-NUM. HEADER FOR NEXT FILE	
9		F.G.
	Phono 1 = 2R.I. Phono 2 = 4L.I. Respiration ECG = Lead 2 Binary Data Recs.	
10		F.G.

jitter) of the wavelets was approximately ± 4 ms. where all onset times were measured from the ECG Q wave. This coherence was observed in all patients included in this study.

As pointed out in Chapter II, in the cardiohemic system the onset time and intensity of the wavelets are functions of the hemodynamics of the heart and the high degree of coherence and reproducibility observed among these selected cycles indicates that these cardiocycles are produced under identical hemodynamic conditions. In conclusion, equivalent cardiocycles at a listening site are defined here as cardiocycles which are produced at the same respiration phase and whose Q-Q interval variations are within 10 percent.

Equivalent Data Ensembles. Clearly, equivalent cycles may be averaged at any respiration phase, but to observe the maximum phonocardiogram signal changes produced by respiration, equivalent cycles are selected at mid-inspiration and mid-expiration.

Mid-inspiration (and mid-expiration) cardiocycles are defined as those cardiocycles where the maximum (and minimum) values of the respiration signal occur at the middle of the cycle. Thus, these cardiocycles are obtained at approximately maximum (and minimum) lung volumes. Fig. 12 shows the systole and early diastole of five mid-inspiration cardiocycles selected as discussed above. Note

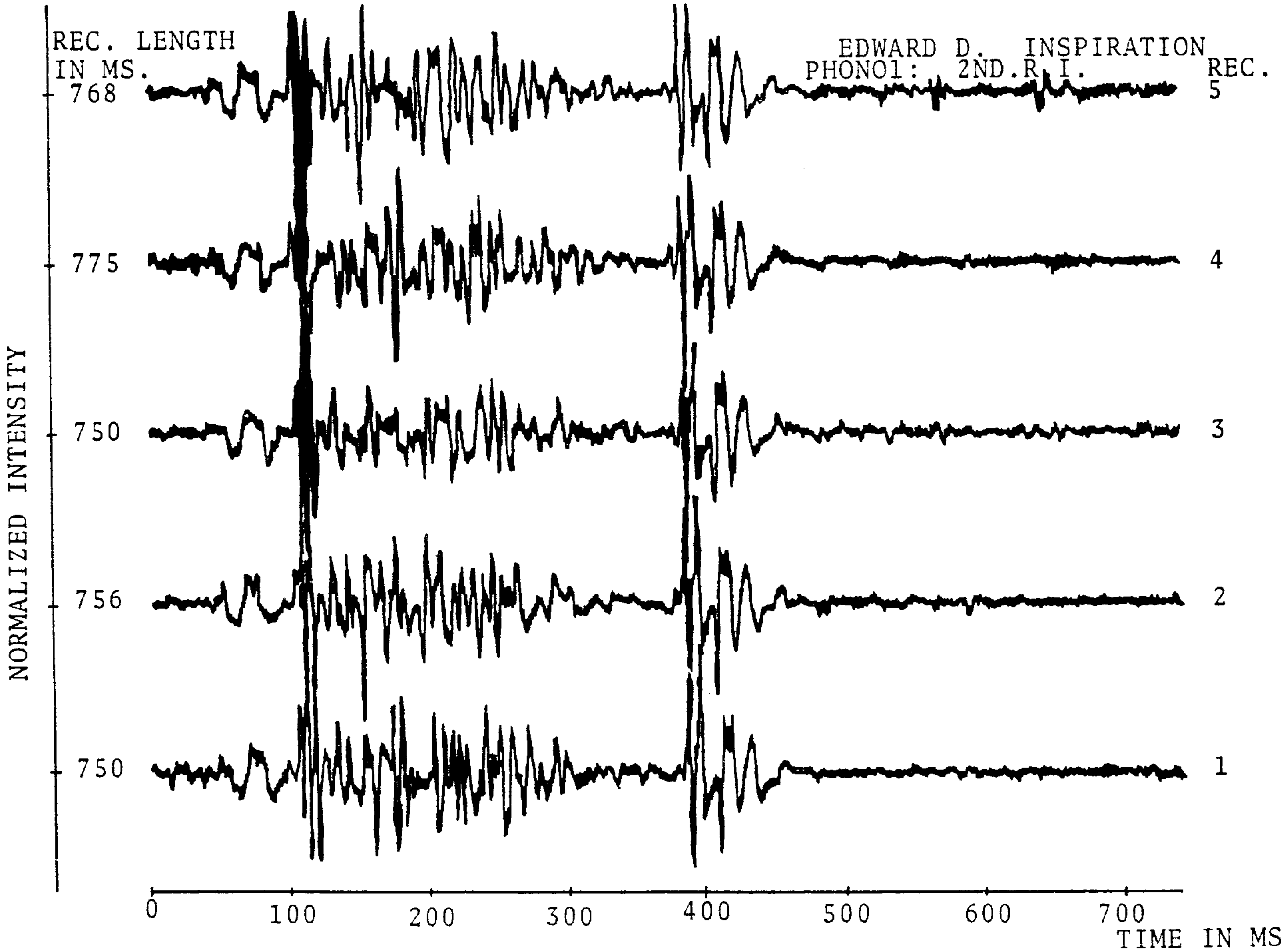

Fig. 12. Five typical equivalent phonocardiogram records

that the onset time and shape of the wavelets are independent of the record length (Q-Q interval).

PASS 2-3 DATA

Equivalent data ensembles (files) are generated with a two-step data reduction process. In the "initial step", equivalent cardiocycles are selected and approximately timed to contain a single Q-Q interval. The data output in this step is referred to as Pass 2 data. During this step the four-channel Pass 1 data is displayed on the graphics terminal; from this display, equivalent Q-Q interval cardiocycle records are selected with the "graphics cursor" and are output to the digital tape recorder. Excessively noisy cycles are omitted at this time.

During the second step the previously selected cardiocycles are aligned and timed to start precisely at the ECG Q wave and the data output in this step is referred to as Pass 3 data. Prior to alignment the ECG waveforms are examined and the largest and most rapidly changing signal feature (R or S wave) is selected as the alignment point. The time interval between the alignment point and the Q wave is measured and defined as the IDQ interval. This interval is stored as a parameter in the "align program" and serves as a common reference within a patient data set. Alignment is accomplished by a computer program which searches for the alignment point (local maximum or minimum) and slides the cardiocycles to the left or right to cause an alignment about the point mentioned above. To start the aligned records at the ECG Q wave, data points to the left of the IDQ interval are deleted. Selection and timing of the four data channels occur simultaneously, maintaining a time correlation between data channels of 400 μs. Typical aligned cardiocycle records are shown in Fig. 13. As a final check on alignment and timing, ECG records of each file are "stack plotted" and carefully examined. With this two-step process, cardiocycle alignment precision (i.e., Q wave onset jitter) is approximately ± 1.6 ms.

Pass 2-3 Data Tape Formats. Both Pass 2 and Pass 3 data outputs have identical data tape record and file formats as shown in Tables 5 and 6. Note that each data file is preceded by a header file describing it. Each patient "data block" consists of seven data files; two mid-inspiration, two mid-expiration, two carotid, and one calibration file.

Data pertaining to a cardiocycle consists of four records: Phono 1, Phono 2, ECG, and Respiration or Carotid. The first three words of each record are the record length, record number and record identification character or the Pass 1 record number respectively.

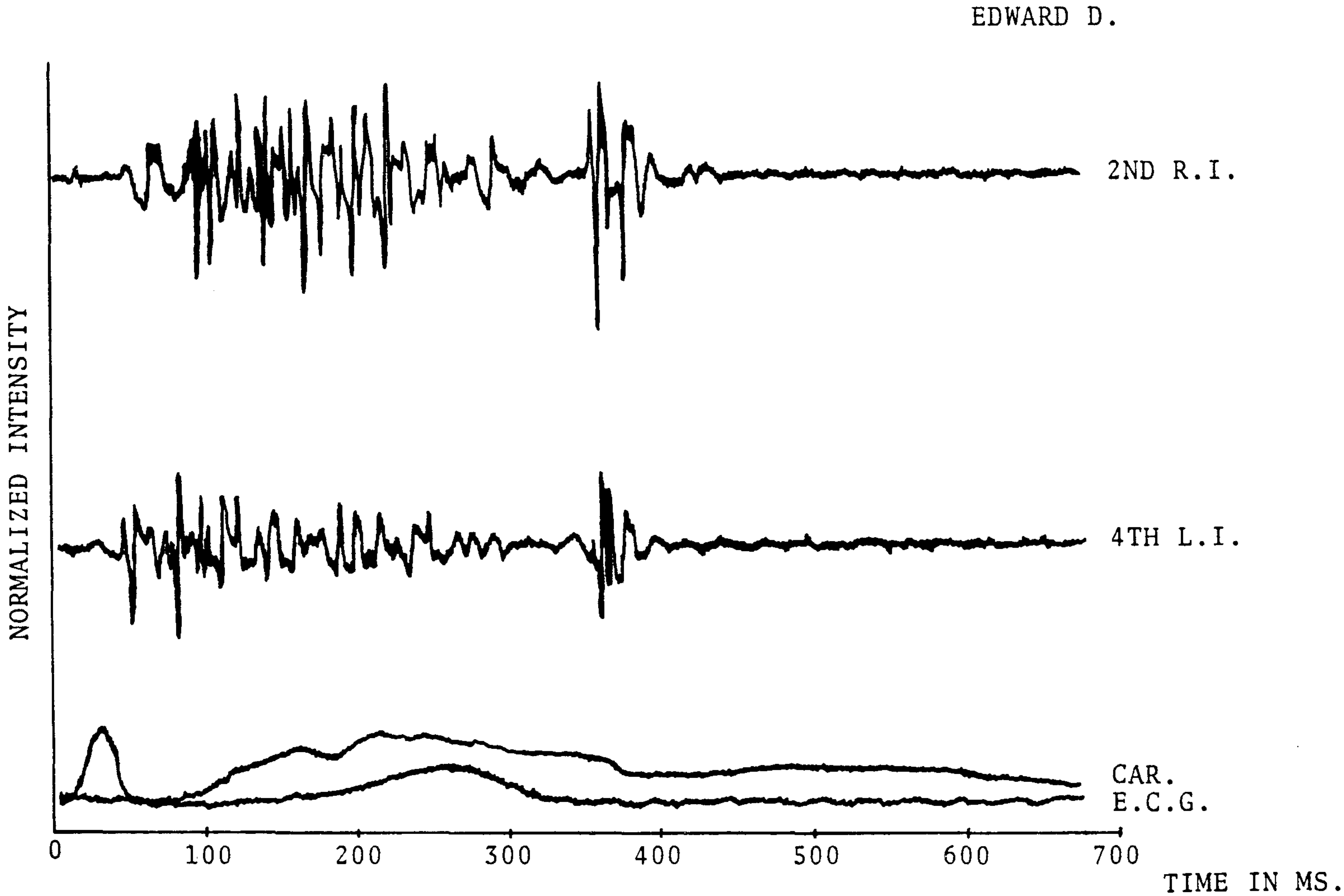

Fig. 13. A typical aligned four-channel cardiocycle record

TABLE 5

PASS 2-3 DIGITAL DATA TAPE RECORD FORMAT

15	6 — 0 BIT No.	
RECORD LENGTH		
PASS 2-3 REC. No.		
PASS 1 REC. No.		
Phono 1 Samp. 1	Phono 1 Samp. 2	Phono 1 Data Rec.
	Phono 1 Last Samp.	
RECORD GAP		
RECORD LENGTH		
PASS 2-3 REC. No.		
Record P	ID. Char. 2	
Phono 2 Samp. 1	Phono 2 Samp.	Phono 2 Data Rec.
	Phono 2 Last Samp.	
RECORD GAP		
RECORD LENGTH		
PASS 2-3 REC. No.		
Record E	ID. Char. C	
ECG Samp. 1	ECG Samp. 4	ECG Data Rec.
	ECG Last Samp.	

One Cadio-cycle (spanning all records above)

TABLE 5--Continued

RECORD GAP

RECORD LENGTH	
PASS 2-3 REC. No.	
Record R	ID. Char. P
Pulse/Resp. Samp. 1	Pulse/Resp. Samp. 4
	Pulse/Resp. Last Samp.

Pulse/Resp. Data Rec.

TABLE 6

PASS 2-3 DIGITAL DATA TAPE FILE FORMAT

File	Gap
ALPHA-NUMERIC PATIENT HEADER	F.G. (FILE GAP)
Phono 1/Phono 2 Tone Cal Binary Data Recs.	F.G.
ALPHA-NUM. HEADER FOR NEXT FILE	F.G.
Phono 1 = 2 L.I. Phono 2 = Apex Pulse = Carotid ECG = Lead 2 Binary Data Recs.	F.G.
ALPHA-NUM. HEADER FOR NEXT FILE	F.G.
Phono 1 = 2 L.I. Phono 2 = Apex Inspiration ECG = Lead 2 Binary Data Recs.	F.G.
ALPHA-NUM. HEADER FOR NEXT FILE	F.G.
Phono 1 = 2 L.I. Phono 2 = Apex Expiration ECG = Lead 2 Binary Data Recs.	F.G.
ALPHA-NUM. HEADER FOR NEXT FILE	F.G.
Phono 1 = 2 R.I. Phono 2 = 4 L.I. Pulse = Carotid ECG = Lead 2 Binary Data Recs.	F.G.

One Patient Data Block

TABLE 6--Continued

ALPHA-NUM. HEADER FOR NEXT FILE	
	F.G.
Phono 1 = 2 R.I. Phono 2 = 4 L.I. Inspiration ECG = Lead 2 Binary Data Recs.	
	F.G.
ALPHA-NUM. HEADER FOR NEXT FILE	
	F.G.
Phono 1 = 2 R.I. Phono 2 = 4 L.I. Expiration ECG = Lead 2 Binary Data Recs.	
	F.G.

CHAPTER IV

SIGNAL PROCESSING TECHNIQUES

In this chapter phonocardiogram signal processing techniques are described in detail. Time and frequency domain sampling is discussed along with the discrete Fourier transform (DFT) and the fast Fourier transform (FFT). A description of a stochastic process and its power spectrum are presented. The final sections of the chapter are devoted to envelope analysis and a description of the Hilbert transform.

TIME DOMAIN SAMPLING

The sampling process can be represented as amplitude modulation of a discrete carrier by a continuous data function [64]. This modulation process is defined by Eq. 1.

$$\overset{*}{s}(t) = s(t)p(t) \qquad \text{Eq. 1}$$

where $\overset{*}{s}(t)$ = sampled data function

$s(t)$ = continuous data function

$p(t)$ = periodic carrier

If p(t) is a finite pulse duration, unit amplitude, periodic pulse sequence, then the process is called "pulse sampling" and Eq. 1 describes a practical sampling process. If p(t) is a periodic sequence of unit delta functions, then the process is called "impulse sampling."

Let p(t) be a finite duration, periodic pulse sequence with

Δt = sampling period

T_p = sampling pulse duration

where p(t) is defined as

$$p(t) = 1 \quad \text{when} \quad |t| \leq \frac{T_p}{2}$$

$$p(t) = 0 \quad \text{when} \quad \frac{T_p}{2} < |t| \leq \frac{\Delta t}{2}$$

Since p(t) is periodic, it can be expanded in the Fourier series as

$$P(t) = \sum_{k=-\infty}^{\infty} c_k \; e^{j\frac{2\Pi kt}{\Delta t}}$$

where c_k's are the Fourier coefficients and $j = \sqrt{-1}$

$$c_k = \frac{1}{\Delta t} \int_{-\frac{T_p}{2}}^{\frac{T_p}{2}} s(t) \; e^{-j\frac{2\Pi kt}{\Delta t}} \, dt$$

$$\text{and } \overset{*}{s}(t) = \sum_{k=-\infty}^{\infty} c_k s(t) \; e^{j\frac{2\Pi kt}{\Delta t}}$$

Using the equations given below and denoting the transformed functions with capital letters, the Fourier transform of $\overset{*}{s}(t)$ is obtained below.

$$\int_{-\infty}^{\infty} \overset{*}{s}(t) \; e^{-j\omega t} dt = \overset{*}{S}(\omega)$$

$$\int_{-\infty}^{\infty} s(t) \; e^{at} e^{-j\omega t} dt = S(\omega - a)$$

$$\overset{*}{S}_p(\omega) = \sum_{k=-\infty}^{\infty} c_k \; S(\omega - k\omega_s) \qquad \text{Eq. 2}$$

where $\omega_s = \frac{2\Pi}{\Delta t}$ = sampling rate

When impulse sampling is used

$$p(t) = \sum_{n=-\infty}^{\infty} \delta(t - n\Delta t)$$

where $\delta(t)$ = unit impulse function.

For this type of sampling the Fourier coefficients in Eq. 2 are

$$c_k = \frac{1}{\Delta t} \quad \text{for all k's}$$

and Eq. 2 reduces to

$$\overset{*}{S}_\delta(\omega) = \frac{1}{\Delta t} \sum_{k=-\infty}^{\infty} S(\omega - k\omega_s) \qquad \text{Eq. 3}$$

The amplitude spectra of $\overset{*}{S}(\omega)$ along with $\overset{*}{s}(t)$ for pulse and impulse sampling are given in Fig. 14. From these amplitude plots and from Eqs. 2 and 3, the following properties can be shown:

1. Sampling in the time domain produces a repetitive spectrum in the frequency domain. When impulse sampling is used, the spectrum becomes a periodic extension of $\frac{1}{\Delta t} S(\omega)$.

2. If $s(t)$ is bandwidth-limited to B (i.e., $S(\omega) = 0$ for $|\omega| \geq B$) and the sampling rate ω_s is $\omega_s \geq 2B$, then $S(\omega)$ can be recovered from $\overset{*}{S}(\omega)$ by low-pass filtering. Consequently, $s(t)$ can be uniquely determined from $\overset{*}{s}(t)$. If $\omega_s < 2B$, then the adjacent "lobes" of $\overset{*}{S}(\omega)$ are overlapping

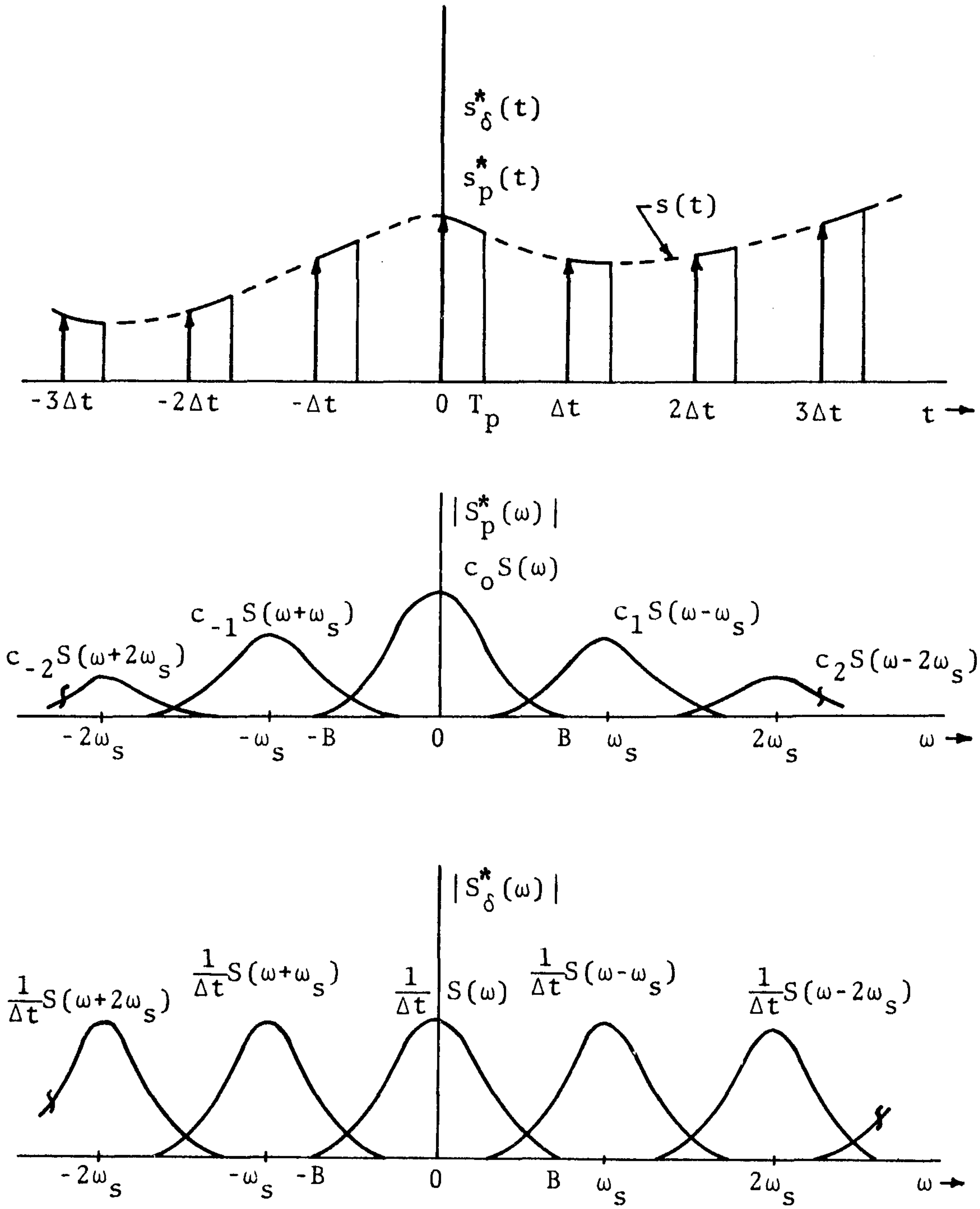

Fig. 14. Pulse and impulse sampling of s(t) and corresponding amplitude spectra

as shown in Fig. 14 and $S(\omega)$ cannot be recovered from $\overset{*}{S}(\omega)$. This latter condition is referred to as "alaising" [76], while statement 2 is referred to as the sampling theorem [64,65,66,71].

Point Sampling. Let $S(\omega)$ be the Fourier transform of a signal $s(t)$, then

$$s(t) = \frac{1}{2\Pi} \int_{-\infty}^{\infty} S(\omega)\ e^{j\omega t} d\omega$$

From the above equation a discrete sequence $\{s_n\}$ is obtained by substituting discrete values for t into $s(t)$. This form of sampling will be referred to as point sampling. It is shown by Cooley et al. [63] that point sampling $s(t)$ produces a periodic Fourier spectrum which is the superposition of the shifted spectra of $S(\omega)$. This periodic property is outlined below.

Point sampling $s(t)$ with a sampling rate of F produces time samples at the intervals of $n\Delta t = \frac{n}{F}$, $n = 0, \underline{+}1, \underline{+}2, \ldots$, where

$$s(n\Delta t) = \frac{1}{2\Pi} \int_{-\infty}^{\infty} S(\omega)\ e^{j\frac{\omega n}{F}}\ d\omega$$

Recalling that $e^{j\frac{\omega n}{F}}$ is a periodic function of ω with a period $2\pi F$, the above equation is rewritten as

$$s(n\Delta t) = \frac{1}{2\Pi} \sum_{k=-\infty}^{\infty} \int_{k2\Pi F}^{(k+1)2\Pi F} S(\omega)\ e^{j\frac{\omega n}{F}}\ d\omega$$

Assuming well behaved functions and making the substitution $\omega = u + 2\Pi kF$ (recalling that $e^{j2\Pi kn} = 1$ for all integers k and n), then the above equation is expressed as

$$s(n\Delta t) = \frac{1}{2\Pi} \int_0^{2\Pi F} S_p(\omega) e^{j\frac{\omega n}{F}} d\omega \qquad \text{Eq. 4}$$

$$\text{where } S_p(\omega) = \sum_{k=-\infty}^{\infty} S(\omega + k2\Pi F) \qquad \text{Eq. 5}$$

and u is replaced by ω.

Comparison of Eqs. 3 and 5 reveals that impulse and point sampling are identical within a constant of $\frac{1}{\Delta t}$. Additionally, if the signal s(t) is bandwidth-limited to B (i.e., $S(\omega) = 0$ for $|\omega| \geq B$) and if the sampling rate $F \geq \frac{2B}{2\pi}$, then the periodic function $S_p(\omega)$ is an unaliased (nonoverlapping) extension of $S(\omega)$ [63,66]. Since $S_p(\omega)$ is a periodic function of ω with period $2\pi F$, it can be represented by Fourier series as

$$S_p(\omega) = \sum_{n=-\infty}^{\infty} A_n e^{-j\frac{\omega n}{F}} \qquad \text{Eq. 6}$$

$$\text{where } A_n = \frac{1}{2\Pi F} \int_0^{2\Pi F} S_p(\omega)\, e^{j\frac{\omega n}{F}} d\omega$$

Comparing Eq. 4 with the Eq. above reveals that the Fourier coefficients A_n's can be expressed in terms of the sample values as

$$A_n = \frac{s(n\Delta t)}{F}$$

Substituting these Fourier coefficients into Eq. 6 we obtain

$$S_p(\omega) = \frac{1}{F} \sum_{n=-\infty}^{\infty} s(n\Delta t)\, e^{-j\frac{\omega n}{F}} \qquad \text{Eq. 7}$$

It is clear from the above that the periodic function $S_p(\omega)$ is completely defined by the sample points $s(n\Delta t)$.

FREQUENCY DOMAIN SAMPLING

Let s(t) be a signal waveform defined on the interval of $|t| < T/2$ and zero for $|t| > T/2$, where T is the record length. The Fourier transform of this signal is defined below.

$$S(\omega) = \int_{-T/2}^{T/2} s(t)\ e^{-j\omega t}\ dt \qquad \text{Eq. 8}$$

Expanding s(t) in Fourier series on the interval of -T/2 to T/2, we obtain a periodic function $s_p(t)$ given by

$$s_p(t) = \sum_{k=-\infty}^{\infty} c_k\ e^{j\frac{2\Pi kt}{T}} \qquad \text{Eq. 9}$$

$$\text{where } c_k = \frac{1}{T} \int_{-T/2}^{T/2} s(t)\ e^{-j\frac{2\Pi kt}{T}}\ dt \qquad \text{Eq. 10}$$

and comparing Eqs. 8 and 10, we obtain

$$c_k = \frac{S(\frac{2\Pi k}{T})}{T} \qquad \text{Eq. 11}$$

Note that the Fourier coefficients c_k's are determined from the sample values of $S(\omega)$ and consequently, define the periodic function $s_p(t)$. The above result can be restated as point sampling of $S(\omega)$ at $\frac{2\Pi k}{T}$ angular frequency intervals corresponding to a periodic extension of s(t) in the time domain [60,63,66,77] as shown in Fig. 15.

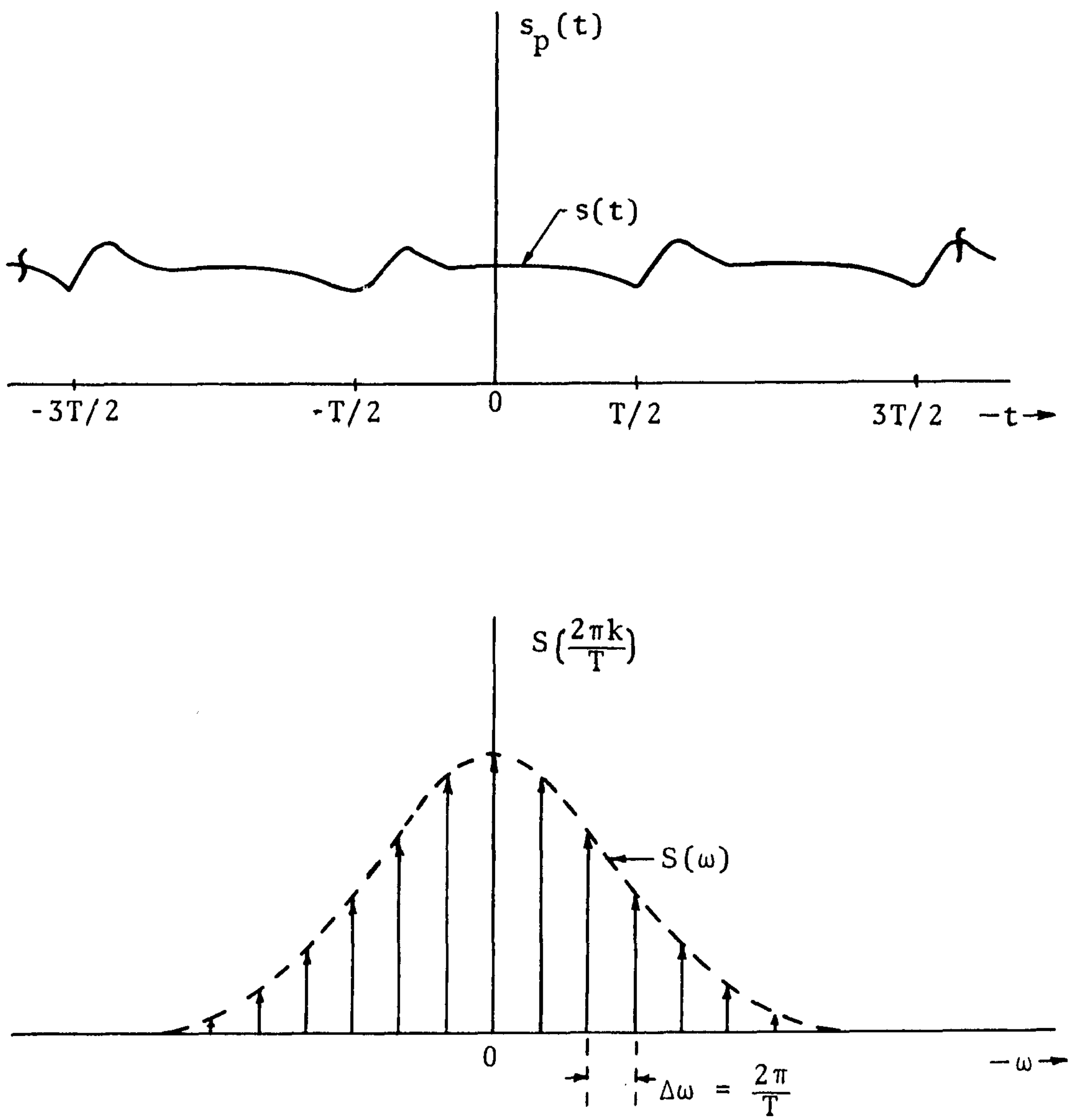

Fig. 15. A sampled amplitude spectrum and the corresponding periodically extended s(t)

DISCRETE FOURIER TRANSFORM

To compute Fourier transforms with a digital computer, one must consider a finite number of discrete samples in the time as well as in the frequency domain.

Suppose that a finite-duration, bandwidth-limited function $g(t)$ can be represented by a sequence of N equally-spaced samples in the time domain. The sequence is denoted by $\{g(n\Delta t)\}$ where

$$n = \text{time sample index and}$$
$$\Delta t = \text{sample time interval.}$$

Similarly, let $G(\omega)$ (Fourier transform of $g(t)$) be represented by a sequence of N equally-spaced samples in the frequency domain where the sequence is denoted by $\{G(k\Omega)\}$ and

$$k = \text{frequency sample index and}$$
$$\Omega = \frac{2\Pi}{N\Delta t} = \text{sample frequency interval.}$$

Consistent with the above discussion, the discrete Fourier transform (DFT) of the sequence $\{g(n\Delta t)\}$ is defined as the sequence $\{G(k\Omega)\}$, where each component of $\{G(k\Omega)\}$ is computed from Eq. 12 [58,60].

$$G(k\Omega) = \frac{1}{N} \sum_{n=0}^{N-1} g(n\Delta t)\ e^{-j\Omega\Delta t n k} \qquad \text{Eq. 12}$$

The original time sequence $\{g(n\Delta t)\}$ can be recovered by the inverse discrete Fourier transform (IDFT) where each component of $\{g(n\Delta t)\}$ is computed from Eq. 13.

$$g(n\Delta t) = \sum_{k=0}^{N-1} G(k\Omega)\, e^{j\Omega\Delta tnk} \qquad \text{Eq. 13}$$

The discrete Fourier transform pair is often referred to as the finite Fourier transform pair and within a constant, is equal to the sampled version of the periodically-extended continuous functions g(t) and G(ω) [58,60,61,62,63,75]. The periodic property of the DFT is a clear consequence of time and frequency domain sampling. Derivation of the DFT from the continuous Fourier transform is outlined below.

Consider a finite-duration and bandwidth-limited signal s(t), where s(t) = 0 for $|t| \geq T/2$ and its Fourier transform S(ω) = 0 for $|\omega| \geq B$. Point sampling of s(t) with a sampling rate $\omega_s \geq 2B$ produces a finite, discrete sequence in the time domain and an unaliased, continuous periodic extension of S(ω) in the frequency domain [58,60,61,63] as described in the previous section. This periodic function $S_p(\omega)$ is defined by Eq. 7. If we point sample $S_p(\omega)$ by replacing ω with kΩ, Eq. 7 can be expressed as

$$S_p(k\Omega) = \frac{T}{N} \sum_{n=-\infty}^{\infty} s(n\Delta t)\, e^{-j\frac{2\Pi nk}{N}} \qquad \text{Eq. 14}$$

where $N = \frac{T}{\Delta t}$ = number of sample points per record length T. Note that time and frequency sampling yields N term periodic discrete sequences in the frequency, as well as in the time domain, as shown in Figs. 14 and 15 [58,60,61,63]. We can express Eq. 14 as a finite sum by recognizing that s(nΔt) and $e^{-j2\Pi nk/N}$ are periodic in n with period N where any arbitrary integer n can be expressed as

$$n = rN + n_o$$

where r = integer and

n_o = n modulo N.

$$S_p(k\Omega) = T\left(\frac{1}{N}\sum_{n=0}^{N-1} s_p(n\Delta t)\, e^{-j\frac{2\Pi nk}{N}}\right) \qquad \text{Eq. 15}$$

$$\text{where } s_p(n\Delta t) = \sum_{\ell=-\infty}^{\infty} s(n\Delta t + \ell T) \qquad \text{Eq. 16}$$

The righthand side of Eq. 15 is the record length T times the DFT of the signal s(t), while the lefthand side is the point sampled and periodically-extended $S(\omega)$.

The Fast Fourier Transform (FFT). The fast Fourier transform (FFT) introduced by Cooley and Tukey [59,63] is an efficient computational algorithm used to compute discrete Fourier transform pairs. A brief examination of Eqs. 12 and 13 reveals that for a complex sequence, N^2 complex operations (multiplications and additions) are required to compute the DFT or IDFT from the definitions. In comparison, the FFT algorithm requires approximately $\frac{3N}{2}\log_2 N$ complex operations and at N = 1024, it offers a factor of approximately 200 computational savings [60,62,63]. Using Cooley and Tukey's notation, the FFT algorithm used to compute IDFT involves evaluating the complex sum given below.

$$X(n) = \sum_{k=0}^{N-1} A(k)Q^{kn} \qquad \text{Eq. 17}$$

$$\text{for } n = 0, 1, \ldots, N-1 \text{ and } Q = e^{j\frac{2\Pi}{N}}$$

Note that the DFT defined by Eq. 12 can be expressed as

$$S(k\Omega) = \frac{1}{N} \left[\sum_{n=0}^{N-1} \overset{*}{s}(n\Delta t)Q^{kn} \right]^* \qquad \text{Eq. 18}$$

where * denotes conjugation. A comparison of Eqs. 17 and 18 reveals that they differ only by a constant and by conjugations; therefore, the same algorithm can be used to compute forward as well as inverse DFT's.

When the sequence length N is equal to the powers of 2, for example N = 8, then it is convenient to represent both n and k as a binary number; that is, for n = 0, 1, ..., 7 and k = 0, 1, ..., 7 we can write

$$n = 4n_2 + 2n_1 + n_o$$

$$k = 4k_2 + 2k_1 + k_o$$

where n_o, n_1, n_2, k_o, k_1 and k_2 can take on values of 0 or 1 only. Substituting their values into Eq. 17 and omitting Δt and Ω for notational clarity, we may obtain

$$X(n_2,n_1,n_o) = \sum_{k_o=0}^{1} \sum_{k_1=0}^{1} \sum_{k_2=0}^{1} A(k_2,k_1,k_o)\, Q_T$$

where

$$Q_T = Q^{(4n_2+2n_1+n_o)(4k_2+2k_1+k_o)}$$

Completing the products of exponents and noting that $Q^{k+n} = Q^k \cdot Q_n$, it is apparent that some of the product terms reduce to unity by the periodic property of the exponential function (i.e., $Q^{m8} = 1$ where m is an integer). This leads to

$$X(n_2,n_1,n_o) = \sum_{k_o=0}^{1} \sum_{k_1=0}^{1} \sum_{k_2=0}^{1} A(k_2,k_1,k_o) Q^{y_2} Q^{y_1} Q^{y_o} \qquad \text{Eq. 19}$$

$A_1(n_o,k_1,k_o)$ 1st stage

$A_2(n_o,n_1,k_o)$ 2nd stage

$A_3(n_o,n_1,n_2)$ 3rd stage

reorder

$X(n_2,n_1,n_o)$

where $y_2 = 4n_ok_2$ $y_1 = 2k_1(2n_1+n_o)$ $y_o = k_o(4n_2+2n_1+n_o)$

Note that the computation of $x(n_2,n_1,n_o)$ involves successive computation of A_1, A_2 and A_3, each containing 8 complex terms where the last step is a simple reordering operation. It is clear that each new complex term to be computed requires only the previous set of terms; consequently, the same storage area can be shared in computations of stages. The FFT formula, Eq. 19, shows 48 complex computations; however, note that the first multiplication in each sum involves multiplication by +1 and $Q^o = -Q^4$, $Q^1 = -Q^5$, etc. When each of these time saving steps is accounted for, the number of operations is reduced to $\frac{3}{2}$ $N\log_2 N$ complex operations.

A 1024 complex number FFT program (DAS FFT), using the computational steps outlined above, is given in Appendix I. This program was developed by E. Nichols, M. Stern and the author and is written in the Varian 620/I assembly language.

DESCRIPTION OF A STOCHASTIC PROCESS

In the following analysis the phonocardiogram murmur signals obtained over a short time duration are approximated as a finite stationary stochastic process. This approximation is particularly reasonable for a "flat" envelope murmur and for ejection murmurs where the ensemble elements are composed of short records centered about the peak intensity of the murmur.

Definition of a Stochastic Process. When a random time series data record is analyzed, it can be regarded as one of the many data records which may have occurred. Representation of such a process is accomplished by associating with each point of time t in the range of $(-\infty \leq t \leq \infty)$, a random variable $X(t)$ which has a sample space $\{-\infty \leq X(t) \leq \infty\}$ and a corresponding probability density function (pdf), $f(x)$. Consequently, a time series can be described as an ordered set of random variables $\{X(t)\}$ defined on $(-\infty \leq t \leq \infty)$ for a continuous time series and an ordered set of random variables $\{X_t\}$, $t = 0, 1, 2, \ldots$, for a discrete time series.

The ordered set of random variables is called a stochastic process [67,68,70] and provides a probabilistic description of the physical process as it changes with time. The double infinite set of time functions defined on this sample space is called an ensemble [67].

Moments of a Stochastic Process. At any point in time we can define the univariant moments of a stochastic process by

$$E[(X(t))^k] = \int_{-\infty}^{\infty} x^k f(x)dx \qquad \text{Eq. 20}$$

and the bivariant moments by

$$E\{(X(t_1))^k(X(t_2))^n\} = \int_{-\infty}^{\infty}\int_{-\infty}^{\infty} x_1^k x_2^n f(x_1,x_2)dx_1dx_2 \qquad \text{Eq. 21}$$

where $f(x)$ = probability density function at time t

$f(x_1,x_2)$ = joint probability density function at time t_1,t_2

The most important univariant moments are the mean function $E[X(t)]$ and the second central moment, or variance function $Var[X(t)]$. These moments are defined by the equations given below.

$$E[X(t)] = \eta(t) = \int_{-\infty}^{\infty} x\ f(x)dx \qquad \text{Eq. 22}$$

$$Var[X(t)] = \sigma^2(t) = \int_{-\infty}^{\infty} (x-\eta(t))^2 f(x)dx \qquad \text{Eq. 23}$$

In addition we may define the autocorrelation function (acf), $R(t_1,t_2)$ and the autocovariance function (acvf), $C(t_1,t_2)$ by

$$R(t_1,t_2) = E[X(t_1)X(t_2)] = \int_{-\infty}^{\infty} x_1x_2f(x_1,x_2)dx_1dx_2 \qquad \text{Eq. 24}$$

$$C(t_1,t_2) = E[(X(t_1)-\eta(t_1))(X(t_2)-\eta(t_2))] \qquad \text{Eq. 25}$$

where $\eta(t_i)$ = the mean of $X(t_i)$ at time t_i.

A Stationary Stochastic Process. In general, the properties of a stochastic process are time dependent. The assumption is often made that the process has reached a steady equilibrium in the sense that the statistical properties of the series are independent of absolute time. In this case the process is called stationary or strictly stationary [67,68,70]. The minimum requirement for this to hold is that the pdf, $f(x)$ and the joint pdf of the process, $f(x_1,x_2,...,x_n)$ be independent of absolute time. The clear consequences of the stationary requirement are that the mean $E[X]$ and the variance $Var[X]$ are constant, and in addition, the autocorrelation and covariance functions are independent of absolute time and are functions of the lag variable $\tau = t_1 - t_2$.

POWER SPECTRUM ANALYSIS

In this section power spectrum analysis is introduced to study the power distribution of abnormal phonocardiograms as the function of frequency. Later, in

Chapter V the signal features of the murmur power spectrum are examined and correlated to the severity of valvar aortic stenosis.

The Power Spectral Density of a Deterministic Signal. The true power spectral density B(f) of a continuous deterministic signal s(t) is defined by

$$B(f) = \lim_{T \to \infty} B_i(f) \qquad \text{Eq. 26}$$

where $B_i(f)$ = power spectral density estimate

and is derived from the Fourier transform of a signal of T seconds duration by the equation given below.

$$B_i(f) = \frac{1}{T} |S_i(f)|^2 \qquad \text{Eq. 27}$$

For a deterministic signal, as the record length T approaches infinity, $B_i(f)$ converges "smoothly" to the theoretical spectrum B(f) in the sense that for all values of f, the error $B(f) - B_i(f)$ approaches zero as T approaches infinity [67]. It is shown by Papoulis, Jenkins and Watts; Davenport and Root [66,67,68], that for the power spectral density of a stochastic signal, the above definition cannot be applied. The basic difference between the Fourier analysis of a stochastic signal and a deterministic signal is that for the former, the variance of $B_i(f)$ does not approach zero as the record length T approaches infinity. Consequently, $B_i(f)$ does not approach smoothly to B(f) with increasing record length.

Power Spectral Density of a Stochastic Process.

More general definitions for the true power spectral density are given below and apply to deterministic as well as to stationary stochastic processes. The power spectral density B(f) can be defined from the autocorrelation function $R(\tau)$ as

$$B(f) = \int_{-\infty}^{\infty} R(\tau)\, e^{-j2\Pi f\tau}\, d\tau \qquad \text{Eq. 28}$$

If the sample functions of the process are real, then the autocorrelation function $R(\tau)$ is real and is an even function of τ; consequently, B(f) is real and is an even function of f. Since B(f) and $R(\tau)$ are Fourier transform pairs, we gain an insight to B(f) by examining the equation given below at $\tau = 0$.

$$E[s(t+\tau)s(t)] = R(\tau) = \int_{-\infty}^{\infty} B(f)e^{j\omega\tau}\, df \qquad \text{Eq. 29}$$

$$R(0) = E[s^2(t)] = \text{Var}\,[s(t)] + (E[s(t)])^2 = \int_{-\infty}^{\infty} B(f)df \qquad \text{Eq. 30}$$

It is clear from Eq. 30 that B(f) is a positive real-valued function which describes how the total signal power is distributed in frequency.

It is shown by Papoulis [66,70] that the true power spectral density B(f) of a stationary random process can be alternatively defined by the equation given below.

$$B(f) = \lim_{T\to\infty} E[B_i(f)] \qquad \text{Eq. 31}$$

where ensemble averaging of the power spectral density estimates is required to reduce spectrum variance.

Prior to development of the FFT algorithm, power spectral density estimates were most often computed from the autocorrelation function using Eq. 28 since it was the fastest method available. With the advent of the FFT algorithm, the second expression, given by Eq. 31, is now most often used. This method is the faster of the two and therefore was employed to compute power spectral density estimates in this study.

<u>The Discrete Power Spectral Density Estimate</u>. To take advantage of the computational speed of the digital computer and the FFT algorithm, the discrete power spectral density function, $B_i(k\Delta f)$ is defined by replacing f by $k\Delta f$ in Eq. 27 giving

$$B_i(k\Delta f) = \frac{1}{T} |S_i(k\Delta f)|^2 \qquad \text{Eq. 32}$$

Using Eq. 15 to compute $S_i(k\Delta f)$, the above equation is written for $0 \leq k \leq \frac{N}{2}-1$ as

$$B_i(k\Delta f) = T \left| \frac{1}{N} \sum_{n=0}^{N-1} s(n\Delta t)\ e^{-j\frac{2\Pi nk}{N}} \right|^2 \qquad \text{Eq. 33}$$

$$B_i(k\Delta f) = \frac{\Delta t}{N} [R_{eal}^2(k\Delta f) + I_m^2(k\Delta f)]$$

where $R_{eal}(k\Delta f)$ and $I_m(k\Delta f)$ are the real and imaginary components of $B_i(k\Delta f)$. Note that $B_i(k\Delta f)$ is an even function of f; therefore, Eq. 33 also provides values for negative frequency components.

It is shown by Jenkins and Watts [67] that for a white Gaussian random signal with zero mean, $B_i(k\Delta f)$ is chi-square distributed. The mean $E[B_i(f_k)]$ and variance $Var[B_i(f_k)]$ of $B_i(k\Delta f)$ are given in terms of the variance of the signal Var[s] as

$$E[B_i(f_k)] = (\Delta t)Var[s] = B(k\Delta f) \qquad \text{Eq. 34}$$

$$Var[B_i(f_k)] = \{(\Delta t)Var[s]\}^2 = B^2(k\Delta f) \qquad \text{Eq. 35}$$

It is clear from the above that $E[B_i(f_k)]$ and $Var[B_i(f_k)]$ are independent of record length T and consequently a $B_i(f_k)$ estimate will not converge to the theoretical power spectral density with increasing record length. It is important to note that even if the signal is not Normally distributed, the random variables $R_{eal}(k\Delta f)$ and $I_m(k\Delta f)$ for $N > 30$ computed from the DFT have nearly a Normal distribution as can be shown by the central limit theorem. Therefore, the distribution of $B_i(k\Delta f)$ will be very nearly chi-square.

Bartlett's Smoothing Procedure. The variance of spectral estimates can be reduced by spectral smoothing. One of the first smoothing procedures was introduced by Bartlett [81]. The procedure involves splitting up the random time series into m sub-series where each has a record length M. The spectral estimate for each sub-series is computed, and an averaged spectrum for $0 \le k \le \frac{N}{2}-1$ is calculated according to the equation given below.

$$\bar{B}(k\Delta f) = \frac{1}{m} \sum_{i=1}^{m} B_i(k\Delta f) \qquad \text{Eq. 36}$$

When the signal s(t) is white noise, the sub-series are independent and the mean $E[\bar{B}(f_k)]$ and variance $Var[\bar{B}(f_k)]$ of $\bar{B}(k\Delta f)$ are defined by the sample statistics [67,79]. If the sample size m is greater than 30, then the sampling distribution is asymptotically normal [79] and the mean and variance of $\bar{B}(f_k)$ are related to the mean and variance of $B_i(f_k)$ by equations given below.

$$E[\bar{B}(f_k)] = E[B_i(f_k)]$$

and

$$Var[\bar{B}(f_k)] = \frac{Var[B_i(f_k)]}{m}$$

From the above it can be concluded that the $Var[\bar{B}(f_k)]$ is inversely proportional to the number of sub-series (records) averaged, m, while the relative error, defined below, is inversely proportional to $\sqrt{m}$.

$$\frac{\sqrt{Var[\bar{B}(f_k)]}}{E[\bar{B}(f_k)]} = \frac{1}{\sqrt{m}} \qquad \text{Eq. 37}$$

Clearly, this smoothing procedure can be applied to non-sequential but independent random records such as phonocardiogram murmur signals.

Bartlett's Spectral Window. The Bartlett smoothing procedure outlined in the previous section now will be re-examined and its effect on spectral resolution and bias will be described.

Since the Fourier transform is a linear operation, the smoothed estimate $\bar{B}(f)$ can be expressed in terms of the averaged autocorrelation function $\bar{R}(\tau)$ as

$$\overline{B}(f) = \int_{-M}^{M} \overline{R}(\tau)\, e^{-j2\Pi f\tau}\, d\tau \qquad \text{Eq. 38}$$

For the i^{th} sub-series we may find the autocorrelation estimate for $\tau \geq 0$ by

$$R_i(\tau) = \frac{1}{M} \int_{(i-1)M}^{iM-\tau} s(t)s(t+\tau)dt \qquad \text{Eq. 39}$$

$$\text{where } \overline{R}(\tau) = \frac{1}{m} \sum_{i=1}^{m} R_i(\tau)$$

It is shown by Jenkins and Watts, and Richards [67,71] that $\overline{R}(\tau)$ is given by

$$\overline{R}(\tau) = \frac{T-m|\tau|}{T-|\tau|} \left(\frac{1}{T}\right) \int_{0}^{T-|\tau|} s(t)s(t+\tau)dt \qquad \text{Eq. 40}$$

$$\text{where } \overline{R}(\tau) = 0 \text{ for } |\tau| > M.$$

Examination of Eq. 40 reveals that the segmented averaging described earlier is statistically equivalent to multiplying the original autocorrelation function by a "window" function $w(\tau)$ where

$$w(\tau) = \frac{T-m|\tau|}{T-|\tau|} \qquad \text{when } |\tau| \leq M$$

$$w(\tau) = 0 \qquad \text{when } |\tau| > M$$

When M << T, then the denominator of $w(\tau)$ is approximately equal to T. The corresponding window (Bartlett lag window) is given below.

$$w_B(\tau) = T - \frac{|\tau|}{M} \quad \text{when } |\tau| \leq M$$

$$w_B(\tau) = 0 \quad \text{when } |\tau| > M \qquad \text{Eq. 41}$$

Substituting the windowed autocorrelation function into Eq. 38 and assuming that the number of segments m approaches infinity, we obtain the smoothed spectrum estimate as

$$\overline{B}(f) = \int_{-\infty}^{\infty} w_B(\tau)R(\tau)\ e^{-j2\Pi f\tau}\ d\tau \qquad \text{Eq. 42}$$

Recalling that the product in the lag domain is convolution (denoted by *) in the frequency domain, the above equation can be expressed as

$$\overline{B}(f) = W_B(f)*B(f) = \int_{-\infty}^{\infty} W_B(x)B(f-x)dx \qquad \text{Eq. 43}$$

and the corresponding Bartlett spectral window is given below.

$$W_B(f) = M\left(\frac{\sin(\Pi fM)}{\Pi fM}\right)^2 \qquad \text{Eq. 44}$$

It is clear from Eq. 43 that the estimate $\overline{B}(f)$ is a biased estimator of the true spectral density B(f), where the bias $B_{ias}(f)$ is defined below.

$$B_{ias}(f) = \overline{B}(f) - B(f) \qquad \text{Eq. 45}$$

For an arbitrary spectrum containing spectral peaks, the bias will be zero only if the window width M approaches infinity.

It has been shown in the previous section that for a random signal with finite record length T, the spectrum variance is reduced by decreasing the sub-series length M. However, for the Bartlett window $W_B(f)$, the first zero crossing occurs at 1/M and a small M implies smoothing over a wider range of frequencies. Consequently, with this estimation, one is forced to compromise between variance reduction and spectrum bias.

Several windows are commonly used in power spectrum spectroscopy, most often these are the Bartlett, Tukey, or Parzen windows [67,69,72,74]. These offer various degrees of compromise between bias and variance. However, all the windows must satisfy the following conditions [67] in the lag domain.

1. $w(0) = 1$
2. $w(\tau) = w(-\tau)$
3. $w(\tau) = 0$ for $|\tau| > M$

The Bartlett window is used in this study because it offers computational simplicity and good reduction of variance at a moderate bias.

Variance of Smoothed Spectral Estimators. To investigate the statistical error of a smoothed spectral estimator $\overline{B}(f)$, the variance of this function is defined below. It is shown by Jenkins and Watts [67], that for any bandwidth-limited, normal stochastic signal s(t), the variance of $B_i(f)$ is

$$Var[B_i(f)] \approx B^2(f) \qquad \text{Eq. 46}$$

Similarly, for a smoothed spectral estimator $\overline{B}(f)$ (used to estimate B(f)) the mean and variance are

$$E[\overline{B}(f)] \approx B(f) \qquad \text{Eq. 47}$$

$$Var[\overline{B}(f)] \approx \frac{B^2(f)}{T} \int_{-\infty}^{\infty} w^2(\tau)d\tau = \frac{B^2(f)I}{T} \qquad \text{Eq. 48}$$

For the Bartlett window

$$I = \int_{-M}^{M} (1-\frac{|\tau|}{M})^2 d\tau = \frac{2}{3} M \qquad \text{Eq. 49}$$

and consequently,

$$Var[\overline{B}(f)] \approx \frac{B^2(f)}{T} (\frac{2}{3} M) \qquad \text{Eq. 50}$$

We may define a reduction factor

$$\frac{I}{T} = \frac{Var[\overline{B}(f)]}{B^2(f)}$$

which compares the variance of a smoothed spectrum versus the variance of the estimate. For the Bartlett window this ratio is expressed as

$$\frac{I}{T} = .667 \ (\frac{M}{T}) \qquad \text{Eq. 51}$$

<u>Confidence Interval for the Smoothed Spectrum</u>. When $\overline{B}(f)$ is computed from a finite number of phonocardiogram records, the precise value of B(f) cannot be predicted. However, for this case it is possible to define a confidence

region where B(f) is found with a specified probability or confidence level. It is shown by Jenkins and Watts [67] that for a smoothed spectrum, the probability density distribution function of $\overline{B}(f)$ can be approximated by $a\chi^2$ where

$$\chi^2 = \text{chi-square distribution}$$

$$a \approx \frac{E[\overline{B}(f)]}{v}$$

$$\text{and} \quad v \approx \frac{2(E[\overline{B}(f)])^2}{Var[\overline{B}(f)]} = \text{degree of freedom}$$

Substituting from the previous section for the mean and variance of the Bartlett window (Eqs. 47 and 50), $v = 3\,\frac{T}{M}$. Knowing that the distribution is chi-square, the confidence interval for B(f) at each value of $\overline{B}(f)$ is obtained from the probabilistic equation given below.

$$Pr\{\chi_L < B(f) \leq \chi_H\} = 1 - \alpha$$

The percent confidence level is $100(1-\alpha)$ for the limits given below.

$$\chi_L = \frac{v\ \overline{B}(f)}{x(1-\frac{\alpha}{2})}$$

$$\chi_H = \frac{v\ \overline{B}(f)}{x\ \frac{\alpha}{2}}$$

For a given confidence level, the confidence limits are usually evaluated from chi-square tables or charts [67,79]. As the degree of freedom approaches infinity, the chi-square distribution approaches the Normal distribution. Consequently, for v > 30, the confidence limits can be closely approximated from the Normal distribution and the spectrum is estimated with a desired confidence level by the equation below.

$$B(f) = \overline{B}(f) \pm z\sqrt{Var[\overline{B}(f)]} \qquad \text{Eq. 52}$$

In the above equation z is a confidence parameter; for 99.73% confidence level, z = 3.00, for a 95% confidence level, z = 1.96, and for a 68.27% confidence level, z = 1. For the Bartlett window, Eq. 52 can be expressed as

$$B(f) \approx \overline{B}(f)(1 \pm z \frac{\sqrt{\frac{2}{3}}}{\sqrt{m}}) \qquad \text{Eq. 53}$$

where m is the number of sub-intervals or records averaged.

<u>Bandwidth of a Spectral Window</u>. It has been shown in the previous sections that the variance, bias and resolution of $\overline{B}(f)$ is determined by the shape and width of the spectral window W(f). In this section the equivalent bandwidth of a spectral window is defined which determines the above-mentioned properties of the spectrum. Consider a rectangular spectral window with a bandwidth h defined by the equation given below.

$$W_R(f) = \frac{1}{h} \quad \text{for } -\frac{h}{2} \leq f \leq \frac{h}{2}$$

The total AC power or variance within this window is given below.

$$Var[\overline{B}(f)] \approx \frac{B^2(f)}{T} \cdot \frac{1}{h}$$

For a nonrectangular spectral window, we define its bandwidth b as the width of a rectangular window which gives the same variance or AC power [67].

$$\mathrm{Var}[\overline{B}(f)] \approx \frac{B^2(f)}{T} \cdot \frac{1}{\overline{b}} = \frac{B^2(f)}{T} \int_{-\infty}^{\infty} w^2(\tau)\,d\tau$$

This definition is sometimes referred to as equivalent bandwidth and spectrum smoothing occurs within it. Consistent with the above discussion, the bandwidth of an arbitrary window is defined [67] as

$$b = \frac{1}{\int_{\infty}^{\infty} w^2(\tau)\,d\tau} = \frac{1}{\int_{-\infty}^{\infty} W^2(f)\,df} = \frac{1}{I} \qquad \text{Eq. 54}$$

and the bandwidth for the Bartlett spectral window is given below.

$$b_B = \frac{3}{2M} \qquad \text{Eq. 55}$$

<u>Summary of Bartlett Window Properties</u>. The essential properties of the Bartlett window described in this section are summarized in the table below.

TABLE 7

SUMMARY OF BARTLETT WINDOW PROPERTIES

Spectral Window $W(f)$	Variance Ratio I/T	Degree of Freedom	Bandwidth
$M\left(\frac{\sin(\Pi fM)}{\Pi fM}\right)^2$	$\frac{2}{3}\frac{M}{T}$	$3\frac{T}{M}$	$\frac{3}{2M}$

<u>Computation of the Discrete Power Spectral Estimate</u>. A discrete power spectral function is defined below in order to study the power distribution of a phonocardiogram signal as a function of frequency. More specifically, the discrete power spectral estimate $P_i(k\Delta f)$ of a signal for $0 \leq k \leq (\frac{N}{2}-1)$ is defined as

$$P_i(k\Delta f) = \frac{B_i(k\Delta f)}{T} \qquad \text{Eq. 56}$$

Note that $B_i(k\Delta f)$ is a power density function while $P_i(k\Delta f)$ is a power function and each harmonic term $k\Delta f$ represents the signal power in a bandwidth $\frac{1}{T}$ centered at $k\Delta f$. With this definition, the power spectrum is merely the square of the magnitude of the discrete Fourier spectrum as defined by Eq. 12 and the total signal power is computed from the equation given below.

$$P_s = \sum_{k=-\frac{N}{2}+1}^{\frac{N}{2}-1} P_i(k\Delta f) \qquad \text{Eq. 57}$$

The power spectral estimate of a phonocardiogram signal is computed here by using the steps outlined below.

1. Select the required signal in the time domain using the rectangular Bartlett data window.
2. Remove the DC bias introduced by the analog-to-digital converter.
3. Divide each signal amplitude by the rms value of the calibration signal. This normalization step removes microphone and other gain setting errors.
4. Compute the complex DFT spectrum as defined by Eq. 12 using an $N = 1024$ fixed length FFT algorithm. When the time series record length is < 1024, the additional buffer values are set equal to zero. The effect of lengthening the time sequence by extra zeros is merely interpolation in the frequency domain [58].
5. Compute the single-sided $(0 \leq k \leq 511)$ power spectral estimate as prescribed by Eq. 56. That is, for each harmonic interger k, find the sum of the squared real and squared imaginary components of the DFT spectrum.

The power spectral estimates were computed either interactively using the program "AUTOFREQ" or in batch mode using the subroutine FANAL. The programs, along with their descriptions, are given in Appendix I. A typical V.A.S.

murmur power spectral estimate smoothed by a 100 ms. Bartlett window is shown in Fig. 16. Explanations of the plot labels are given in the next section, while the analysis and interpretations of the spectrum are given in Chapter V.

Explanations of the Plot Labels. An explanation of the plot labels is as follows: the first and second lines contain the patient's first name, identification number, respiration phase, and microphone location. The respiration phases are inspiration, expiration, and minspiration (mixed inspiration and expiration). On the third line, T is the plotting time interval measured in ms. from the Q wave of the ECG signal. On the fifth line, N is the number of records averaged and R is the last record number acquired for analysis. The remaining letters describe the channel number, type of analysis performed (TIM. = time, PWS = power spectrum, ENV. = envelogram), and the analysis sampling rate (DEF. = 2.5 KHz, SUM. = 1.25 KHz). The vertical scales are normalized intensity scales. Prior to computations, the PCG records are amplitude-normalized by the rms value of the appropriate calibration records. This step removes microphone and other gain setting errors, allowing direct data comparison among patients.

ENVELOPE ANALYSIS

In this section a real-valued function, called an envelogram, is derived from the phonocardiogram signal by complex demodulation. The envelogram is essentially a

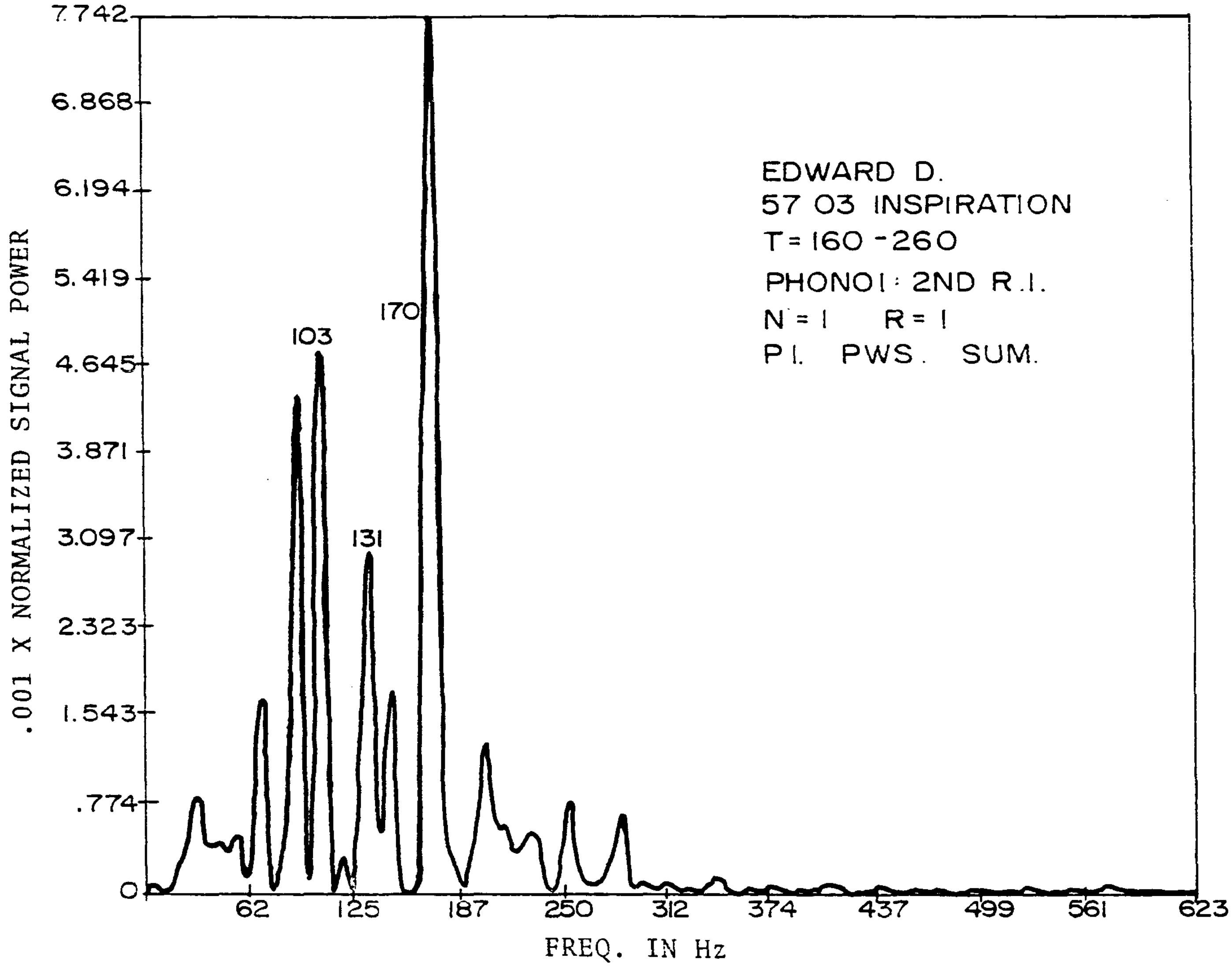

Fig. 16. A typical V.A.S. murmur power spectrum estimate

high-resolution intensity plot of the phonocardiogram signal and is used to locate the epochs, measure durations, and estimate the intensity of phonocardiogram wavelets and murmurs.

In the development of an envelogram, the Hilbert transform and the analytic signal representation of the phonocardiogram signal are required. These **are** defined and their properties explored in the two sections that follow.

The Hilbert Transform. Let s(t) be a real signal with a Fourier transform $S(\omega)$. The Hilbert transform [66,70,73,80] of s(t), denoted by $\overset{\Delta}{s}(t)$ is defined by the convolution (denoted by *) integral given below.

$$\overset{\Delta}{s}(t) = s(t)*(\frac{1}{\Pi t}) = P[\frac{1}{\Pi} \int_{-\infty}^{\infty} \frac{s(\lambda)}{t-\lambda} d\lambda] \qquad \text{Eq. 58}$$

where P stands for the Cauchy principal value of the integral. The Fourier transform of $\frac{1}{\Pi t}$, [66,73] is

$$\int_{-\infty}^{\infty} \frac{1}{\Pi t} e^{-j\omega t} dt = -j \ \mathrm{sgn}(\omega)$$

$$\text{where } \mathrm{sgn}(\omega) = 1 \text{ when } \omega > 0$$

$$\mathrm{sgn}(\omega) = 0 \text{ when } \omega = 0$$

$$\mathrm{sgn}(\omega) = -1 \text{ when } \omega < 0$$

The Fourier transform of $\overset{\Delta}{s}(t)$, denoted by $\overset{\Delta}{S}(\omega)$, can be computed in the frequency domain from the equation given below by recalling that convolution in the time domain is the product in the frequency domain.

$$\hat{S}(\omega) = -j\ \mathrm{sgn}(\omega)S(\omega) \qquad \text{Eq. 59}$$

It is clear from the above that $\hat{s}(t)$ is produced by shifting the phase of s(t) by -90° for $\omega > 0$ and +90° for $\omega < 0$. The singular case when f = 0 is covered by defining sgn(0) = 0. It is shown below that if s(t) is real, then $\hat{s}(t)$ is also real. The necessary and sufficient condition for a signal to be real [66,73] is as follows:

$$S(-\omega) = \overset{*}{S}(\omega)$$

Applying the above definition to Eq. 59 and realizing that $\mathrm{sgn}(\omega)$ is an odd function of ω, gives

$$\hat{S}^*(\omega) = \hat{S}(-\omega)$$

and consequently $\hat{s}(t)$ is real. This property of $\hat{s}(t)$ is required when the analytic signal representation s(t) is developed.

<u>The Analytic Signal</u>. Using the Hilbert transform, the analytic signal [66,70,73,80,89] denoted by z(t) is defined as

$$z(t) = s(t) + j\hat{s}(t) \qquad \text{Eq. 60}$$

Since s(t) and $\hat{s}(t)$ are real signals, it is clear from the definition that z(t) is complex; consequently, $Z^*(\omega)$ is not equal to $Z(-\omega)$. In fact $Z(\omega)$ is a signal which contains only positive frequency components (i.e., $Z(\omega)$ is an upper single-sideband signal). To show this, one merely needs to take the Fourier transform of Eq. 60 and substitute Eq. 59 for $\overset{\Delta}{S}(\omega)$ resulting in

$$Z(\omega) = S(\omega)\ [1 + \mathrm{sgn}(\omega)] \qquad \text{Eq. 61}$$

Recalling the definition of sgn(ω), the above equation can be rewritten as

$$\begin{aligned} Z(\omega) &= 2S(\omega) && \text{for } \omega > 0 \\ Z(\omega) &= S(\omega) && \text{for } \omega = 0 \\ Z(\omega) &= 0 && \text{for } \omega < 0 \end{aligned} \qquad \text{Eq. 62}$$

Envelope, Phase and Frequency of the Phonocardiogram Signal. Let s(t) be the phonocardiogram signal and z(t) be the corresponding analytic signal of s(t). The envelope of the signal e(t) is defined here as

$$e(t) = |z(t)| = [s^2(t) + \overset{\Delta}{s}{}^2(t)]^{1/2} \qquad \text{Eq. 63}$$

while the phase $\theta_s(t)$ and frequency $\omega_s(t)$ of the signal s(t) are defined as

$$\theta_s(t) = \arctan\left(\frac{\overset{\Delta}{s}(t)}{s(t)}\right) = \mathrm{ph}(z(t)) \qquad \text{Eq. 64}$$

$$\omega_s(t) = \frac{d\theta_s(t)}{dt} \qquad \text{Eq. 65}$$

The envelope, phase and frequency as defined above coincide with the normally used descriptors of narrow band signals [73,80]. The envelope is of particular interest in phonocardiogram signal analysis since it can be employed to time narrow band wavelets and to identify murmur intensity patterns.

<u>Envelope of Heart Sounds and Clicks</u>. In this study heart sounds and clicks are represented as the modulated signal given below.

$$s(t) = a(t)\cos(\omega_c t + \phi(t)) \qquad \text{Eq. 66}$$

where $a(t)$ = modulating signal envelope

ω_c = carrier or mean frequency

and $\phi(t)$ = phase deviation

It will be shown that if the bandwidth of $a(t)\cos\phi(t)$ and $a(t)\sin\phi(t)$ are less than ω_c, then $a(t)$ is equal to the magnitude of the analytic signal. To show this, one must investigate the Hilbert transform of the products of two functions. It is shown by Bennett [73] that if $f(t)$ and $g(t)$ are low-pass and high-pass signals respectively (i.e., $f(t)$ and $g(t)$ are two real functions with nonoverlapping Fourier spectra and the spectrum of $f(t)$ is confined below the spectrum of $g(t)$), then

$$H[f(t)g(t)] = f(t)H[g(t)] \qquad \text{Eq. 67}$$

where H is the Hilbert transform operator. In addition, we must recall that

$$H[\sin(\omega_c t)] = -\cos(\omega_c t)$$

and $$H[\cos(\omega_c t)] = \sin(\omega_c t)$$

Using the trigonometric identities, Eq. 66 is expressed as

$$s(t) = a(t)(\cos\phi(t))\cos\omega_c t - a(t)(\sin\phi(t))\sin\omega_c t$$

Requiring that $a(t)\cos\phi(t)$ and $a(t)\sin\phi(t)$ be low-pass signals with bandwidths below ω_c, we obtain

$$\overset{\Delta}{s}(t) = a(t)[(\cos\phi(t))\sin\omega_c t + (\sin\phi(t))\cos\omega_c t]$$

$$\overset{\Delta}{s}(t) = a(t)\sin(\omega_c t + \phi(t)) \qquad \text{Eq. 68}$$

The corresponding analytic signal is

$$z(t) = s(t) + j\overset{\Delta}{s}(t)$$

$$z(t) = a(t)[\cos(\omega_c t+\phi(t)) + j\ \sin(\omega_c t+\phi(t)] \qquad \text{Eq. 69}$$

$$z(t) = a(t)e^{j\omega_c t+\phi(t)}$$

Taking the magnitude of the above equation gives the desired result.

$$|z(t)| = e(t) = a(t)$$

For a general modulated signal in the form of Eq. 66, but with overlapping frequency spectra between the carrier and $a(t)\cos\phi(t)$ or $a(t)\sin\phi(t)$, the Hilbert transform of this signal is given by Rihaczek [80] as

$$\overset{\Delta}{s}(t) = a(t)\sin(\omega_c t+\phi(t)) + K(t) \qquad \text{Eq. 70}$$

where the significance of the correction terms $K(t)$ diminish as the essential frequencies in $a(t)$ and $\phi(t)$ decrease compared to ω_c. It is clear from the above that the envelope of this signal derived from $z(t)$ is not equal to $a(t)$;

however, in most cases the error is reasonably small [90]. It is shown by Rubin and DiFranco [90], that for a wide-band signal defined by Eq. 66, the rms error between z(t) and a(t) is a function of the percent bandwidth, where the percent bandwidth is defined as 100% times the modulating signal bandwidth divided by f_c. For a Gaussian pulse envelope at 50% bandwidth, the error is approximately 2%.

Envelope of the Murmur Signal. In this section it will be shown that the analytic signal can be used to find the intensity patterns of heart murmurs. When s(t) is a wide-band signal with a bandwidth approximately equal to ω_s, the modulating signal a(t) as defined by Eq. 66 loses its meaning [80]. However, the envelope e(t) as defined by Eq. 63 can still be used to identify a slowly changing modulating signal. To demonstrate this, let v(t) be a positive-valued, high-pass random Gaussian signal where the Fourier transform $V(f) = 0$ for $500 \text{ Hz} \leq |f| \leq 30 \text{ Hz}$. We define the murmur signal s(t) as the product of these two signals.

$$s(t) = m(t)v(t)$$

and the Hilbert transform of this product as defined by Eq. 67 is

$$\overset{\Delta}{s}(t) = m(t)\overset{\Delta}{v}(t)$$

and the corresponding analytic signal is

$$z(t) = m(t)(v(t)+j\overset{\Delta}{v}(t))$$

and

$$|z(t)| = e(t) = m(t)|v(t)+j\overset{\Delta}{v}(t)| \qquad \text{Eq. 71}$$

Note that Eq. 71 is the product of two positive-valued functions. Since v(t) is a bandwidth-limited random signal, the ensemble average of e(t) will produce

$$E[e(t)] = m(t)K \qquad \text{Eq. 72}$$

where K is a constant approximately equal to one and therefore, the murmur intensity envelope shape is preserved in this analysis.

Computation of the Discrete Envelogram Estimate. The discrete envelope of a phonocardiogram cycle, as defined by the equation given below, is referred to as the envelogram estimate.

$$|IDFT\{Z(k\Delta f)\}| = |IDFT\{S(k\Delta f)(1+sgn(k\Delta f))\}| \qquad \text{Eq. 73}$$

where IDFT denotes the inverse discrete Fourier transform operation. The envelogram estimate is a high-resolution intensity plot of the phonocardiogram signal and is rapidly computed in the frequency domain using Eq. 73 and the FFT algorithm as outlined below.

1. Input the sample points of a phonocardiogram cycle to the real buffer of the FFT subroutine. The number of data points must be less than or equal to 1024.
2. Remove the DC bias introduced by the analog-to-digital converter.
3. Divide each signal amplitude by the rms value of the calibration signal. This normalization

step removes microphone and other gain setting errors.

4. Compute the complex DFT spectrum as defined by Eq. 12 using an N = 1024 fixed-length FFT algorithm. When the phonocardiogram cycle length is less than 1024, the additional buffer values are set equal to zero.
5. Set all negative frequency terms equal to zero (i.e., all terms for $512 \leq k \leq 1023$).
6. Multiply the positive frequency terms by 2 (i.e., all terms for $1 \leq k \leq 511$). Note that the DC value k = 0 remains unchanged.
7. Take the 1024 point inverse discrete Fourier transform using the FFT algorithm.
8. Compute the magnitude of the complex function obtained in Step 7 (i.e., for each integer, find the square root of the sum of squared real and squared imaginary components). The resulting real-valued function is the envelogram estimate of a phonocardiogram cycle.

A typical phonocardiogram cycle and its corresponding envelogram estimate are shown in Figs. 7 and 17. Note that the large, narrow-band wavelet (aortic ejection click) occurring at approximately 90-113 ms. is demodulated and represented on the envelogram as a single pulse, where its value is equal to the intensity of the wavelet. Similarly, wavelets in the 350-440 ms. time range (s_2) are demodulated

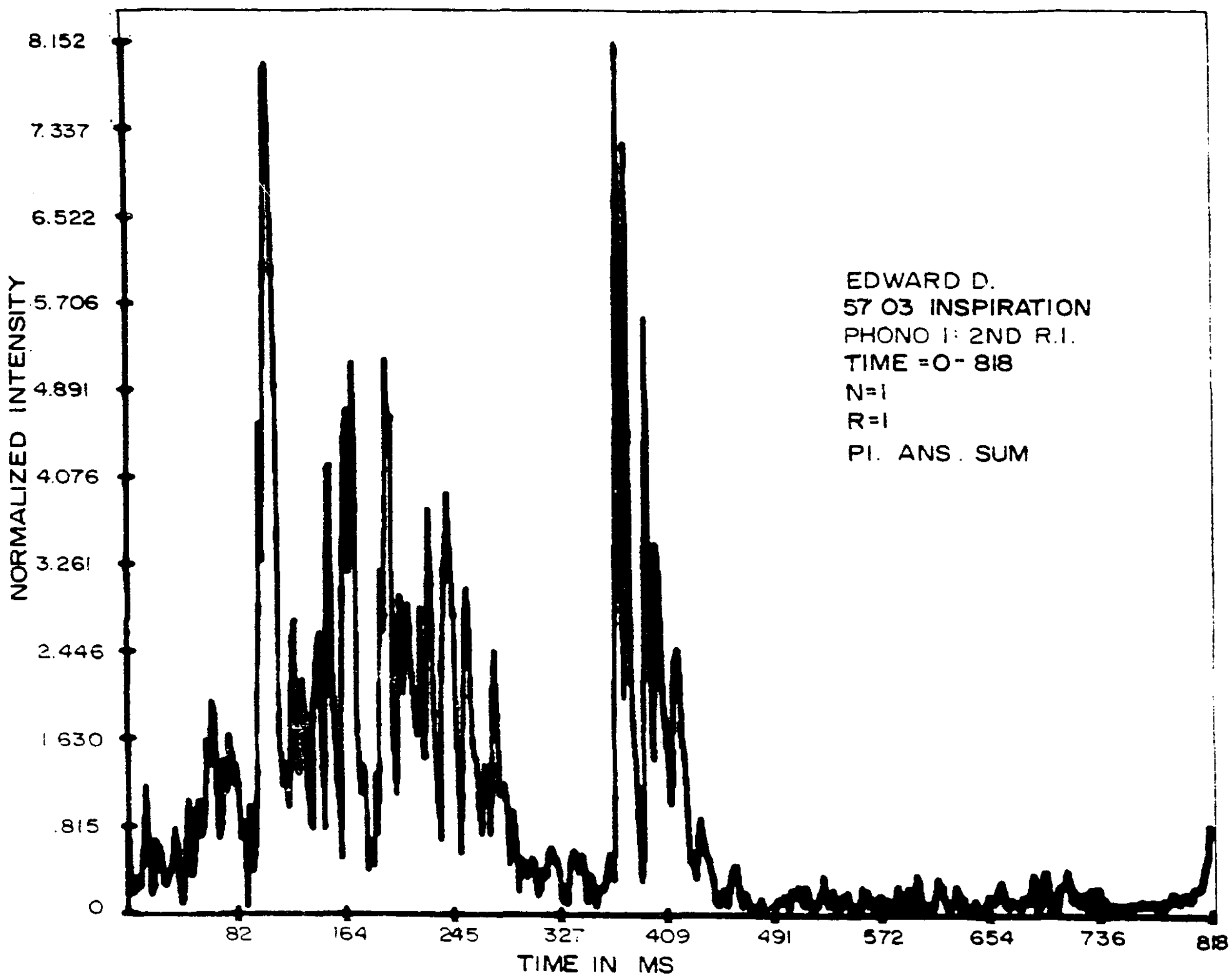

Fig. 17. Envelogram estimate of Fig. 7

and separated into four major components. The demodulation process resembles the absolute value function for the wide-band random signals occurring in the 120-350 ms. and 440-800 ms. time ranges.

CHAPTER V

RESULTS

In this chapter a complete data set is described and the analysis results are presented in two parts. The first part contains averaged envelogram and phonocardiogram plots and their descriptions. These plots aid in the positive diagnosis of systolic heart diseases and condense the large volume of phonocardiogram time series data into a single display. The plots can be used for rapid identification and accurate timing of phonocardiogram events. It is demonstrated that the essential aortic identification signal features are preserved or enhanced in these displays.

In the second part, selected segments of aortic ejection murmurs are gated and an average power spectrum is computed. From this spectrum, quantitative murmur diagnosis parameters (first spectral moment and bandwidth) are defined and computed. For the thirteen catheterized patients, correlation studies between the calculated power spectrum parameters and the peak systolic ejection gradient (P.S.E.G. measured by catheterization) are presented. These studies indicate that good correlation exists between the first spectral moment and the P.S.E.G. and that this noninvasive technique is useful in assessing the severity of aortic stenosis.

DESCRIPTION OF THE PATIENT DATA SET

Fourteen catheterized and four clinically-diagnosed aortic stenosis patients were recorded for this study. One of the catheterized patients, Raymond S., Hosp. #80-62-02, was later omitted from the analysis when post-operative diagnosis indicated that his disease was severe congenital deformation of the aorta rather than valvar aortic stenosis. All the catheterized patients had either mild or no aortic regurgitation. For the catheterized patients, the personal data, the diagnosis, the degree of aortic regurgitation (Aortic Regurg), and the peak systolic ejection gradient (P.S.E.G.), (obtained from Children's Hospital catheterization data charts) are tabulated in Table 8.

In addition, six normal patients were included in this study to facilitate the identification of aortic stenosis signal features. Personal data for the normal and clinically-diagnosed (uncatheterized) aortic stenosis patients are given in Table 9.

Prior to data recording, the chest wall thickness of each patient was classified as thin, medium, or thick, gauged by the following criteria: thin-walled if the ribs were clearly visible, medium-walled if the ribs were not distinguishable but had no appreciable fatty deposit, and thick-walled if the ribs were covered by a fatty layer. All of the patients included in the study had no chest deformities and all had normal body temperatures.

TABLE 8

THIRTEEN CATHETERIZED VALVAR AORTIC STENOSIS PATIENTS DATA

Personal Data				Catheterization Data		
Name	Hosp. #	Age/Sex	Chest Wall	Cath. Diagnosis	Aortic Regurg.	P.S.E.G. mm Hg
Roger F.	47-99-27	16 M	Thick	Mod. V.A.S.	---	75
Tommy K.	63-77-80	10 M	Thin	Mild V.A.S.	---	9-18
Donald G.	62-12-80	10 M	Thin	Triv. V.A.S.	Mild	16
Natalie K.	70-89-05	8 F	Med.	Mild V.A.S.	Triv.	23
Bryan K.	60-91-88	14 M	Thin	Mild V.A.S.	---	39
Robert M.	53-91-59	19 M	Med.	Mild-Mod. V.A.S.	Mild	45
Elizabeth R.	55-01-61	12 F	Thin	Mod. V.A.S.	---	45
Rudolph B.	68-97-78	9 M	Thin-Med.	Mod. V.A.S.	---	45
Richard F.	57-53-27	11 M	Med.	Mod.-Sev. V.A.S.	Mild	61-68
Jean S.	58-79-24	15 F	Med.	Mod.-Sev. V.A.S.	Mild	70-90
Mark M.	68-95-48	10 M	Thin	Triv. V.A.S.	Triv.	6-8
Jonathan F.	64-87-14	9 M	Thin	Triv. V.A.S.	Triv.	5-9
Barry F.	60-50-48	10 M	Med.	Mild V.A.S.	---	16-24

TABLE 9

PERSONAL DATA FOR NORMAL AND CLINICALLY DIAGNOSED VALVAR AORTIC STENOSIS PATIENTS

Clinically-Diagnosed Valvar Aortic Stenosis Patients				
Name	Hospital #	Age	Sex	Chest Wall
Edward D.	57-03-63	14	M	Thin
John B.	58-29-30	9	M	Thick
John R.	66-12-34	7	M	Med.
Donald D.	79-41-95	15	M	Thin

Normal Patients				
Name	Hospital #	Age	Sex	Chest Wall
Kenneth S.	---	10	M	Thin
Sherry C.	---	13	F	Med.
Steven C.	---	10	M	Thin
Cameron C.	---	15	M	Med.
Lynne S.	---	13	F	Thin
Sheldon W.	---	10	M	Thin

ENSEMBLE-AVERAGED ENVELOGRAMS

As the initial step of the interactive diagnostic analysis, an ensemble-averaged envelogram was computed for each data file as defined below.

$$\bar{e}(n\Delta t) = \frac{1}{N.REC} \sum_{i=1}^{N.REC} e_i(n\Delta t)$$

where N.REC = Number of records averaged

$e_i(n\Delta t)$ = value of the i^{th} envelogram estimate at time $n\Delta t$

and $\bar{e}(n\Delta t)$ = value of the averaged envelogram at time $n\Delta t$.

The computed ensemble-averaged envelograms were plotted on the graphics terminal and hard copies were generated. The plots were examined and the maximum murmur intensity site was noted. For nearly all of the aortic stenosis patients studied, the maximum intensity site was at the 2nd R.I. space. The interactive diagnosis program and its description are given in Appendix II.

Ensemble-averaged envelogram plots at the 2nd R.I. for inspiration and expiration are shown in Figs. 18 and 19. A comparison of Figs. 17 and 18 reveals that in the averaged envelogram, "fine wavelet structures" are preserved while murmur intensity variance is reduced by approximately a factor of three. Note that good correlation exists between Figs. 18 and 19 in the 113-177 ms. time interval.

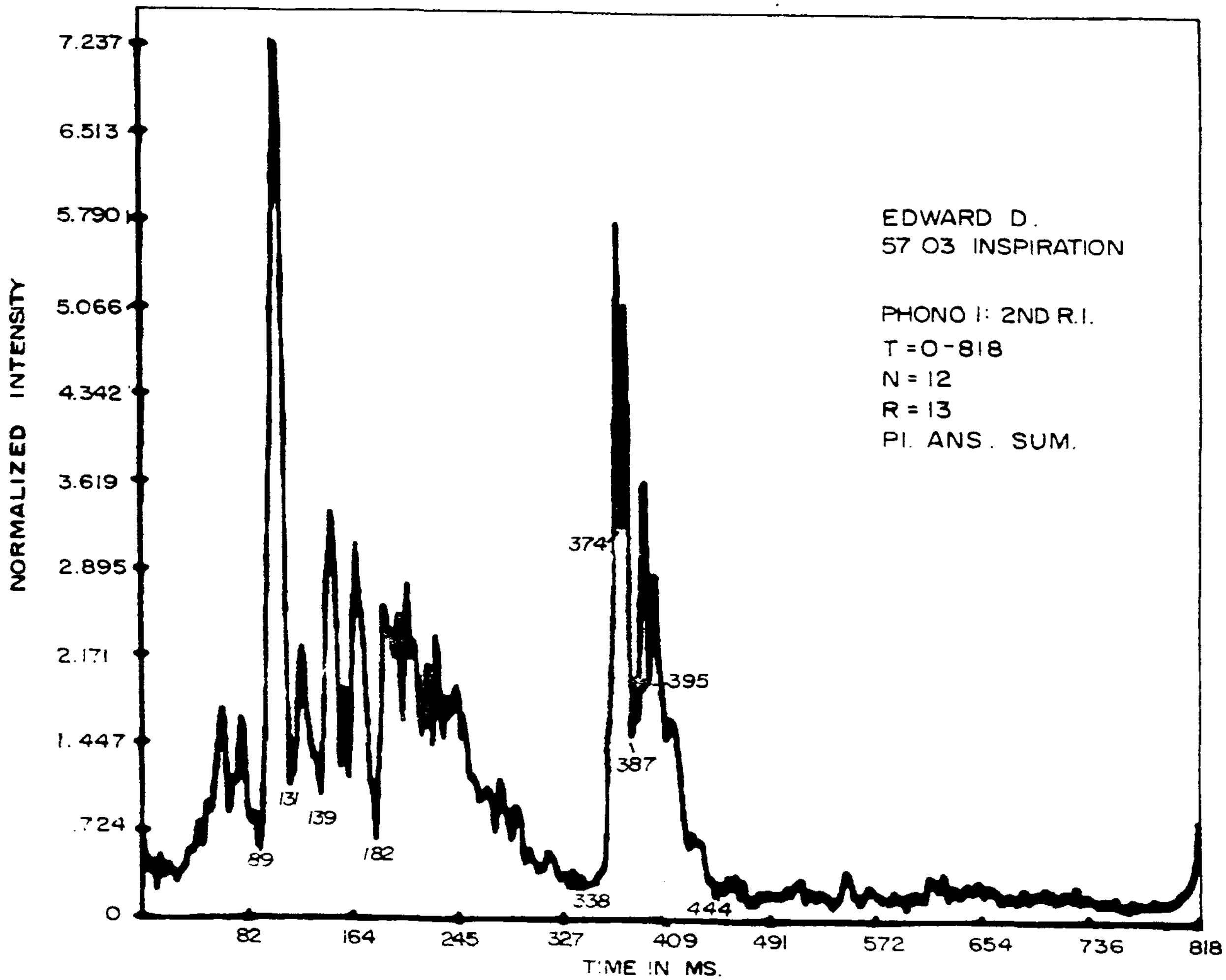

Fig. 18. Averaged V.A.S. envelogram for inspiration

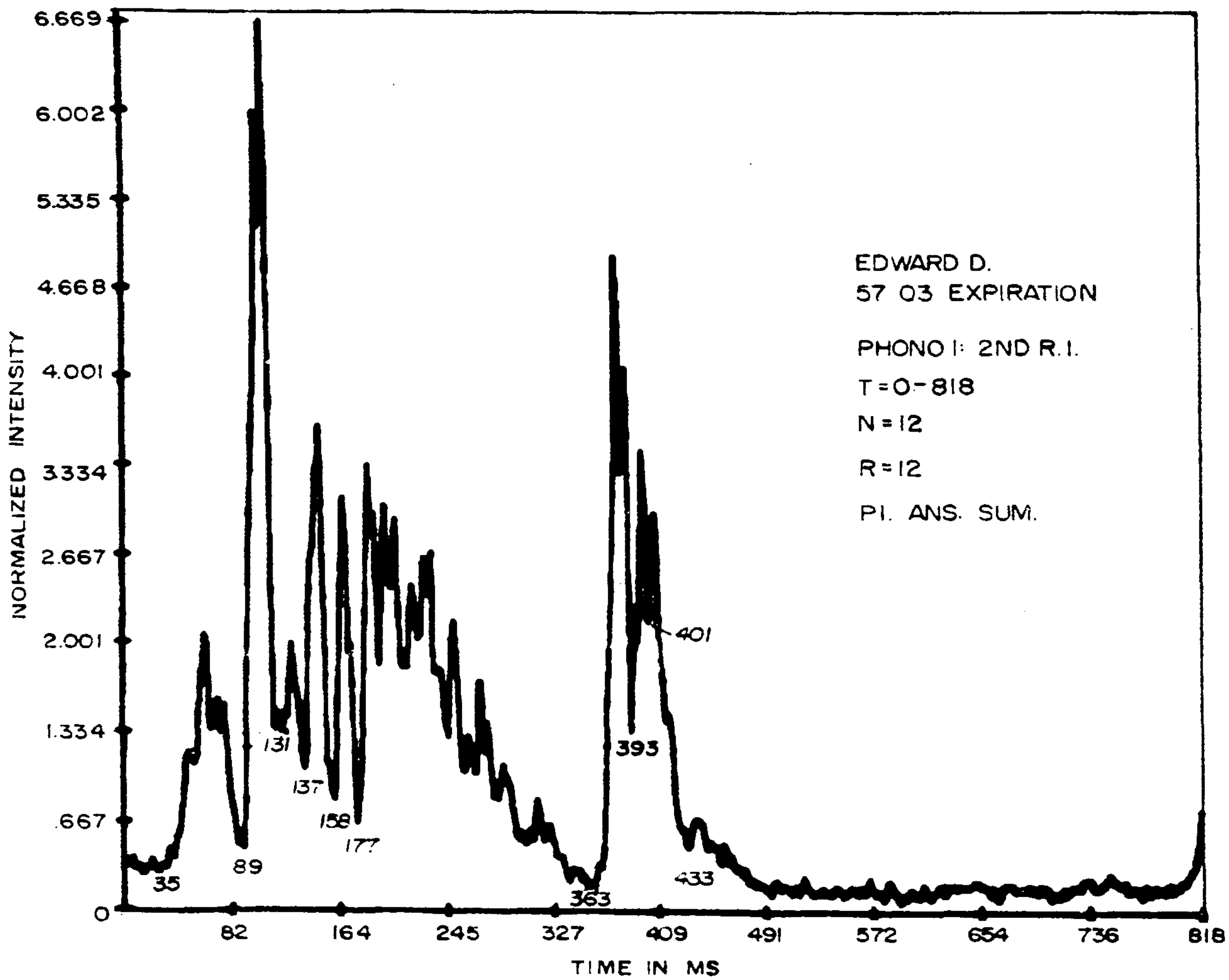

Fig. 19. Averaged V.A.S. envelogram for expiration

Consequently, these peaks are probably not produced by random intensity fluctuations, but are more likely produced by murmur amplitude modulation. This interpretation is supported by the following observations: (1) the pressure fluctuations (trill) occur in the carotid pulse waveform during the 113-177 ms. time interval as shown in Fig. 20 and correlate with the intensity fluctuation observed in their corresponding envelogram, and (2) the gated averaged power spectrum of this region does not contain strong line structures, indicating that the signal is random.

The large intensity increase in the 89-113 ms. range shown in Fig. 18 is identified as an aortic ejection click. Identification is based on the following observations:

1. It correlates well with the upstroke of the carotid pulse.
2. Maximum intensity occurs at the 2nd R.I.
3. Intensity and onset time of the event are not affected by respiration.

Observation 1 suggests that the intensity increase is an ejection click, where 2 and 3 suggest aortic origin.

The intensity change in the 358-448 ms. range shown in Fig. 18 is identified as the aortic component of the second heart sound. Identification is supported by the following observations:

1. It radiates well to all four listening areas, particularly to the 2nd R.I. and to the apex.

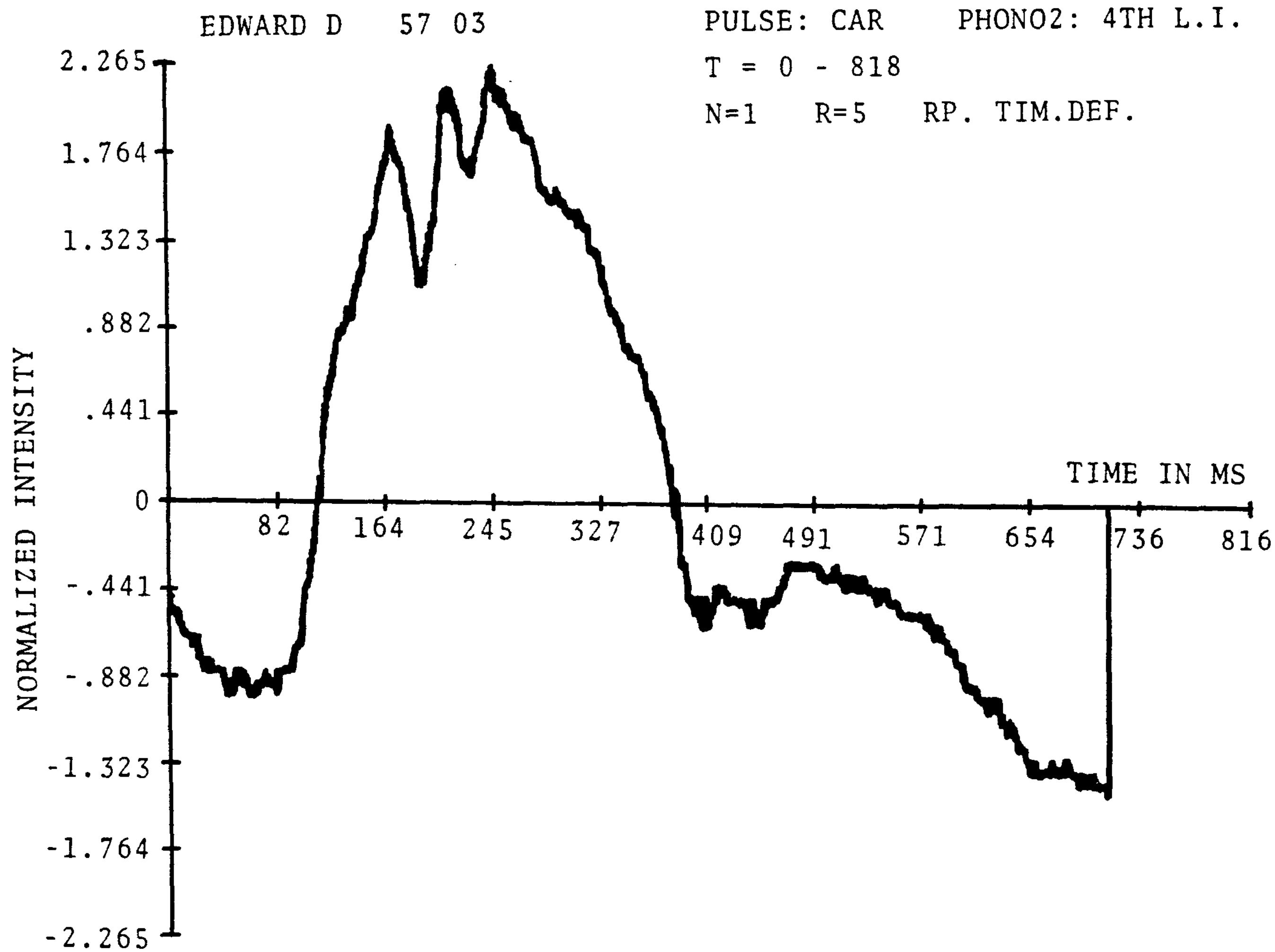

Fig. 20. A typical V.A.S. carotid pulse

2. The entire wavelet occurs earlier upon inspiration than upon expiration.

The intensity increase in the 130-358 ms. range shown in Fig. 18 is identified as an aortic ejection murmur. Its timing and diamond shape imply that the murmur is ejection type and its maximum intensity location suggests aortic origin.

ENSEMBLE-AVERAGED WAVELETS

Heart sounds and murmurs are identified and accurately timed from the averaged envelogram plots. Knowing the time of occurrence, wavelets of special interest can be gated and an ensemble-averaged wavelet (averaged signal waveform) can be computed as defined by the equation given below.

$$\bar{s}(n\Delta t) = \frac{1}{N.REC} \sum_{i=1}^{N.REC} s_i(n\Delta t)$$

where $s_i(n\Delta t)$ = signal intensity of i^{th} estimate at time $n\Delta t$

and $\bar{s}(n\Delta t)$ = averaged signal intensity at time $n\Delta t$.

As pointed out in Chapter III, wavelets within an equivalent ensemble are highly reproducible in both time and waveshape. The approximate onset time jitter of wavelets is 4 ms. measured from the ECG Q wave while the difference in mean onset time from inspiration to expiration is approximately 16 ms. In addition, waveshapes of the aortic wavelets (i.e., aortic ejection click and A_2) are independent of respiration. The onset time jitter of an aortic wavelet can be removed by searching for and locating a particular signal feature (local maximum or minimum) within a narrow time window. Thus, wavelets can be aligned prior to averaging.

Aligned averaging is equivalent to time domain filtering where superimposed signals can be separated, and reliable average wavelet waveforms can be obtained. When two wavelets with similar frequency characteristics have nearly identical onset times, large segments of their waveforms are superimposed. Due to overlapping frequency components, separation by frequency filtering is not possible. Examples of such events are the aortic-pulmonic components of the second heart sound and the first heart sound ejection click. The onset time jitter of these wavelets tends to be independent, since they are generated by different physical events. Alignment of the early event and ensemble averaging cause enhancement of the early component and suppression of the later event. This effect is shown in Figs. 21 and 22. A typical, single, normal second heart sound of Sherry C., consisting of aortic (373-400 ms.) and pulmonic (406-430 ms.) components is shown in Fig. 21, with the aligned and averaged aortic wavelet shown in Fig. 22. Prior to averaging, alignment was performed on the aortic component. Note that in Fig. 22 the pulmonic component (second wavelet) is suppressed, while the aortic component is preserved.

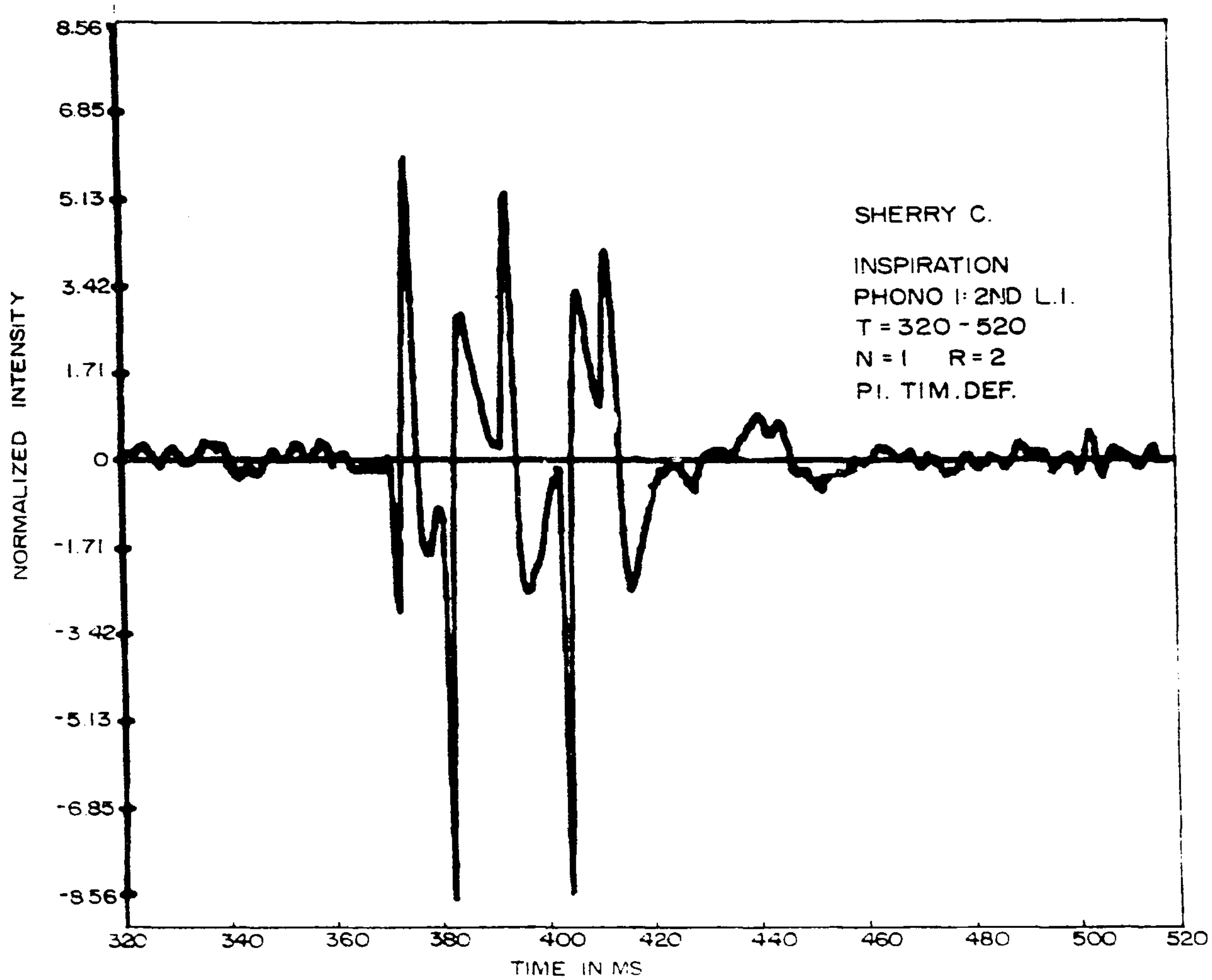

Fig. 21. A typical normal second heart sound

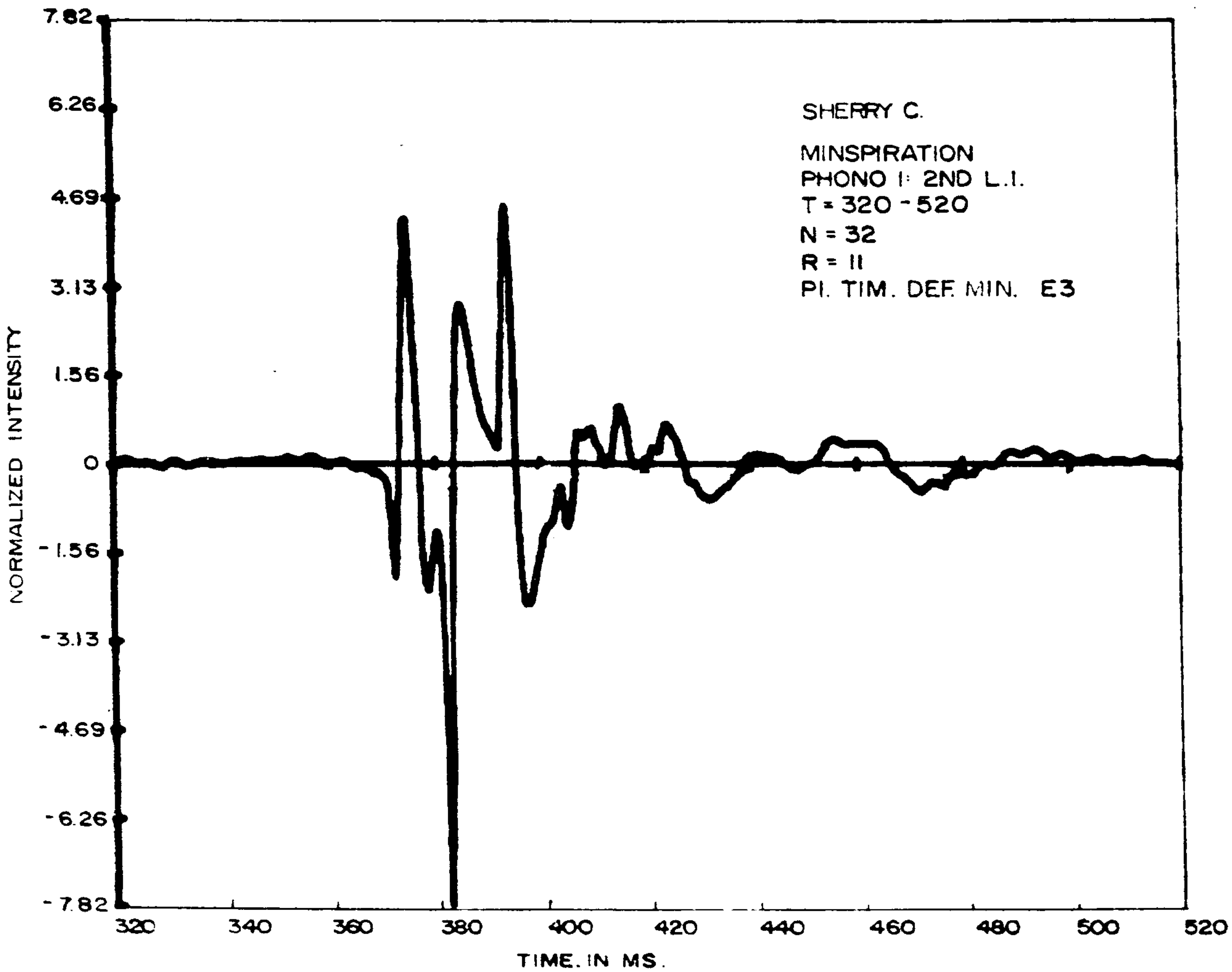

Fig. 22. The aligned averaged aortic component of Fig. 21

Similarly, aligned averaging can be used to separate wavelets (e.g., mid and late systolic clicks, ejection clicks, etc.) from superimposed random signals (e.g., murmurs). To demonstrate this, a 100 ms. time segment containing the click of Edward D. is gated, and the aligned-averaged time waveform is computed. Note that a high-frequency component is evident in the single record (95-117 ms.), Fig. 23, but that an additional low-frequency component observed in the averaged plot (115-135 ms.), Fig. 24, is obscured by the murmur.

ESTIMATING THE SEVERITY OF AORTIC STENOSIS USING MURMUR POWER SPECTRAL ANALYSIS

As the first step of the severity assessment analysis, averaged envelogram plots at the 2nd R.I. space are examined, and a 100 ms. "rectangular data window" is chosen centered around the peak intensity of the systolic ejection murmur. Since the duration of the systole is usually 300-400 ms., this data window encompasses approximately one-third of the murmur signal. During this time interval the murmur is at a reasonably constant intensity and is approximated as a stationary random process. In addition, this data window is sufficiently delayed from the first heart sound and the ejection click; consequently, these signals contribute a negligible amount to the total signal intensity. Using the selected data window, the required murmur signals are gated at the 2nd R.I. and an averaged power spectrum is computed.

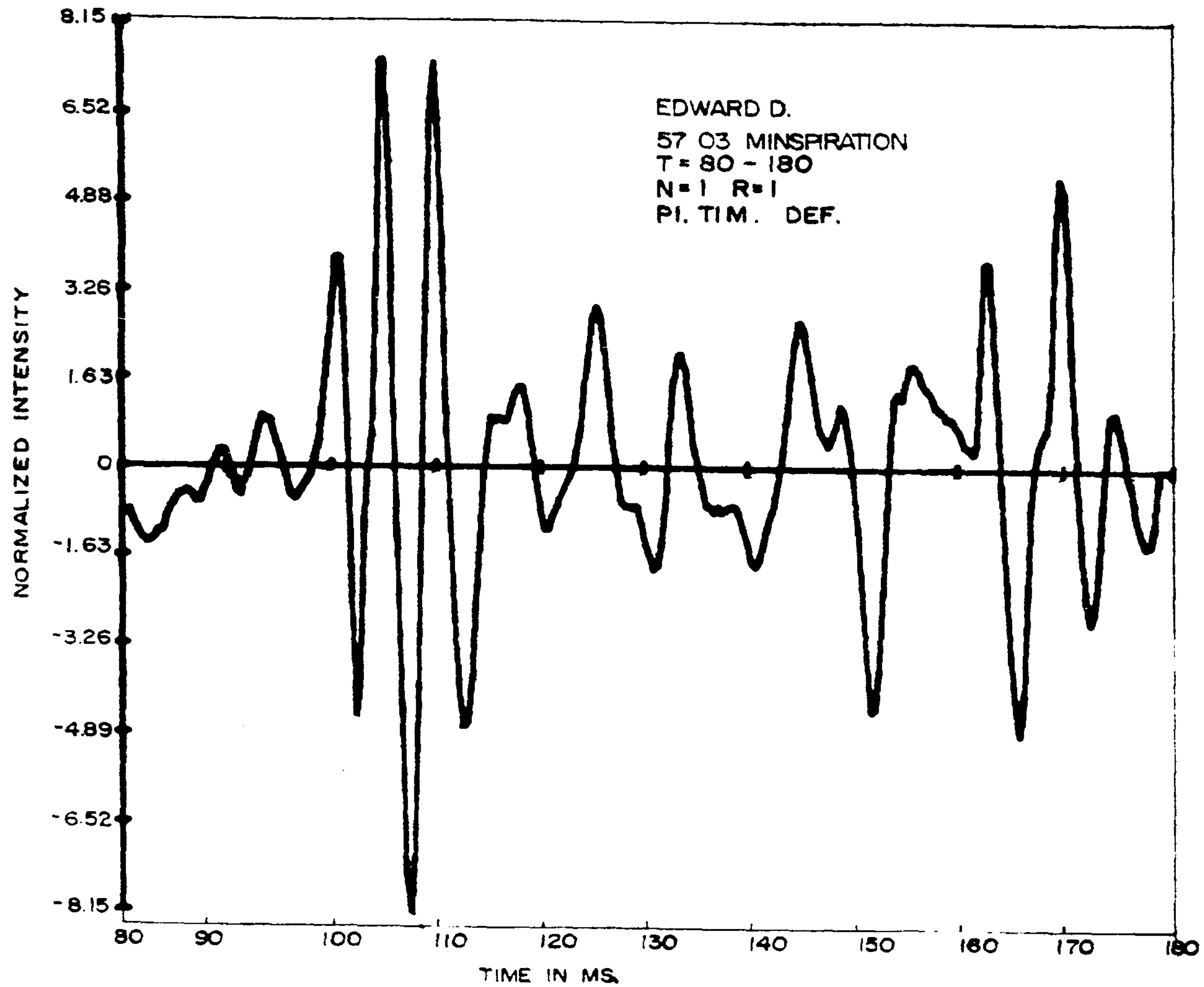

Fig. 23. A typical aortic ejection click

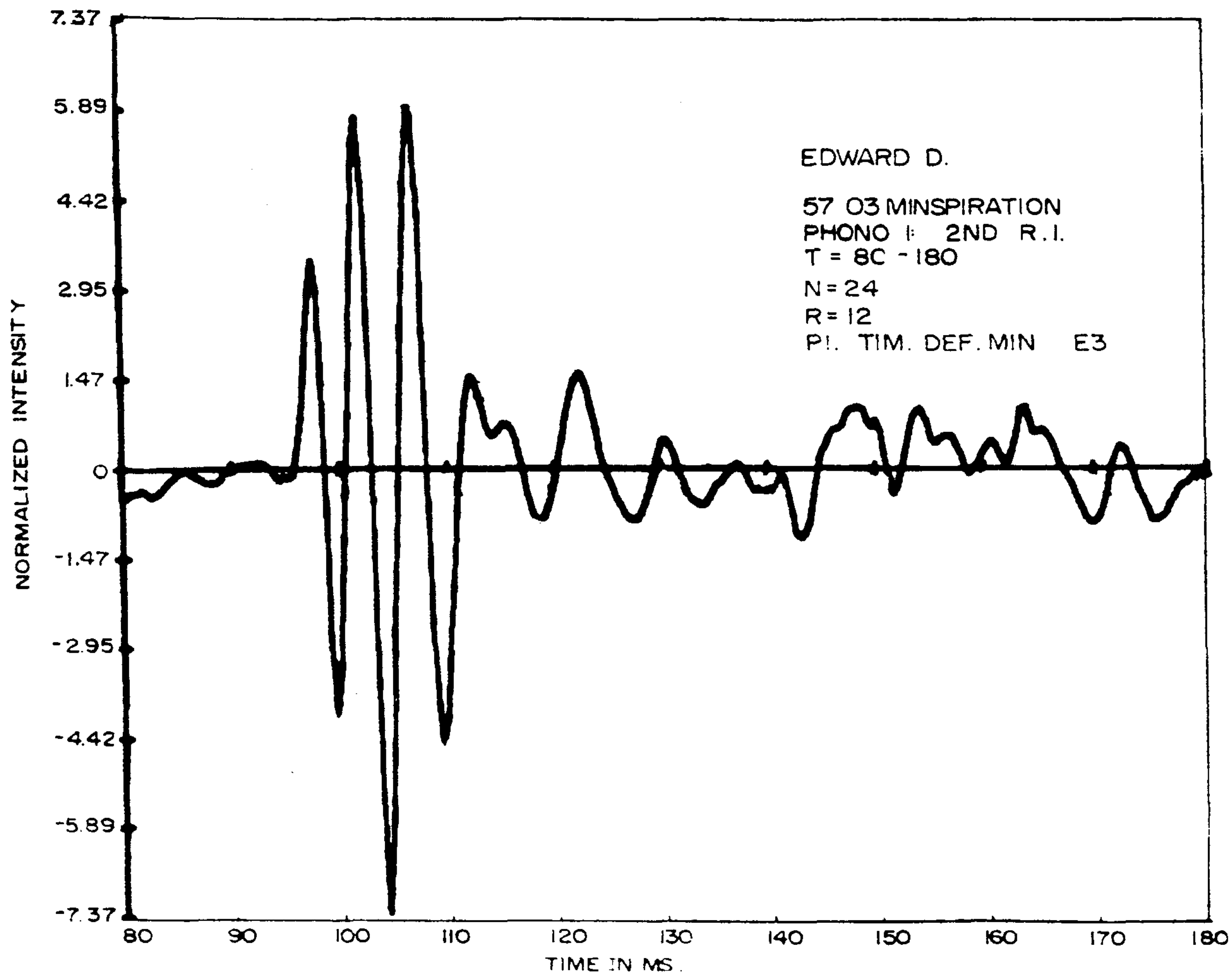

Fig. 24. A typical aligned averaged aortic ejection click

The averaged murmur power spectrum of Edward D., computed from inspiration and expiration data files as described in Chapter IV, is shown in Fig. 25. The spectral resolution provided by the rectangular data window (computed by Eq. 55) is 15 Hz. The confidence interval of the averaged spectrum (computed by Eq. 53) at Z = 1 (68.27% confidence level) is $\pm$ .16 $\bar{B}(f)$. Comparison of the averaged murmur power spectrum (Fig. 25) with a spectral estimate (Fig. 16), reveals that the estimate is inherently random and unreproducible, while the averaged spectrum obtained from twenty-four estimates converges to a spectral shape which appears to contain four major peaks.

For each averaged power spectrum, the first spectral moment $\bar{f}$ (AVE. FRQ.) and the spectrum bandwidths (%F) at 10% area increments are computed. The first spectral moment $\bar{f}$ is defined by the equation given below,

$$\bar{f} = \frac{\sum_{k=0}^{511} (k\Delta f)\ \bar{P}(k\Delta f)}{\sum_{k=0}^{511} \bar{P}(k\Delta f)}$$

where $\bar{P}(k\Delta f)$ = average k^{th} spectral component

$$\bar{P}(k\Delta f) = \frac{1}{N.REC} \sum_{i=1}^{N.REC} P_i(k\Delta f)$$

$$\Delta f = 1.2207 \text{ Hz}$$

and N.REC = number of records averaged

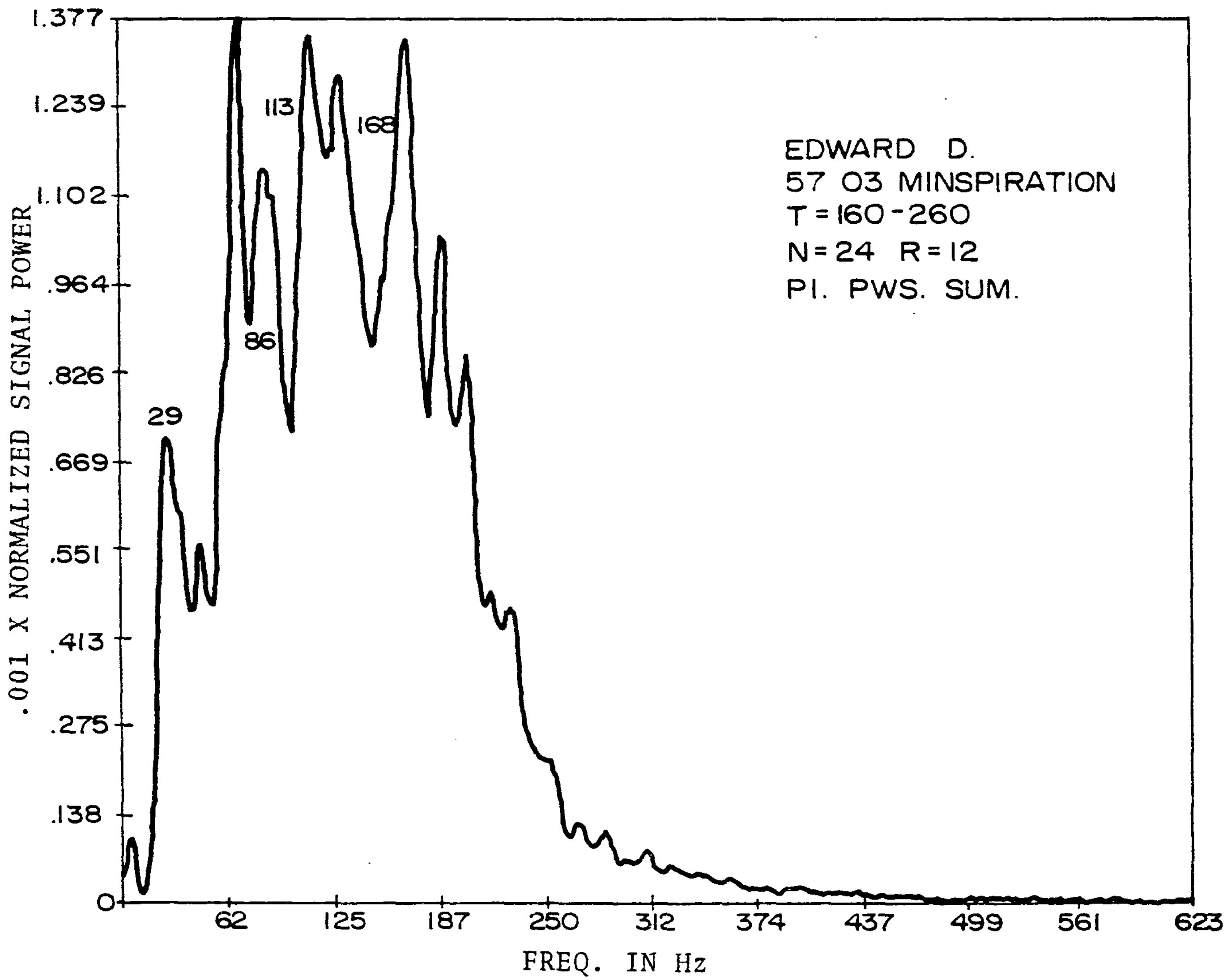

Fig. 25. A typical averaged V.A.S. murmur power spectrum

and the spectrum bandwidth is defined as the frequency increment centered about $\bar{f}$, which includes a specified fraction of the total spectral area. These parameters. calculated at the 2nd R.I. from inspiration, expiration and carotid data files for Natalie K., are given in Table 10. Note that in addition, the table contains the maximum spectral magnitude times 10^4 (M.M*10K), the frequency of the maximum magnitude (FM.MAG), the total area of the spectrum times 100 (AREA100), the number of records averaged (N.REC), the analysis performed (ANAL), and the start and end times for the spectral window (S.TIM & E.TIM). The severity analysis computer programs and their descriptions are given in Appendix II.

The murmur power spectrum analysis results, along with the personal and catheterization data for the thirteen catheterized aortic stenosis patients, are summarized in Table 11. These results were obtained at the 2nd R.I. from inspiration, expiration, and carotid data files as described above. The table contains the first spectral moment ($\bar{f}$), the estimated standard deviation of the first moment ($\sigma_{\bar{f}}$), the spectral bandwidth at 50% total area (50%F), the total number of records averaged (N.REC), and the murmur signal-to-diastolic-noise ratio (S/N). The signal-to-noise ratio was estimated from the averaged envelogram plots, where the peak murmur intensity is defined as the signal (S) and the mean intensity in the diastole is defined as the noise (N). The analysis for $\sigma_{\bar{f}}$ is given in Appendix II.

TABLE 10

BANDWIDTH AND FIRST MOMENT OF MEAN POWER SPECTRUM
COMPUTED FROM INSPIRATION, EXPIRATION AND
CAROTID DATA FILES AT 2ND. R.I.

NATALIE K 70 89 05 PHONO1: 2ND. R.I.

N. REC= 60 S. TIM=160.00MS. E. TIM=260.00MS. SAMP.= 1.22Hz. ANAL.=PWS.

AVE. FRQ= 124.53Hz. F.M.MAG= 91.55Hz. AREA100= 13.45 M.M*10K= 14.06

10%F	20%F	30%F	40%F	50%F	60%F	70%F	80%F
22.0Hz.	41.5Hz.	58.6Hz.	75.7Hz.	95.2Hz.	114.7Hz.	136.7Hz.	161.1Hz.

TABLE 11

SUMMARY OF MURMUR SPECTRUM ANALYSIS AT 2ND. R.I. FOR THE CATH. V.A.S. PATIENTS

Cath. and Personal Data				Phonocardiogram Data				
Name	Hosp. #	Chest Wall	P.S.E.G. mm Hg	$\bar{f}$ In Hz	$\sigma_{\bar{f}}$ In Hz	50% F In Hz	N.Rec.	S/N
Roger F.	47-99-27	Thick	75	134.98	1.52	100.1	54	20
Tommy K.	63-77-80	Thin	9-18	85.79	2.26	78.1	32	10
Donald G.	62-12-80	Thin	16	89.70	2.00	61.0	40	11
Natalie K.	70-89-05	Med.	23	124.53	1.48	95.2	60	10
Bryan K.	60-91-88	Thin	39	127.97	1.62	73.2	49	15
Robert M.	53-91-59	Med.	42-45	124.53	1.58	90.3	53	12
Elizabeth R.	55-01-61	Thin	45	147.77	1.54	80.6	48	26
Rudolph B.	68-97-78	Thin-Med.	45	142.86	1.43	97.7	58	12
Richard F.	57-53-27	Med.	61-68	168.56	1.38	78.1	54	24
Jean S.	58-79-24	Med.	70-90	201.84	1.70	68.4	30	13
Mark M.	68-95-48	Thin	6-8	95.89	1.71	78.1	53	10
Jonathan F.	64-87-14	Thin	5-9	93.12	2.06	36.6	37	11
Barry F.	60-50-48	Med.	16-24	104.15	2.08	56.2	34	10

The correlation coefficient between the peak systolic ejection gradient (P.S.E.G.) and the 50% bandwidth is equal to .32. Calculations are given in Table 1,AII. The correlation coefficient between the P.S.E.G. and the first moment of the mean power spectrum based on all thirteen subjects is .89 and the corresponding scatter diagram is given in Fig. 26. Careful examination reveals that a single point belonging to Roger F., Hosp. #47-99-27, exhibits a lower frequency moment than expected. Since this patient was the only one with a thick chest wall, the observed spectral moment difference may possibly be due to the increased chest wall thickness. The correlation coefficient between the P.S.E.G. and the first moment of the mean power spectrum $\bar{f}$ based on the twelve thin-medium chest walled patients is .96. The corresponding least square regression line calculated for the twelve points is shown in Fig. 26. Calculations are given in Table 2,AII.

To investigate the affect of respiration on the correlation between P.S.E.G. and $\bar{f}$, separate power spectral moments for inspiration and expiration were also computed. The corresponding calculations are given in Tables 3,AII and 4,AII. The resulting correlation coefficients for the twelve thin-medium chest walled patients were .95 for inspiration and .96 for expiration. Results of the correlation studies are summarized in Table 12.

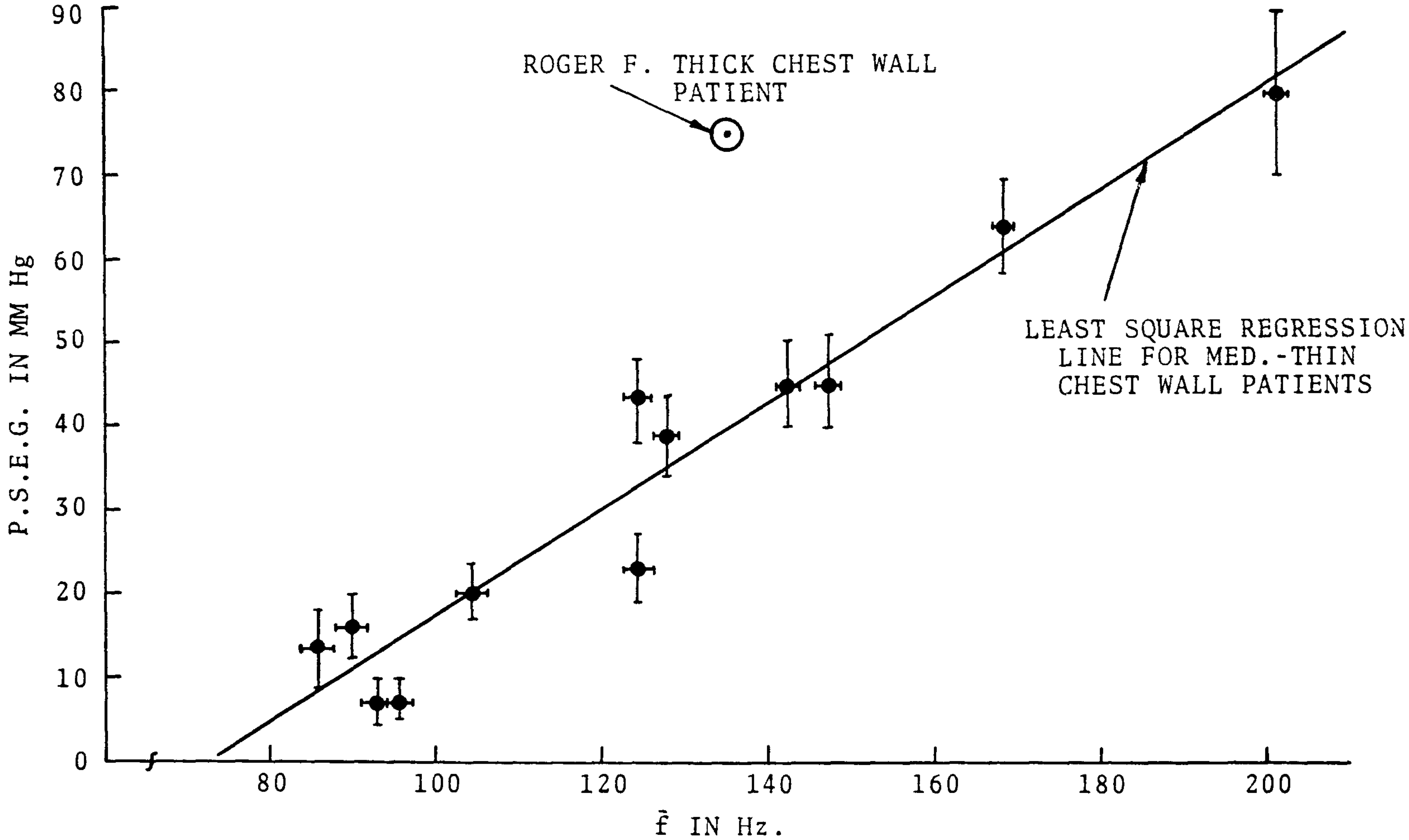

Fig. 26. Scatter diagram for the catheterized V.A.S. patients at the 2nd. R.I. for inspiration + expiration + carotid data

TABLE 12

SUMMARY OF CORRELATION STUDY BETWEEN P.S.E.G. AND MEAN MURMUR POWER SPECTRUM PARAMETERS, CALCULATED AT THE 2ND. R.I. FOR THE CATH. V.A.S. PATIENTS

Chest Wall Thickness and Data Files Av. at 2nd. R.I.	Corr. Coeff. between P.S.E.G./$\bar{f}$	Corr. Coeff. between P.S.E.G./50% F
For 1 Thick + 12 (Med.-Thin) Inspir. + Expir. + Car.	.89	---
For 12 (Thin-Med.) Inspir. + Expir. + Car.	.96	.32
For 12 (Thin-Med.) Inspir.	.95	---
For 12 (Thin-Med.) Expir.	.96	---

CHAPTER VI

DISCUSSION OF RESULTS

ADVANTAGES OF ENSEMBLE AVERAGING

As pointed out earlier in Chapter IV, the envelogram and power spectral estimates derived from a single phonocardiogram cycle are statistically unreliable and consequently, are unsuitable for the positive identification of phonocardiogram signal features. In Chapter V ensemble averaging of estimates was introduced to reduce the variance and the averaged plots were interpreted. Ensemble averaging of estimates offers the following advantages:

1. Reduces the variance of power spectral and envelogram estimates by approximately a factor of $\sqrt{N}$. Ensemble averaging is particularly required to smooth power spectra and to obtain consistent severity estimates.
2. Improves the detection sensitivity and timing of heart murmurs in the envelograms by approximately a factor of $\sqrt{N}$.
3. Unsynchronized respiratory and other external noise events are approximately evenly distributed and appear as a constant bias in the averaged envelograms.

The murmur detection sensitivity of ensemble-averaged envelograms was clearly demonstrated in the case of a normal patient, Lynne S., where prior to recording, no systolic murmur was detected by a cardiologist using auscultation techniques. However, the averaged envelogram computed from fourteen equivalent cardiocycles indicated a late systolic murmur of a grade 1-2 level, and was later confirmed by a second careful ausculatory examination. The high murmur detection sensitivity makes this technique particularly attractive in the assessment and study of mild regurgitant-type murmurs which occur in mild prolapsed mitral valves and in mild aortic and pulmonic insufficiency.

Unsynchronized noise smoothing (advantage 3) is especially useful in the detection of mild heart murmurs in infants and young children. The detection of these murmurs is, at best, difficult with the usual ausculatory and phonocardiogram techniques due to large respiratory and body background noise.

DISCUSSION OF V.A.S. SEVERITY ESTIMATES

The accurate noninvasive assessment of the severity of valvar aortic stenosis is an important clinical problem, and presently, is possible only by cardiac catheterization (an invasive surgical procedure which requires three days of hospital care). In contrast, the severity estimation procedure outlined in Chapter V is a completely noninvasive technique where the measurements and data analysis are performed within minutes. For this technique to gain wide acceptance in clinical cardiology, it is suggested that it first be employed to follow the case history of catheterized valvar aortic stenosis patients, thus eliminating additional catheterizations while increasing the cardiologist's confidence in the technique.

Estimating the severity of valvar aortic stenosis from the murmur power spectrum has been tried unsuccessfully by several investigators, notably by Jacobs et al. and McKusick [17,56]. The basic difference between the technique employed by these investigators and that presented in Chapter V is as follows. The estimation parameters for the former were obtained from a power spectral estimate computed from a single murmur signal, while for the latter, these parameters were computed from an averaged power spectrum computed from 30-50 murmur signals. The accurate severity estimation of valvar aortic stenosis is made possible by the ensemble averaging of spectral estimates.

For the twelve thin-medium chest walled patients discussed earlier in Chapter V, excellent correlation exists between the peak systolic ejection gradient and the first spectral moment of the mean murmur spectrum. The correlation can be clearly observed from the scattering diagram, Fig. 26, and from Table 12. These results, however, do not appear to apply to thick chest walled patients where additional fatty deposits can produce high-frequency attenuation.

This observation is implied by the lower $\bar{f}$ of the single thick chest walled patient, Roger F.

The linear least square regression line fitted to the twelve thin-medium chest walled patients shown in Fig. 26 was used to estimate the severity of the four clinically-diagnosed V.A.S. patients. The corresponding predicted peak systolic ejection gradients are tabulated with other pertinent data in Table 13. From the calculations these patients are classified as having mild to moderate valvar aortic stenosis.

During the severity estimation it may be well remembered that while Fig. 26 can be used to estimate the severity of thin-medium chest walled patients, prior to the use of this plot the diagnosis of valvar aortic stenosis must be established as outlined in Chapter V.

SUGGESTIONS FOR FURTHER STUDY

A significant improvement in the positive diagnosis of heart disease by phonocardiogram signals can be made if echo phonocardiograms were to be included as an extra time series data channel in this analysis. This signal could be used to improve the timing of the aortic ejection click and could possibly be used to measure chest wall thickness between the listening site and the aortic valve cusps. The measured chest wall thickness could in turn be incorporated to improve severity estimates and to extend the correlation results to include thick chest walled patients.

The envelogram and power spectral analysis techniques employed in this study could be adopted in a computerized phonocardiogram diagnostic system.

TABLE 13

PREDICTED MEAN P.S.E.G. AND STANDARD DEVIATION FOR THE CLINICALLY DIAGNOSED VALVAR AORTIC STENOSIS PATIENTS

Name	Hosp. #	Chest Wall	N. Rec.	S/N	$\sigma_{\bar{f}}$ In Hz	$\bar{f}$ In Hz	Predicted Mean P.S.E.G. In Hg mm	Predicted $\sigma_{P.S.E.G.}$ In Hg mm
Edward D.	57-03-63	Thin	31	15	1.98	138.8	42	1.25
John B.	58-29-30	Thick	54	14	1.47	147.1	> 47	---
John R.	66-12-34	Med.	38	8	2.0	100.8	18	1.26
Donald D.	79-41-95	Thin	40	8	1.85	117.5	28	1.17

BIBLIOGRAPHY

1. Rushmer, R. F., Cardiovascular Dynamics, 3rd Ed., W. B. Saunders Co., Philadelphia, 1970.

2. Attinger, E. O., "The Cardiovascular System" in Pulsatile Blood Flow, McGraw-Hill, New York, 1964.

3. Attinger, E. O., Pulsatile Blood Flow, McGraw-Hill, New York, 1964.

4. Watts, R. N., "A Mathematical Model for Studying the Mechanical Properties of the Impaired Left Ventricle", Ph.D. Dissertation, Rutgers Univ., New Brunswick, N. J., Jan., 1974.

5. Bellhouse, B. J. and Bellhouse, F. H., "Mechanism of Closure of the Aortic Valve", Nature, Vol. 217, Jan., 1968.

6. Bellhouse, B. J. and Bellhouse, F. H., "Fluid Mechanics of the Aortic Root with Application to Coronary Flow", Nature, Vol. 219, Sept., 1968.

7. Bellhouse, B. J. and Talbot, L., "The Fluid Mechanics of the Aortic Valve", J. Fluid Mech., Vol. 35, Part 4, 1969.

8. Bellhouse, B. J., Phil, D., and Bellhouse, F., "Fluid Mechanics of Model Normal and Stenosed Aortic Valves", Circ. Res., Vol. XXV, Dec., 1969.

9. Klatte, E. D., Tapas, J. P., Campbell, J. A., and Lurie, P. R., "The Roentgenographic Manifestation of Aortic Stenosis and Aortic Valvular Insufficiency", Amer. J. Roent., Vol. 88, 1962.

10. Braunwald, E. and Friedman, W. F., "Aortic Stenosis" in Paediatric Cardiology, Ed. by Nadas, A., Saunder, Philadelphia, 1963.

11. Private Communication with Roberta Williams, M.D.

12. Blackman, J. R. and Murray, John A., "Valvular Heart Disease" in Cardiovascular Dynamics, 3rd Ed., W. B. Saunders Co., Philadelphia, 1970.

13. Whittaker, A. V., Shaver, J. A., Gray, S., III, and Leonard, J. J., "Sound-Pressure Correlates of the Aortic Ejection Sound, An Interactive Sound Study", Circ., Vol. XXXIX, April, 1969.

14. Brackenbrough, E. C., Braunwald, E., and Ross, J., "Transseptal Left Heart Catheterization", Circ., Vol. 25, 1962.

15. Seldinger, S. I., "Catheter Replacement of the Needle in Percutaneous Arteriography", Acta. Radiol., Vol. 39, 1953.

16. Gorlin, R., and Gorlin, S. G., "Hydraulic Formula for Calculation of the Area of the Stenotic Mitral Valve, Other Cardiac Valves, and Central Circulatory Shunts", Amer. Heart J., Vol. 41, 1951.

17. Jacobs, J. E., Horikoshi, Kazuo, and Petrovick, M. A., "Feasibility of Automated Analysis of Phonocardiograms", J. Audio Engin. Soc., Vol. 17, Jan., 1969.

18. Rushmer, R. F., Morgan, C. L., and Harding, D. D., "Electronic Aids to Auscultation", Med. Res. Engin., Vol. 7, No. 4, 1968.

19. Holford, F. D., Dartmouth Med. School, Classroom Notes on Heart Sounds and Murmurs.

20. Shah, P. M., Mori, M., MacCanon, D. M. and Luisada, A. A., "Hemoeynamic Correlates of the Various Components of the First Heart Sound", Circ., Res., Vol. 12, 1963.

21. Tavel, M. E., Clinical Phonocardiography and External Pulse Recording, 2nd Ed., Year Book Medical Publisher, Inc., Chicago, 1972.

22. MacCanon, E. M., Arevalo, F. and Meyer, E. C., "Direct Detection and Timing of Aortic Valve Closure", Circ. Res., Vol. 14, 1964.

23. Piemme, T. E., Barnett, G. O., and Dexter, L., "Relationship of Heart Sounds to Acceleration of Blood Flow", Circ. Res., Vol. 18, March, 1966.

24. Kusukawa, R., Bruce, D. W., Sakamoto, T., MacCanon, D. M., and Luisade, A. A., "Hemodynamic Determinants of the Amplitude of the Second Heart Sound", J. Appl. Physiol., Vol. 21, 1966.

25. Sakamoto, T., Kusukawa, R., MacCanon, D. M., and Luisade, A. A., "Hemodynamic Determinants of the Amplitude of the First Heart Sound", Circ. Res., Vol. 16, Jan., 1965.

26. Hultgren, H. N., Reeve, R., Cohn, K., and McLeod, R., "The Ejection Click of Valvular Pulmonic Stenosis", Circ. Res., Vol. XL, Nov., 1969.

27. Epstein, E. J., Criley, J. M., Raftery, E. B., Humphries, J. O'Neal, and Ross, R. S., "Cine-radiographic Studies of the Early Systolic Click in Aortic Valve Stenosis", Circ. Res., Vol. 31, June, 1965.

28. "The Normal Heart", Clinical Educational Aid, No. 7, Ross Laboratories, Columbus, Ohio.

29. Thorek, P., Anatomy in Surgery, J. B. Lippincott Co., Philadelphia, 1962.

30. Spencer, M., and Edmunds, L. H., Jr., "Evaluation of Operative Left Ventricular Outflow Tract Lesions with a Fluid Impedance Plot", Circ. Res., Vol. 37, 1968.

31. Kennedy, J. W., Twiss, R. D., Blackman, J. R. and Dodge, H. T., "Quantitative Angiocardiography III: Relationships of Left Ventricular Pressure, Volume, and Mass in Aortic Valve Disease", Circ. Res., Vol. 38, 1968.

32. Morrow, A. G., Roberts, W. C., Ross, J. Jr., Fisher, R. D., Behrendt, D. M., Mason, D. T., and Braunwald, E., "Obstruction of Left Ventricular Outflow", Ann. Intern. Med., Vol. 69, 1968.

33. Rappaport, M. B. and Sprague, H. B., "The Graphic Registration of the Normal Heart Sounds", Am. Heart J., Vol. 23, 1942.

34. Leatham, A., Phonocardiology, Brit. M. Bull., Vol. 8, 1952.

35. Bache, R. J., Wang, Y., and Greenfield, J. C., Jr., "Left Ventricular Ejection Time in Valvar Aortic Stenosis", Circ. Res., Vol. XLVII, March, 1973.

36. Caseres, C. A., The Innocent Murmur, Little, Brown and Co., Boston, 1967.

37. Rushmer, R. F., and Morgan, C., "Meaning of Murmurs", Amer. J. Cardiol., Vol. 21, May, 1968.

38. Dock, W., "The Forces Needed to Evoke Sounds from Cardiac Tissues and the Attenuation of Heart Sounds", Circ. Res., Vol. XIX, March 1959.

39. Bruns, D. L., "A General Theory of the Causes of Murmurs in the Cardiovascular System", Amer. J. Med., Sept., 1959.

40. Meismer, J. E., and Rushmer, R. F., "Production of Sounds in Distensible Tubes", Circ. Res., Vol. 12, 1963.

41. Frueham, C. T., "On the Aeolian Theory of Cardiovascular Murmur Generation", New Physician, Vol. 11, 1962.

42. Lighthill, M. J., "On Sound Generated Aerodynamically II: Turbulence as a Source of Sound", Proc. Royal Soc., London, A222, 1954.

43. Yellin, E. L., "Hydraulic Noise in Submerged and Bounded Liquid Jets", Biomed. Fluid Mech. Sym., Denver, April, 1966.

44. Von Gierke, H. E., "Transmission of Vibratory Energy Through Human Body Tissue", Proc. First Natl. Biophy. Conf., Columbus, March, 1957.

45. Faber, J., Job, M. B. and Burton, A. C., "Biophysics of Heart Sounds and Its Application to Clinical Auscultation", Canac. Med. Assn. J., July, 1964.

46. Faber, J. J. and Purvis, J. H., "Conduction of Cardiovascular Sound Along Arteries", Circ. Res., Vol. 12, March, 1963.

47. Faber, J. J., and Burton, A., "Spread of Heart Sounds Over Chest Wall", Circ. Res., Vol. 11, July, 1962.

48. Faber, J. J., "Damping of Sound on the Chest Surface", Circ. Res., Vol. 13, Oct., 1963.

49. Zalter, R., Hardy, H. C. and Luisada, A. A., "Acoustic Transmission Characteristics of the Thorax", Appl. Physiol., Vol. 18, 1963.

50. Bergel, D. H., "The Dynamic Elastic Properties of the Arterial Wall", J. Physiol., 156, 1961.

51. Burton, A. C., Physiology and Biophysics of the Circulation, Year Book Med. Pub., Inc., Chicago, 1965.

52. Takagi, S., Yoshimura, S. and Okamura, T., "Transmission Problems of Sounds from Heart to Phonograph", 8th ICMBE, Chicago, July, 1969.

53. Anliker, M., Histand, M. B. and Ogden, E., "Dispersion and Attenuation of Small Artificial Pressure Waves in the Canine Aorta", Circ. Res., Vol. 23, Oct., 1968.

54. Levine, M. D., "Feature Extraction: A Survey", Proceedings of IEEE, Vol. 57, No. 8, August, 1969.

55. McKusick, V. A., Murry, G. E., Peeler, R. G. and Webb, G. H., "Musical Cardiovascular Murmurs", Bull. Hopkins Hosp., Vol. 97, 1955.

56. McKusick, V. A., "Spectra Phonocardiography", Am. J. Cardio., Vol. 4, 1959.

57. Remington, R. D., "Editorial: Statistics", Circ. Res., Vol. 39, April, 1969.

58. Gold, B. and Rader, C. M., Digital Processing of Signals, McGraw-Hill, New York, 1969.

59. Cooley, J. W. and Tukey, J. W., "An Algorithm for the Machine Calculation of Complex Fourier Series", Math. Comp., Vol. 19, April, 1965.

60. Bergland, G. D., "A Guided Tour of the Fast Fourier Transform", IEEE Spectrum, July, 1969.

61. Brigham, E. O. and Morrow, R. E., "The Fast Fourier Transform", IEEE Spectrum, December 1967.

62. Cochram, W., Cooley, J. W., Favin, D. L., Helms, H.D., Kaenel, R. A., Lang, W. W., Maling, G. C., Jr., Nelson, D. E., Rader, C. M., and Welch, P. D., "What is the Fast Fourier Transform?" IEEE Trans. on Audio & Electroacoustics, Vol. AU-15, No. 2, June, 1967.

63. Cooley, J. W., Lewis, P. A. W., and Welch, P. D., "Application of the Fast Fourier Transform to Computation of Fourier Integrals, Fourier Series, and Convolution Integrals", IEEE Trans. on Audio & Electroacoustics, Vol. AU-15, No. 2, June, 1967.

64. Ragazzini, J. R. and Franklin, G. F., Sampled-Data Control Systems, McGraw-Hill, New York, 1958.

65. Goldman, S., Information Theory, Dover Publications, Inc., New York, 1953.

66. Papoulis, A., The Fourier Integral and Its Applications, McGraw-Hill, New York, 1962.

67. Jenkins, G. M. and Watts, D. G., Spectra Analysis and Its Applications, Holden-Day, Inc., San Francisco, 1968.

68. Davenport, W. B., Jr., and Root, W. L., An Introduction to the Theory of Random Signals and Noise, McGraw-Hill, New York, 1958.

69. Blackman, R. B. and Tukey, J. W., The Measurement of Power Spectra, Dover Publications, New York, 1962.

70. Papoulis, A., Probability, Random Variables, and Stochastic Processes, McGraw-Hill, New York, 1965.

71. Richards, P. I., "Computing Reliable Power Spectra", IEEE Spectrum, January, 1967.

72. Bingham, C., Godfrey, M. D. and Tukey, J. W., "Modern Techniques of Power Spectrum Estimation", IEEE Trans. on Audio and Electroacoustics, Vol. AU-15, No. 2, June, 1967.

73. Bennett, W. R., Introduction to Signal Transmission, McGraw-Hill, New York, 1970.

74. Singleton, R. C. and Poulter, T. C., "Spectral Analysis of the Call of the Male Killer Whale", IEEE Trans. on Audio and Electroacoustics, Vol. AU-15, No. 2, June, 1967.

75. Rabiner, L. R. and Rader, C. M., Ed., Digital Signal Processing, IEEE Press, New York, 1972.

76. Helms, H. D. and Rabiner, L. R., Ed., Literature in Digital Signal Processing: Terminology and Permuted Title Index, IEEE Press, New York, 1972.

77. "Technical Report on Recommended Practices for Burst Measurements in the Frequency Domain", IEEE Trans. on Audio and Electroacoustics, Vol. AU-15, No. 1, March, 1967.

78. Beers, Y., Introduction to the Theory of Error, Addison-Wesley, Palo Alto, 1957.

79. Spiegel, M. R., Theory and Problems of Statistics, Schaum's Outline Series, McGraw-Hill, New York, 1961.

80. Rihaczek, A. W., Principles of High-Resolution Radar, McGraw-Hill, New York, 1969.

81. Bartlett, M. S., An Introduction to Stochastic Processes with Special Reference to Methods and Applications, Cambridge University Press, Cambridge, 1953.

82. Cambron, T. M., "Pattern Recognition Applied to Phonocardiogram Diagnosis", Ph.D. Thesis, Department of Electrical Engineering, University of South Carolina, 1971.

83. Vocker, M. C., "An Adaptive Method of Epoch Location for Repetitive Signals", Ph.D. Thesis, Department of Electrical Engineering, University of Iowa, 1971.

84. Stephens, J., "The Diagnostic Value of a Frequency Analysis of the Isovolumic Phase of the First Heart Sound", Ph.D. Thesis, Department of Electrical Engineering, University of Cincinnati, 1969.

85. Perry, L. W., Sherman, D., Winer, D. E., Weihrer, A. L., Hodgson, D., and Caceres, C. A., "Computer Analysis of the Phonocardiogram", in Engineering in the Practice of Medicine, Williams and Wilkins Co., Baltimore, 1967.

86. Frome, E. L., and Frederickson, E. L., "Digital Spectrum Analysis of the First and Second Heart Sounds", Computer and Biomedical Research, Vol. 7, pp. 421-431, 1974.

87. Gerbarg, S. D., Taranta, A., Spagnuolo, M., and Hotlev, J. J., "Computer Analysis of Phonocardiograms", Progress in Cardiovas. Disease, Vol. 5, No. 4, Jan., 1963.

88. Townes, W. H., Bosers, M. J. and Braun, A. H., "Characteristics of Innocent and Stenotic Cervical Bruits", Amer. Heart J., Vol. 79, No. 6, June, 1970.

89. Schroeder, M.R., Flanagan, J. L., and Lundry, E. A., "Bandwidth Compression of Speech by Analytic-Signal Rooting", Proceedings of IEEE, Vol. 55, No. 3, March, 1967.

90. Rubin, W. L., and DiFranco, J. V., "Analytic Representation of Wide-band Radio Frequency Signals", J. Franklin Inst., Vol. 275, pp. 197-204, 1963.

APPENDIX I

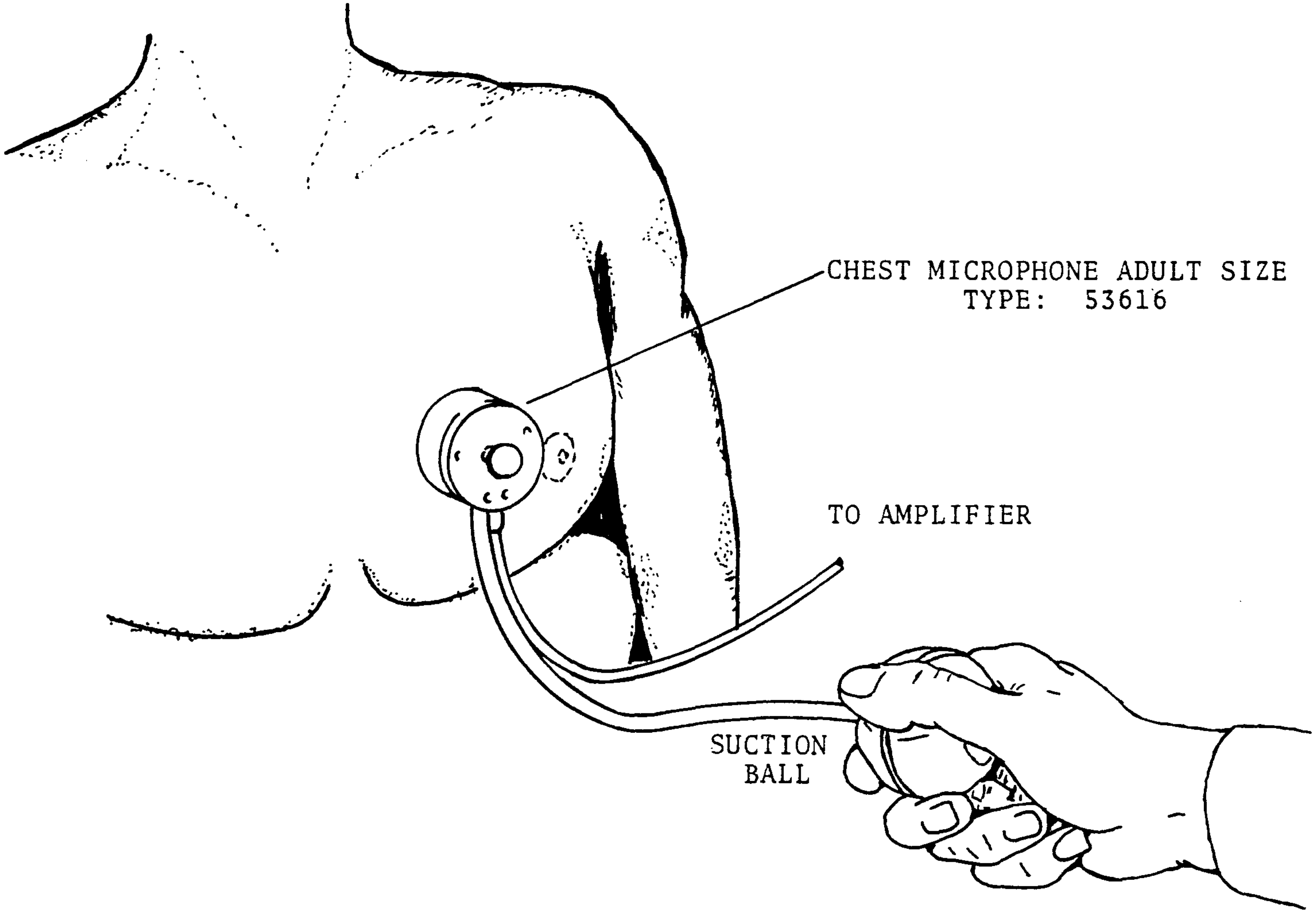

Fig. 1,AI. Microphone placement on the chest

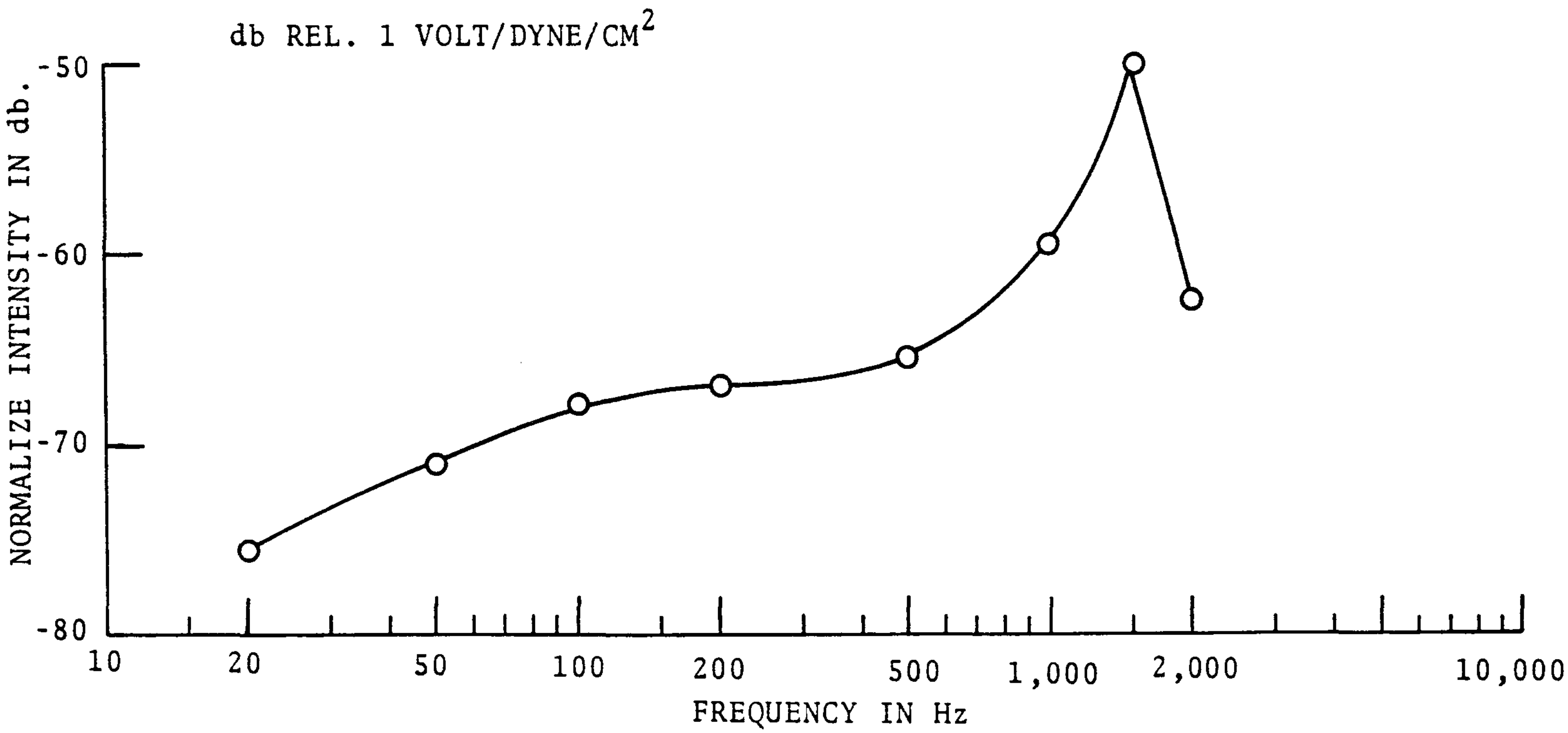

Fig. 2, AI. Amplitude response curve of a type 53616 microphone

TABLE 1,AI

ACOUSTICAL COMPARISON OF MICROPHONE 2 VERSUS MICROPHONE 1

Frequency of Tone Generator	Relative Error* of Mic. 2 vs. Mic. 1
125 Hz	- 19.1%
250 Hz	- 6.15%
500 Hz	0.0%
1000 Hz	- 10.8%
2000 Hz	+ 19.2%

*The relative error of microphone 2 $E_2(f)$ is defined as

$$E_2(f) = \left(\frac{\bar{R}_2(f) - \bar{R}_1(f)}{\bar{R}_1(f)} \right) 100\%$$

where $\bar{R}_i(f) = \dfrac{R_i(f)}{R_i(500)}$ = Normalized voltage response of microphone 1 to a constant intensity acoustical source. Reference response is chosen at 500 Hz.

TABLE 2,AI

PATIENT HEADER FORMAT

Name/Hosp. # :

Exam Date :

Diagnosis :

Sex :

Age :

Chest Wall :

Chest Deformity:

Fever :

Catheter Data Available ?:

Analog Tape #, Record # :

Comments on Analog Tape :

Pass 1 Conversion Date :

Next File:

Phono 1: Phono 2:

ECG Lead: Pulse/Resp:

TABLE 3,AI

DATA HEADER FORMAT

Name/Hosp. #:

Next File: Phono 1: Phono 2:

ECG Lead: Pulse/Resp:

```
*
*       MOD16
* ANALOG READ BINARI DUMP
* A. SARKADY 4/8/73
* TEM1 =MODUL 4 COUNT INI VAL =077777
* TEM2=MODUL 3200 COUNTER INI VAL =071600
* P1B= STAR ADD OF IN BUF
* P2B =STAR ADD OF OUT BUF
* B REG=ADD OF SOUND DATA
* EIGHT M. S. B.  = PHONO 1
* EIGHT L. S. B.  = PHONO 2
* X REG = ADD OF PULSE AND E. C. G.  DATA  INI = 010640
* EIGHT M. S. B.  = PULSE DATA
* EIGHT L. S. B. =E. C. G DATA
*  SEN SW1 UP =STOP AND CONT WITH READ WHEN DOWN
*  SEN SW2 UP=STOP AND PULL FILE GAP
*
* INIT TEM1,TEM2,OTEM,ITEM,XREG,BREG,BIC
*
*
*
        NAME    ANAL
*
*
P1B     EXT
P2B     EXT
*
ANAL    ENTR
        STX     SAVX
        STB     SAVB
ENT     ROF
        TZA
        IAR
        STA     TEM3            PASS1 REC COUNT
        LDAI    077777

        STA     TEM1
        LDAI    071600

        STA     TEM2
        LDAI    P2B

        STA     OTEM
        LDBI    P1B

        STB     ITEM
        LDAI    P1B

        ADDI    3200

        TAX     INI X REG
```

```
*
JOY     SEN     0050,SEN1

        NOP
        JMP     JOY

*
*
* MAIN PROG
*
SEN1    CIA     050
        SEN     0150,G01     PULSE AND RESP DATA

        NOP
        JMP     *-3

G01     INR     TEM1
        JOF     PE

*
        SEN     0250,*+5

        NOP
        JMP     *-3

        CIA     050
*
SEN3    SEN     0350,G02    SOUND 1 D

        NOP
        JMP     *-3

G02     CIA     050
        LRLA    8
        SEN     0050,G03    SOUND 2 D

        NOP
        JMP     *-3

G03     INA     050
        STA     0,2         B=2
        IBR
        INR     TEM2
        JOF     BIC

        JMP     SEN1+1

*
*
* READ PULSE AND E.C.G.  DATA
*
PE      ROF
        CIA     050
```

```
        LRLA    8
        SEN     0250,G04
        NOP
        JMP     *-3
G04     INA     050
        STA     0,1         X=1
        IXR
        LDAI    077774      INI TAMP 1 MOD 4
        STA     TEM1
        JMP     SEN3
*
* BIC BUSSY ?,ERR MES,SWAP POINT,BIC WRITE
*
BIC     ROF
        SEN     0210,CON     MTU  READY
        JMP     BB
CON     SEN     021,BS      BIC  ABNORM STOP
        SEN     020,SWAP    BIC,NOT BUSSY
        JMP     BB
SWAP    LDA     ITEM
        LDB     OTEM
        STA     OTEM
        STB     ITEM
        EXC     021         INIT BIC
        DAR
        OAR     020         BIC INI ADD
*
        TAX
        LDA     TEM3
        STA     0,1
        TXA
*
        ADDI    4000
        OAR     021         BIC FINAL ADD
*
        LDA     ITEM
        ADDI    3200
        TAX
        LDAI    071600      INI TEM2
        DATA    0104110
        STA     TEM2
*
```

```
*
        EXC     020         ACT BIC
        EXC     0210        WRITE MTOO
        JSS1    HALT
        JSS2    FILE
        INR     TEM3
        JMP     GO1
*
*
* ERROR ROUTINE
*
BS      LDAI    'SB'
        JMP     OCH
BB      LDAI    'BB'
        JMP     OCH
OCH     ROF
        SEN     0101,*+5
        NOP
        JMP     *-3
        OAR     01
        JOF     HALT
        SOF
        LRLA    8
        JMP     OCH+1
HALT    HLT
        JMP     ENT
*
FILE    SEN     0210,FG     MTU READY
        NOP
        JMP     *-3
FG      EXC     0410
        LDX     SAVX
        LDB     SAVB
        JMP*    ANAL
*
TEM3    DATA    0
*
```

```
SAVX    BSS     1
SAVB    BSS     1
TEM1    BSS     1
TEM2    BSS     1
OTEM    BSS     1
ITEM    BSS     1
*
*
        END     ENT
```

```
ENTRY NAMES
 000000 R ANAL
EXTERNAL NAMES
 000024 E P1B     000016 E P2B
```

```
SYMBOLS
 000000 R ANAL
 000125 R CON
 000043 R GO1
 000217 R HALT
 000241 R OTEM
 000236 R SAVB
 000133 R SWAP

000176 R BB      000120 R BIC     000172 R BS
000003 R ENT     000227 R FG      000222 R FILE
000061 R GO2     000070 R GO3     000110 R GO4
000242 R ITEM    000030 R JOY     000202 R OCH
000024 E P1B     000016 E P2B     000100 R PE
000235 R SAVX    000035 R SEN1    000054 R SEN3
000237 R TEM1    000240 R TEM2    000234 R TEM3
```

```
*** DASFFT   N MAX=1024 F NICHOLS/A SARKADY 8-5-73
*****************************************************
*                                                   *
*          COMPLEX                                  *
*          FAST FOURIER TRANSFORM                   *
*          FOR INTEGER VALUES                       *
*                                                   *
*         CALL INFFT(ICSTB,N)
*          TO INITIALIZE COS TABLE                  *
*         DIMENSION ICSTB(N/4+1)
*                                                   *
*         CALL FFTM(IREAL,IMAG,NSHFTS)
*          TO TAKE TRANSFORM                      . *
*          *** NSHFTS ***                           *
*          ON INPUT    0+ => IDFT , - => DFT        *
*          ON OUTPUT, SCALE FACTOR=2**NSHFTS        *
*                                                   *
*****************************************************
*
          NAME      INFFT,FFTM,ICSTB
*
*SF       EXT
*
*          MACRO TO COMPLEMENT AND INCREMENT
*          FROM SOURCE TO DESTINATION
*
MINUS     MAC
          COMPL     0200+P(1)+010+P(2)
          INCR      0100+P(2)+010+P(2)
          EMAC
*
B         EQU       02              INDEX WITH B
X         EQU       01              INDEX WITH X
AR        EQU       01              A REGISTER
BR        EQU       02              B REGISTER
XR        EQU       04              X REGISTER
*
*
SFFT      LDA       NOP             INITIALIZE COMMANDS/
          STA       SKIP            CONSTANTS
          LDXE*     OVNUM           DFT OR IDFT '

          STX       FTRN            0+ => IDFT,  - => DFT
          TZA
          STAE*     OVNUM

          LDA       RWORK
          ADD       N
          STA       PASSC           END-OF-STAGE CONSTANT
          ROF
*
          LDA       ND2
          STA       SEPR            INITIAL SPAN
```

```
*
M1       LDA      RWORK       INITIAL POINTS
         STA      REAL
         ADD      SFPR
         STA      RMULT
         LDA      IWORK
         STA      IMAG
         ADD      SFPR
         STA      IMULT
*
*
         TZA                  INITIALIZE
         SUB      ND4         INDEX
         STA      INDX        POINTER
*
M2       TZA                  EXIT WHEN TERMS
         SUB      SFPR        WITH COMMON MULTIPLIER
         STA      EXIT        HAVE BEEN PROCESSED
*
         JMPM     INDEX

*
*          DETERMINE SIN/COS TERMS
*          RETURN WITH ARGUMENT IN A
*
         ROF                  RESET INDICATOR
         TAB
         MINUS    AR,AR


         ADD      ND4         FORM N/4-X
         TAX
         XAP      SOF         SOF IF 0<=X<=N/4

         JAP      M22         SKIP IF 0<=X<=N/4

         MINUS    AR,XR       DO IF N/4<X<N/2


         MINUS    BR,AR


         ADD      ND2
         JMP      M22+1

M22      TBA
         ADD      TABLE
         TAB
         TXA
         ADD      TABLE
         TAX
         LDX      0,X
         LDA      FTRN
```

```
             JAP      M221       JMP IF IDFT

             MINUS    XR,XR      DO IF DFT

     M221    STX      SIN
             LDA      0,B
             JOF      M23        JMP IF 0<=X<=N/4

             MINUS    AR,AR      DO IF N/4<X<N/2
     M23     STA      COS
     *
     M3      TZA                 FORM TERMS
             LDBF*    IMULT

             MUL      SIN
             STA      RTERM
             TZA
             LDBF*    RMULT

             MUL      COS
             SUB      RTERM
             STA      RTERM
     *
     *
             TZA
             LDBF*    RMULT

             MUL      SIN
             STA      ITERM
             TZA
             LDBF*    IMULT

             MUL      COS
             ADD      ITERM
             STA      ITERM
     *
             JOFM     OVFLO      IF O=1, CORRECT/RESET

     *
     M4      LDX      REAL       COMBINE TERMS
             LDA      0,X        CHECK OVERFLOW
             SUB      RTERM      STORE
             TAB
             LDA      0,X
             ADD      RTERM
             JOFM     OVFLO

     REM4    STBF*    RMULT

             STAF*    REAL

     *
```

```
M5      LDX      IMAG
        LDA      0,X
        SUB      ITERM
        TAB
        LDA      0,X
        ADD      ITERM
        JOFM     OVFLO

REM5    STBE*    IMULT

        STAE*    IMAG

*
        INR      REAL         INCREMENT
        INR      RMULT        POINTERS
        INR      IMAG
        INR      IMULT
*
        INR      EXIT
        LDA      EXIT         SKIP IF ALL TERMS
        JAN      M3           WITH COMMON MULT DONE

*
        LDA      RMULT
        ERA      PASSC
        JAZ      FIN          ALL DONE THIS STAGE?

        JMP      NOFIN        NO!!

*
*
OVFLO   ENTR.                 OVERFLOW FIXUP
        INRE*    OVNUM

        LDA      RWORK
        JMPM     SHIFT

        LDA      IWORK
        JMPM     SHIFT

        LDA      RTERM
        ASRA     01
        STA      RTERM
        LDA      ITERM
        ASRA     01
        STA      ITERM
        LDAE     OVFLO

        ERAI     REM4

        JAZ      M4

        LDAE     OVFLO
```

```
         ERAI     REM5
         JAZ      M5
         JMP      M3
*
SOF      SOF                  SET INDICATOR
*
SHIFT    ENTR                 SHIFT ALL DATA
         TAX                  RIGHT ONE BIT
         ADD      N
         STA      DUN
SHT      LDB      0,X
         ASRB     01
         STB      0,X
         IXR
         TXA
         ERA      DUN
         JAZ*     SHIFT
         JMP      SHT
*
DUN      BSS      1
*
NOFIN    LDA      REAL        UPDATE START
         ADD      SEPR        OF BUTTERFLY
         STA      REAL
         ADD      SEPR
         STA      RMULT
         LDA      IMAG
         ADD      SEPR
         STA      IMAG
         ADD      SEPR
         STA      IMULT
         JMP      M2
*
FIN      LDA      SEPR        DIV SEPR BY 2
         ASRA     01
         JAZ      S1          STAGES ALL DONE?
         STA      SEPR        NO!!!
         JMP      M1          START NEXT STAGE
*
*
*          ROUTINE TO GIVE
*          ACCESS TO COS TABLE OR
*          UNSCRAMBLE FINAL VALUES
*
*
INDEX    ENTR                 DETERMINE INDEX
```

```
        LDA     INDX        FOR REVERSE BIT COUNT
        LDB     ND2
        MINUS   BR,BR


SKIP    NOP                 MODIFIED BY S1
        ASRB    01
SKPT    STB     *+2
        ADDI    0

        JAP     SKIP+1

        MINUS   BR,BR


        ASLB    01
        STB     *+2
        ADDI    0

        STA     INDX
        JMP*    INDEX

*
S1      TZA                 UNSCRAMBLE BIT
        SUB     N           REVERSE INDICES
        STA     EXIT
        LDA     RWORK
        STA     RR1
        LDA     IWORK
        STA     II1
*
        TZA
        SUB     ND2
        STA     INDX
        LDA     SKPOVR
        STAE    SKIP

*
S2      JMPM    INDEX

        TAX
        ADD     RWORK
        STA     RR2
        TXA
        ADD     IWORK
        STA     II2
*
        LDA     RR1
        SUB     RR2
        JAP     S3          IF = DON'T SWITCH

*
```

```
*
           LDAE*    RR1         SWITCH REALS
           LDBE*    RR2
           STAE*    RR2
           STBE*    RR1
*
           LDAE*    II1         SWITCH IMAGS
           LDBE*    II2
           STAE*    II2
           STBE*    II1
*
 S3        INR      II1         INCR POINTERS
           INR      RR1
           INR      EXIT
           LDA      EXIT
           JAN      S2          GO SWITCH MORE
           JMP      0           ALL BEEN SWITCHED
 FFTM      BES      0
           CALL     $SE,3
 RWORK     BSS      1           REAL ARRAY ADDRESS
 IWORK     BSS      1           IMAG ARRAY ADDRESS
 OVNUM     BSS      1           OVFL/DFT ADDRESS
           JMP      SFFT        START TRANSFORM
           EJEC
 SIFFT     LDAE*    N
           STA      N
           ASRA     01
           STA      ND2
           ASRA     01
           STA      ND4
           LDB      TABLE
           STB      TPTR
*
*           DETERMINE TABLE VALUE SPACING
*
           TZB
           IBR
 NAGN      TAX
           ERAI     256
```

```
         JAZ     NOUT

         TXA
         LLRL    01
         JMP     NAGN

NOUT     STB     INCR
*
*         STORE TABLE
*
         LDX     TPTR
         LDBI    ICSTB

I1       LDA     0,B
         STA     0,X
         IXR
         JAZ*    INFFT

         TBA
         ADD     INCR
         TAB
         JMP     I1

INFFT    ENTR
         CALL    $SE,2


TABLE    BSS     1
N        BSS     1
         JMP     SIFFT
         EJEC
*         SET UP STORAGE AND DATA
*
FTRN     BSS     1
ND2      BSS     1
ND4      BSS     1
TPTR     BSS     1
INCR     BSS     1
PASSC    EQU     TPTR
SEPR     EQU     INCR
INDX     BSS     1
REAL     BSS     1
RMULT    BSS     1
IMAG     BSS     1
IMULT    BSS     1
COS      BSS     1
SIN      BSS     1
RTERM    BSS     1
ITERM    BSS     1
EXIT     BSS     1
RR1      EQU     TPTR
II1      EQU     INCR
RR2      EQU     REAL
```

```
TIZ     EQU     RMULT
NOP     NOP                     DO NEXT INSTRUCTION
SKPOVR  DATA    01006           SKIP NEXT INSTRUCTION
*
ICSTB   EQU     *
*
*       FIXED POINT COS TABLE
*       0-90 DEGREES 257 POINT
*
        DATA    32767,32766,32765,32761,32757

        DATA    32752,32745,32737,32728,32717

        DATA    32705,32692,32678,32663,32646

        DATA    32628,32609,32589,32567,32545

        DATA    32521,32495,32469,32441,32412

        DATA    32382,32351,32318,32285,32250

        DATA    32213,32176,32137,32098,32057

        DATA    32014,31971,31926,31880,31833

        DATA    31785,31736,31685,31633,31580

        DATA    31526,31470,31414,31356,31297,31237
```

```
368     DATA    31176, 31113, 31050, 30985, 30919

369     DATA    30852, 30783, 30714, 30643, 30571

370     DATA    30498, 30424, 30349, 30273, 30195

371     DATA    30117, 30037, 29956, 29874, 29791

372     DATA    29706, 29621, 29535, 29447, 29358

373     DATA    29268, 29177, 29085, 28992, 28898

374     DATA    28803, 28706, 28609, 28510, 28411

375     DATA    28310, 28208, 28105, 28001, 27896

376     DATA    27790, 27683, 27575, 27466, 27356

377     DATA    27245, 27133, 27019, 26905, 26790

378     DATA    26674, 26556, 26438, 26319, 26198
```

```
379   DATA   26077, 25955, 25832, 25708, 25582
380   DATA   25456, 25329, 25201, 25072, 24942
381   DATA   24811, 24680, 24547, 24413, 24279
382   DATA   24143, 24007, 23870, 23731, 23592
383   DATA   23452, 23312, 23170, 23027, 22884
384   DATA   22739, 22594, 22448, 22301, 22154
385   DATA   22005, 21856, 21705, 21554, 21403
386   DATA   21250, 21096, 20942, 20787, 20631
387   DATA   20475, 20317, 20159, 20000, 19841
388   DATA   19680, 19519, 19357, 19195, 19032
389   DATA   18868, 18703, 18537, 18371, 18204
```

```
390     DATA    18037, 17869, 17700, 17530, 17360

391     DATA    17189, 17018, 16846, 16673, 16499

392     DATA    16325, 16151, 15976, 15800, 15623

393     DATA    15446, 15269, 15090, 14912, 14732

394     DATA    14553, 14372, 14191, 14010, 13828

395     DATA    13645, 13462, 13279, 13095, 12910

396     DATA    12725, 12539, 12353, 12167, 11980

397     DATA    11793, 11605, 11417, 11228, 11039

398     DATA    10849, 10659, 10469, 10278, 10087

399     DATA    9895, 9704, 9511, 9319, 9126

400     DATA    8933, 8739, 8545, 8351, 8156
```

```
401     DATA    7961,7766,7571,7375,7179
402     DATA    6983,6786,6589,6392,6195
403     DATA    5997,5799,5601,5403,5205
404     DATA    5006,4808,4609,4409,4210
405     DATA    4011,3811,3611,3411,3211
406     DATA    3011,2811,2611,2410,2210
407     DATA    2009,1808,1607,1407,1206
408     DATA    1005,804,603,402,201,0
409     END
```

```
ENTRY NAMES
 000405 R FFTM    000511 R ICSTB   000460 R INFFT
EXTERNAL NAMES
 000462 E $SE
```

SYMBOLS

```
000462 E $SE     000001 A AR      000002 A B
000502 R COS     000254 R DUN     000506 R EXIT
000271 R FIN     000470 R FTRN    000446 R I1
000474 R II1     000477 R II2     000500 R IMAG
000474 R INCR    000300 R INDEX   000475 R INDX
000505 R ITERM   000412 R IWORK   000016 R M1
000057 R M22     000073 R M221    000101 R M23
000132 R M4      000146 R M5      000465 R N
000471 R ND2     000472 R ND4     000255 R NOFIN
000442 R NOUT    000200 R OVFLO   000413 R OVNUM
000476 R REAL    000142 R REM4    000156 R REM5
000473 R RR1     000476 R RR2     000504 R RTERM
000325 R S1      000342 R S2      000376 R S3
000000 R SFFT    000236 R SHIFT   000242 R SHT
000503 R SIN     000305 R SKIP    000510 R SKPOVR
000235 R SOF     000464 R TABLE   000473 R TPTR
000004 A XR
                 000002 A BR
                 000405 R FFTM
                 000511 R ICSTB
                 000501 R IMULT
                 000460 R INFFT
                 000031 R M2
                 000102 R M3
                 000431 R NAGN
                 000507 R NOP
                 000473 R PASSC
                 000477 R RMULT
                 000411 R RWORK
                 000474 R SEFR
                 000416 R SIFFT
                 000307 R SKPT
                 000001 A X
```

APPENDIX II

DESCRIPTION OF THE INTERACTIVE ANALYSIS

An interactive analysis program was used to compute envelograms, power spectra, and time-averaged phonocardiograms for the diagnostic analysis procedure.

Prior to data input, the type of record (PHON1, PHON2, etc.), the data window, the sampling rate and the number of records averaged were selected. A record was deleted from the analysis if the record length (Q-Q interval) was not within an acceptable specified range or if the record number was entered in a delete table. During data input, selected records were aligned (time-shifted to the left or right) by a two-pass process.

In the first pass a specified signal feature (local maximum or minimum) was searched for within a specified time range and the location of the signal feature for each record was tabulated in a table. Using this table, a mean alignment time was computed. The sliding increments necessary to cause alignment about this mean time was computed for each record and stored in the same table. During the second pass, the input data tape was repositioned, the same data was acquired and according to the tabulated correction factors, alignment corrections were made prior to analysis.

An analysis routine was composed of modular computational algorithms (such as FFT, magnitude, IFFT, etc.) and was of a standard type (time, envelope, or power spectrum) or was specifically created to suit a special need. In either case, the analysis was implemented from a command table containing a sequence of algorithm characters which defined the required analysis routine.

All the analyzed records were added to a 512 floating-point word accumulator buffer. When the specified number of records were analyzed, the average buffer values were computed and plotted on the graphics terminal or output to magnetic tapes. A listing of the interactive analysis program is shown on the following pages.

PAGE 1

```
***     AUTOFREQ GEN FORT ANALYS VERS#2  3-5-74 A. SARKADY
*       SAMF AS FREQAN BUT LOADS  ANV TIME AND CAL BRANCHES
*       AND CAN ZERO A TIME INTERVAL
*
        COMMON ID( 3 ), IR1( 1024 ), IM1( 1024 ), IDA( 4 )
        COMMON A( 512 )
*
        DIMENSION INT( 6 ), MAT( 12 ), RMS( 2 )
        DIMENSION SAM( 4 ), IH( 2 ), HAD( 6 ), IL( 2 )
        DIMENSION IPW( 2048 ), PW( 1024 )
        DIMENSION AT( 6 )
        DIMENSION MRECS( 40 )
        DIMENSION IZ( 2 )
*
        EQUIVALENCE( IR1( 1 ), IPW( 1 ), PW( 1 ) )
*
        EXTERNAL ICSTB
        EXTERNAL NAMBF
*
        DATA RMS/1. , 1. /
        DATA SAM/8. E-4, 3. 2E-3, 4. E-4, 1. 6E-3/
        DATA IH/0, 0/
        DATA HAD( 1 )/0. /
        DATA IL/2HP1, 2H  /
        DATA AT/4HTIM. , 4HANS. , 4HPWS. , 4HSUM. , 4HDEF. , 4HABS. /
        DATA LUNO, LUN1/0, 1/
        DATA MINCOR/1/
        DATA MAXCOR/2048/
        DATA INT/1, 0, 818, 0, 1, 0/
        DATA IZ/0, 0/
        DATA IBLK/2H  /
*
*
*
*       START INTERACTIVE ANALYSIS
*
*       ENTER FUNCTION COMMENDS FROM TY
*
*       O=79=OUTPUT ARRAY ( A ) TO MT01
*       PLOT ARRAY ( A ) =P=80
*       ENTER INPUT DATA COND COMMENDS =D=68
*       ENTER ANALYSIS COMMENDS =C=67
*       START ANALYSIS A=65
*       R=82=ENTER REC# TO BE SKIPED
*       M= CALL CURSOR =77
*       N=78=NEW ( INIT OUTPUT REC#, AND MRECS ARRAY  )
*
*       S=83=STAND ANAL BRANCH
*       G=71=GO BACK TO START ON MT00
*       J=74=CONTINUE WITH ANALISIS
```

```
*        Z=90=ENTER TIME SFGMENT TO BE ZEROED
*
*
5        IDA( 4 )=0
         =0
         CALL HOLLER( 8HINIT OR#, 8 )
3        CALL INIBUF( 40, MRFCS )
         =0
         CALL HOLLER( 10HINIT MREC  , 10 )
 1       CALL INFFT( ICSTB, 1024 )
         CALL CONTAP( LUNO, LUNO, LUNO, LUN1 )
 6       CALL    BEL
 2       CALL BEL
         CALL CHIN( ICOM )
*
         IF( ICOM. EQ. 90 )GO TO 800
         IF( ICOM-84 )401, 150, 1
 401     IF( ICOM. EQ. 80 )GO TO 15
         IF( ICOM. EQ. 79 )GO TO 20
         IF( ICOM. EQ. 87 )GO TO 700
         IF( ICOM. EQ. 78 )GO TO 5
         IF( ICOM. EQ. 83 )GO TO 600
         IF( ICOM-76 )400, 420, 402
 400     IF( ICOM. EQ. 68 )GO TO 30
         IF( ICOM. EQ. 67 )GO TO34
         IF( ICOM. EQ. 65 )GO TO 40
         IF( ICOM. EQ. 71 )GO TO 451
         IF( ICOM. EQ. 74 )GO TO 42
         GO TO 1
*
*        Z=90=ENTER TIME SEGMENT TO BE ZEROED
*
800      IZ( 1 )=0
         IZ( 2 )=0
         CALL DECIN( IZ( 1 ) )
         CALL DECIN( IZ( 2 ) )
         GO TO 6
*
*        G=71=GO BACK TO START ON MT00
*
451      J=NRFCNT-1
         IF( IOFS. EQ. 0 )J=J+1
         J=4*J+1
         CALL CONTAP( 1, 2HRB, 0, J )
         GO TO 6
*
*        S=83=START STAND ANAL BRANCHS
*
*        E=69=ENVELOP   R, F, D, I, M, V, A
*        T=84=TIME SERIES  R, T, V, A
```

PAGE 3

```
*        C=67=CALIBRATION   R,C,T,P,V,A
*        S=83=POWER SPECTRUM     R,F,S,V,A
*
600      =0
         CALL HOLLER(8H D.TYP= ,8)
         CALL DECIN(INT(1))
         =0
         CALL HOLLER(6HD.AN= ,6)
         CALL BEL
         CALL CHIN(ICOM)
*
         IF(ICOM.EQ.69)GO TO 610
         IF(ICOM.EQ.84)GO TO 620
         IF(ICOM.EQ.67)GO TO 630
         IF(ICOM.EQ.83)GO TO 640
         GO TO 6
*
610      MAT(2)=70
         MAT(3)=68
         MAT(4)=73
         MAT(5)=77
         MAT(6)=86
         MAT(7)=65
612      INT(5)=50
615      MAT(1)=82
         GO TO 40
*
620      MAT(2)=84
         MAT(3)=86
         MAT(4)=65
         GO TO 612
*
630      MAT(2)=67
         MAT(3)=84
         MAT(4)=80
         MAT(5)=86
         MAT(6)=65
         INT(5)=1
         GO TO 615
*
640      MAT(2)=70
         MAT(3)=83
         MAT(4)=86
         MAT(5)=65
         GO TO 612
*
*
*        R=82=ENTER Q-Q MIN,MAX COR LEN AND REC# TO BE SKIPED
*
700      MINCOR=1
```

PAGE 4

```
            MAXCOR=2048
            CALL DECIN(MINCOR)
            CALL DECIN(MAXCOR)
            =0
            CALL HOLLER(6H REC#=,6)
            CALL INIBUF(40,MRECS)
      702   CALL CHOU(13)
            CALL CHOU(10)
            =0
            CALL HOLLFR(4H    ,4)
            CALL DECIN(J)
            IF(J.LE.0)GO TO 6
            IF(J.GT.40)GO TO 6
            MRECS(J)=J
            =J
            CALL DECINA
            GO TO 702
      *
      *
      *     OUTPUT PROSSESED DATA TO MT01
      *
      *     IDA(1)=W LENGTH IA(2)=#IPUT RECORDS AVERAGED
      *     IDA(3)=REC ID  IDA(4)=REC#
      *
       20   IDA(1)=1028
            IDA(2)=IREC
            IDA(3)=IH(1)
            IDA(4)=IDA(4)+1
            CALL IODATA(0,IDA(1),LUN1,IDA(1),IOFS)
            GO TO 6
      *
      *     DIV AVER BUF
      *
       10   DO 12 J=1,512
       12   A(J)=A(J)/FLOAT(IREC)
            LIMP=LIMP/2
            GO TO 6
      *
      *     P=PLOT A
      *
      *
       15   CALL    ERAS
            NSTAR=1
            NEND=512
            CALL DECIN(NSTAR)
            CALL DECIN(NEND)
      11    CALL PHEAD(INT(1))
      16    =32
            CALL BLANKA
            IF(IZS.NE.0)GO TO 17
```

PAGE 5

```
            CALL DECH4( IBLK, 2H Z, IZ( 1 ))
            CALL DECH4( IBLK, IBLK, IZ( 2 ))
   17       =0
            CALL BLANKA
            CALL DECH4( IBLK, 2H T, INT( 2 ))
            CALL DECH4( IBLK, IBLK, INT( 3 ))
            CALL CHOU( 13 )
            CALL CHOU( 10 )
            =30
            CALL BLANKA
            CALL DECH4( IBLK, 2H N, IREC )
            CALL DECH4( IBLK, 2H R, ID( 2 ))
            CALL ENPLOT( A, NSTAR, NEND, SAMP, IH( 1 ))
            GO TO 6
 *
 *          CURSOR=MEASURS TIME AND FREQ FROM AVER PLOTS
 *              T=TIME IN M. SEC   RUBOUT =RET TO 6   OTHERS=FREQ IN
 *
    402     CALL CURSOR( ICHAR, NXP, NYP )
            NXO=FLOAT( NXP )*SAMP
            IF( ICHAR. EQ. 84 )NXO=FLOAT( NXP )*SAMP*1000.
            IF( ICHAR. EQ. 127 )GO TO 6
            =NXO
            CALL DECINA
            GO TO 402
 *
 *
 *  10*LOG10( A )=4. 34*ALOG( A )
 *
   420      GO TO 6
 *
 *
 *
 *          INPUT DATA PARAMETERS
 *
 *          INT( 1 )=DATA TYPE 1. . . 4
 *          INT( 2 )=START TIME IN M. SEC
 *          INT( 3 )=END TIME IN M. SEC
 *          INT( 4 )=0=SUM    INT( 4 )=1=DEFOLD
 *          INT( 5 )=#REC TO BE AVER
 *          INT( 6 )=EXTRA
 *
 *
    30      INT( 4 )=0
            INT( 5 )=100
            INT( 6 )=10
            =0
            CALL HOLLER( 6HIN PAR, 6 )
            L=1
    32      IF( L. GE. 6 )GO TO 6
```

```
          CALL DECIN(INT(L))
          IF(INT(L).LT.0)GO TO 30
          L=L+1
          GO TO 32
*
*
*         LOAD MAT TABLE
*
*
*
 34       =0
          CALL HOLLER(6HAN COM,6)
          L=1
  36      CALL BEL
          CALL CHIN(MAT(L))
          IF(MAT(L)-65)34,6,38
  38      L=L+1
          GO TO 36
*
*
*         INPUT DATA ACORDING TO INT TABLE
*
*
  40      CALL INIBUF(1024,A)
          SAMT=SAM(1)
          IREC=0
          NRECNT=0
          MINLEN=512
          IZS=1
*
          IF(INT(1).GE.3)SAMT=SAM(2)
          ISTART=FLOAT(INT(2))/(SAMT*1000.)
          IEND=FLOAT(INT(3))/(SAMT*1000.)
          RMSV=RMS(1)
          IF(INT(1).EQ.2)RMSV=RMS(2)
          IF(INT(4).GE.1)SAMT=SAMT/2.
          SAMF=1./(1024.*SAMT)
          CALL INIBUF(12,HAD)
*
  42      IWC=IEND-ISTART+1
          CALL INIBUF(2048,IPW)
          CALL IODATA(INT(1),2051,LUNO,ID(1),IOFS)
          IF(IOFS.EQ.0)GO TO 10
          NRECNT=NRECNT+1
          J=ID(2)
          IF(J.EQ.MRECS(J))GO TO 42
          IF(ID(1).GT.MAXCOR)GO TO 42
          IF(ID(1).LT.MINCOR)GO TO 42
          J=ID(1)-ISTART-3
          IF(IWC.GT.J)IWC=J
```

PAGE 7

```
            IF( IWC. GT. 1024 )IWC=1024
            CALL LSRBUF( 2048, ISTART, IFW )
            LWCO=2048-IWC
            CALL INIBUF( LWCO, IFW( IWC+1 ) )
 *
 *          DEFOLD
 *
            IF( INT( 4 ). EQ. 0 )GO TO 43
            CALL DEFOLD( IWC, IR1 )
            IWC=2*IWC
            HAD( 2 )=AT( 5 )
            GO TO 48
 *
 *          SUM
 *
   43       CALL SUMBUF( IWC, IR1 )
            HAD( 2 )=AT( 4 )
 *
   48       IF( INT( 1 ). EQ. 1 )ID( 3 )=IL( 1 )
            IH( 1 )=ID( 3 )
            IH( 2 )=IL( 2 )
 *
 *          TEST COMMAND CHAR
 *
 *          V=AVERAGE=86
 *          T=TIME REMAVER=84
 *          S=POWER SPECTRUM=83
 *          R=REMOVE AVERAGE =82
 *          P=PLOT PW ARRAY=80
 *          O=OUTPUT PW ARRAY=79
 *          N=PHASE( IR1, IM1 )=78
 *          M=MAGNETUD =77
 *          I=INV FFT =73
 *          H=HAN=72
 *          F=FFT=70
 *          E=ENVELOP=69
 *          D=ANALITIC SIGNAL=68
 *          C=CALIBRATIAN=67
 *          A=ANALYZ=65
 *
 *          Z=90=ZERO A SEGMENT OF IR1 ARRAY
 *
 *
   50       IC=0
            IAV=2
            FSCAL=1.
 *
   51       IC=IC+1
   52       ICOM=MAT( IC )
 *
```

```
           IF(ICOM.EQ.90)GO TO 850
   53      IF(ICOM-86)54,86,6
   54      IF(ICOM-83)300,83,84
   300     IF(ICOM-82)55,82,82
   55      IF(ICOM-79)301,79,80
   301     IF(ICOM-77)56,83,78
   56      IF(ICOM-72)57,72,73
   57      IF(ICOM-69)58,69,70
   58      IF(ICOM-68)60,68,69
   60      IF(ICOM-65)6,59,67
 *
 59        IREC=IREC+1
           SAMP=SAMP*FLOAT(IAV)
           CALL CSTOP(127,J)
           IF(J.EQ.0)GO TO 6
           IF(IREC.GE.INT(5))GO TO 10
           GO TO 42
 *
 *
 *         FFT
 *
   70      NSHFT=-1
           CALL FFTM(IR1,IM1,NSHFT)
           FSCAL=FLOAT(2**NSHFT)/1024.
           SAMP=SAMF
           LIMP=1024
           GO TO 51
 *
 *         POWER PECTRUM OR MAGN
 *
   83      CALL ISHUF(1024,IPW)
           Z=(FSCAL*FSCAL)/(RMSV*RMSV)
           DO 100 J=1,1024
           X=IPW(2*J-1)
           Y=IPW(2*J)
   100     PW(J)=(X*X+Y*Y)*Z
           IF(ICOM.EQ.77)GO TO 105
           IAV=1
           HAD(1)=AT(3)
           GO TO 51
 *
 105       DO 106 J=1,1024
   106     PW(J)=SQRT(PW(J))
           GO TO 51
 *
 *         TIME FLOATS ARRAY IR1 AND NORMAL BY RMSV AND FSCAL
 *
   84      DO 180 J=1,1024
           JNUM=1025-J
           PW(JNUM)=IR1(JNUM)
```

```
PAGE     9

  180   PW( JNUM )=PW( JNUM )*FSCAL/RMSV
        HAD( 1 )=AT( 1 )
        GO TO 51
*
*
*
*       REMMOVES AVERAGE VALUE
*
   82   SUMA=0.
        DO 90 J=1, IWC
        XR=IR1( J )
   90   SUMA=SUMA+XR
        SUMA=SUMA/FLOAT( IWC )
        ISUM=SUMA
        DO 91 J=1, IWC
   91   IR1( J )=IR1( J )-ISUM
        SAMP=SAMT
        LIMP=IWC
        IF( IWC. LE. 512 )IAV=1
        GO TO 51
*
*       CALIBRATION=C
*
   67   RMSC=0.
        DO 96 J=1, IWC
        XR=IR1( J )
   96   RMSC=RMSC+XR*XR
        RMSC=RMSC/FLOAT( IWC )
        RMSC=SQRT( RMSC )
        IF( INT( 1 ). EQ. 1 )RMS( 1 )=RMSC
        IF( INT( 1 ). EQ. 2 )RMS( 2 )=RMSC
        IDA( 4 )=0
        SAMP=SAMT
        GO TO 51
*
*       AVERAGE=V  FLOATING POINT ONLY
*
*       IAV=1=AVER EVERY POINT
*       IAV=2=AVER EVERY 2ND POINT
*       MINLEN=MIN REC COR LEN IN AVERAGE
*
*
   86   DO 110 J=1, 512
        JDAM=IAV*J
  110   A( J )=A( J )+PW( JDAM )
        IDA( 2 )=IDA( 2 )+1
        J=LIMP/2
        IF( J. LT. MINLEN )MINLEN=J
        GO TO 51
*
```

PAGE 10

```
*         OUTPUT TO MT01=0
*
79        GO TO 51
*
*         PLOT =P    PW ARRAY ONLY
*
80        CALL ENPLOT( PW, 1, 1024, SAMP, IH( 1 ) )
          GO TO 51
*
*
*         E=69=ABS VAL
*
 69       DO 320 J=1, 1024
320       PW( J )=ABS( PW( J ) )
          HAD( 1 )=AT( 6 )
          GO TO 51
*
*
*         ANALYTIC SIGNAL
*
 68       IR1( 1 )=IR1( 1 )/2
          IM1( 1 )=IM1( 1 )/2
          FSCAL=2.0*FSCAL
          DO 140 J=513, 1024
          IR1( J )=0
140       IM1( J )=0
          HAD( 1 )=AT( 2 )
          GO TO 51
*
*         HANNING WINDOW
*
*
 72       GO TO 51
*
*         INV FFT
*
 73       ISHFT=-1
          SAMP=SAMT
          LIMP=IWC
          DO 500 J=1, 1024
 500      IM1( J )=-IM1( J )
          CALL FFTM( IR1, IM1, ISHFT )
          DO 520 J=1, 1024
 520      IM1( J )=-IM1( J )
          FSCAL=FLOAT( 2**ISHFT )*FSCAL
          GO TO 51
*
*         SYSTEM TEST
*
150       GO TO 6
```

```
PAGE    11

      *
      *       PHASE( IR1, IM1 )
      *
        78    GO TO 51
      *
      *       Z=90=ZERO A SEGMENT OF IR1
      *
       850    X=SAMT*1000.
              J=IZ( 1 )-INT( 2 )
              IZS=FLOAT( J )/X+1.
              J=IZ( 2 )-IZ( 1 )+2
              J=FLOAT( J )/X
              IF( IZS. LE. 1 )GO TO 860
              IR1( IZS )=IR1( IZS )/2
              IZS=IZS+1
       860    CALL  INIBUF( J, IR1( IZS ) )
              J=IZS+J
              IR1( J )=IR1( J )/2
              IZS=0
              GO TO 51
      *
      *
              END
   ENTRY/COMMON BLOCK NAMES
   004353 R
   006007 C COMMON
   EXTERNAL NAMES
   000216 E  ICSTB
   000000 E  NAMBF
   001563 E HOLLER
   004076 E INIBUF
   000215 E  INFFT
   000523 E CONTAP
   001572 E    BEL
   001600 E   CHIN
   001526 E  DECIN
   001330 E   CHOU
   001451 E DECINA
   002041 E IODATA
   004030 E  FLOAT
   004033 E    $QN
   003723 E    $DO
   004113 E    $HN
   001231 E   ERAS
   001246 E  PHEAD
   001335 E BLANKA
   001352 E  DECH4
   003477 E ENPLOT
   001370 E CURSOR
   003762 E    $QM
   004036 E    $IC
   002174 E LSRBUF
   002231 E DEFOLD
   002252 E SUMBUF
   002520 E  CSTOP
   003700 E   FFTM
   003733 E    $HE
   002616 E  ISHUF
   003254 E    $PC
   004007 E    $QK
   003321 E   SQRT
   003410 E    $HM
   003520 E    ABS
```

COMPUTER ANALYSIS PROGRAMS EMPLOYED FOR SEVERITY ESTIMATES

While the diagnostic analysis was performed interactively, "number crunching" involved in the aortic stenosis severity estimates was performed in a batch mode. The severity analysis was accomplished by a two-pass process. During the first pass, an analysis was performed on each patient file and a single, averaged power spectrum and envelogram was computed and stored on magnetic tape. During the second pass, the files were either combined to form a single spectrum at a listening site or were analyzed as independent data files. Second-pass analysis consisted of computing and listing the first moment of spectral bandwidths or involved automated plotting of envelograms and spectra on the graphics terminal.

The programs employed in the first pass are PANAL and the subroutine, FANAL, while the second-pass computations were performed by the program PPAVER. The programs and their descriptions follow.

DESCRIPTION OF THE FIRST-PASS SEVERITY ANALYSIS PROGRAM, PANAL

PANAL = Main program for patient data analysis in batch mode.

Prior to program execution, the following analysis and data parameters must be entered through the teletype.

1. Analysis parameter: a single teletype character

   E = Envelope analysis

   T = Time analysis

   and S = Power spectrum analysis

2. Data parameters: unsigned integers less than 5 digits

   INT(1) = Specifies the data type (integers 1-4)

   If INT(1) = 1 = Phono 1 PCG data

   = 2 = Phono 2 PCG data

   = 3 = ECG data

   = 4 = Respiration or carotid data

   INT(2) = Calibration records start time in ms.

   INT(3) = Calibration records end time in ms.

   INT(4) = Sampling rate

   If INT(4) = 0 = 1.25 KHz (SUM)

   If INT(4) = 1 = 2.50 KHz (DEFOLD)

   INT(5) = Spare

   INT(6) = Data record window start time in ms.

   INT(7) = Data record window end time in ms.

INT(8) = Number of patients to be analyzed

INT(9) = Number of records to skip before Phono 2 calibration

Input Data:

Magnetic tape unit: MT00

Data Format: PASS 2 data format

Output Data:

Magnetic tape unit: MT01

Data format: 1024 data words (or 512 floating-point numbers) preceded by 8-word parameter field as given below.

Parameter Words:

#1 = Data type (fixed-point integer)

#2 = Number of records averaged per file (fixed-point integer)

#3 = Start time in ms. (fixed-point integer)

#4 = End time in ms. (fixed-point integer)

#5 and #6 = Sampling rate (floating-point number)

#7 and #8 = 4 alpha numeric numbers (describing analysis performed)

if #7 and #8 = TIM. = Time analysis

if #7 and #8 = ANS. = Envelope analysis derived
from analytic signal

if #7 and #8 = PWS. = Power spectrum analysis

PAGE 1

```
***     PANAL   FORT ANAL 8-17-74   A. SARKADY
*
*
*       1  ENTER
*
*       AN=TYPE OF ANALYSIS REQUIRED
*
*       E=ENVELOP
*       T=TIME
*       S=POWER SPECTRUM
*
*
*
*       2 ENTER  DATA PARAMETERS
*
*
*       INT( 1 )=DATA TYPE
*       INT( 2 )=CAL START TIME
*       INT( 3 )=CAL END TIME
*       INT( 4 )=SAMP 0=SUM  1=DEFOLD
*       INT( 5 )=NOT USED
*       INT( 6 )=ANAL START TIME
*       INT( 7 )=ANAL END TIME
*       INT( 8 )=#PATIENT TO ANAL
*       INT( 9 )=#REC SKIP BEFORE PHZ CALIB
*
*
*       3 ENTER COMMENDS TO ANALIZ
*
*       A=ANALIZ
*       C=CHANGE PARAM
*
*
*
        COMMON/IBLOCK/INT( 17 )
*
10      CALL ERAS
        CALL BEL
        =0
        CALL HOLLER( 4H AN=, 4 )
        CALL CHIN( ICHAR )
        CALL CHOU( ICHAR )
*
        INT( 1 )=1
        INT( 2 )=0
        INT( 3 )=818
        INT( 4 )=0
        INT( 5 )=100
        INT( 6 )=0
        INT( 7 )=818
```

PAGE 2

```
           INT( 8 )=8
           INT( 9 )=25
      *
           =0
           CALL HOLLER( 4H DP=, 4 )
           DO 15 J=1, 9
           CALL CHOU( 10 )
           CALL DECIN( INT( J ) )
           =INT( J )
      15   CALL DECINA
      *
      20   CALL BEL
           CALL BEL
           CALL CHIN( J )
           IF( J-67 )60, 10, 20
      *
      60   MODE=0
      65   NFILE=0
           CALL ERAS
           CALL CONTAP( MODE, 2HRH, 0, 1 )
           MODE=1
           J=1
           IF( INT( 1 ). GE. 2 )J=INT( 9 )
           CALL CONTAP( MODE, 2HRF, 0, J )
           INT( 2 )=0
           INT( 3 )=818
           INT( 5 )=1
           CALL FANAL( 67, 0 )
           CALL CONTAP( MODE, 2HFF, 0, 1 )
      *
      80   INT( 2 )=INT( 6 )
           INT( 3 )=INT( 7 )
           INT( 5 )=50
           CALL ERAS
           CALL CONTAP( MODE, 2HCP, 0, 1 )
           CALL FANAL( ICHAR, 1 )
           NFILE=NFILE+1
           IF( NFILE. GE. 6 )GO TO 90
           GO TO 80
      *
      90   INT( 8 )=INT( 8 )-1
           IF( INT( 8 ). LE. 0 )GO TO 10
           GO TO 65
      *
           END
ENTRY/COMMON BLOCK NAMES
000420 R
000000 C COMMON
000021 C IBLOCK
EXTERNAL NAMES
```

PAGE 1

```
***      SUBROUT FANAL   VERSION#2  FORT 8-23-74 A. SARKADY
*
*        GEN FORT ANALYSIS ROUTINE
*        USE STOTE INT( 1 ). . INT( 5 ) PARAM IN LABELED COMMON
*        AND CALL FANAL( MANAL, MOUT )
*        MOUT=0, 1 OUTPUT ANALYSIS TO MT01  0=NO 1=YES
*
*        MANAL=ANALYSIS PARM
*
*        IF EQUAL TO
*
*        67=C=CALIB
*        69=E=ENVELOP
*        83=S=POWER SPECTRUM
*        84=T=TIME
*
*        SEARCH IS DELETED
*
*
         SUBROUTINE FANAL( MANAL, MOUT )
*
*
         COMMON/IBLOCK/INT( 17 )
         COMMON ID( 3 ), IR1( 1024 ), IM1( 1024 )
         COMMON IDA( 8 )
         COMMON A( 512 )
*
         DIMENSION MAT( 9 ), RMS( 2 )
         DIMENSION SAM( 2 ), IH( 2 ), HAD( 5 ), IL( 2 )
         DIMENSION IPW( 2048 ), PW( 1024 )
         DIMENSION AT( 7 )
         DIMENSION MRECS( 32 )
         DIMENSION MCUT( 32 )
*
         DIMENSION MCOR( 15 )
*
         DIMENSION DA( 2 )
*
         EQUIVALENCE( IDA( 5 ), DA( 1 ) )
*
*
         EQUIVALENCE( IR1( 1 ), IPW( 1 ), PW( 1 ) )
*
         EQUIVALENCE( MRECS( 1 ), MCUT( 1 ) )
*
         EXTERNAL ICSTB
         EXTERNAL NAMBF
*
         DATA RMS/1. , 1. /
         DATA SAM/8. E-4, 3. 2E-3/
```

PAGE 2

```
              DATA IH/0,0/
              DATA HAD(1)/0./
              DATA IL/2HP1,2H. /
              DATA AT/4HTIM.,4HANS.,4HPWS.,4HSUM.,4HDEF.,4HMAX.,
                     4HMIN./
              DATA LUN0,LUN1/0,1/
              DATA IBLK/2H  /
      *
              DATA IZS/0/
              DATA IZSA/0/
              DATA ICUT/1/
      *
              DATA MCOR/0,2048,0,0,1,1024,2,2,0,0,0,1,2,100,64/
      *
              DATA IDEAL/200/
              DATA LDEAL/700/
      *
              CALL INFFT(ICSTB,1024)
      *
      *
      *
      *       A=65=ALINE TIME AND PLOT R,Z,P,T,V,A
      *       E=69=ENVELOP    R,F,D,I,M,V,A
      *       T=84=TIME SERIES   R,T,V,A
      *       C=67=CALIBRATION R,C,P,T,V,A
      *       S=83=POWER SPECTRUM     R,F,S,V,A
      *       Z=90=SEARCH A FILE AND GO BACK
      *
      *
      *
      600     IF(MANAL.EQ.65)GO TO 635
              IF(MANAL.EQ.69)GO TO 610
              IF(MANAL.EQ.84)GO TO 620
              IF(MANAL.EQ.67)GO TO 630
              IF(MANAL.EQ.83)GO TO 640
              IF(MANAL.EQ.90)GO TO 39
              GO TO 6
      *
      610     MAT(2)=70
              MAT(3)=68
              MAT(4)=73
              MAT(5)=77
              MAT(6)=86
              MAT(7)=65
      612     INT(5)=50
      615     MAT(1)=82
              GO TO 40
      *
      620     MAT(2)=84
              MAT(3)=86
              MAT(4)=65
```

PAGE 3

```
             GO TO 612
*
630          INT(5)=1
             INT(4)=0
             MAT(2)=67
632          MAT(3)=80
             MAT(4)=84
             MAT(5)=86
             MAT(6)=65
             GO TO 615
*
635          MAT(2)=90
             GO TO 632
*
640          MAT(2)=70
             MAT(3)=83
             MAT(4)=86
             MAT(5)=65
             GO TO 612
*
*
*            Q=81=ENTER PARM
*            P=80=PLOT
*            J=74=CONT WITH ANALYS
*            M=77=MEASUR
*
6            =0
             CALL HOLLER(4HAN= ,4)
5            CALL BEL
             CALL BEL
             CALL CHIN(J)
*
*
             IF(J.EQ.80)GO TO 15
             IF(J.EQ.81)GO TO 700
             IF(J.EQ.74)GO TO 44
             IF(J.EQ.77)GO TO 402
             GO TO 6
*
*
*            Q=81=ENTER PARAMETERS
*
*            MCOR(1)=MIN REC CORE LENGTH
*            MCOR(2)=MAX REC COR LENGTH
*            MCOR(3)=REC# TO BE DELETED
*            MCOR(4)=REC# TO BE DELETED
*
*            MCOR(5)=PLOT IR1 START CORE
*            MCOR(6)=PLOT IR1 END CORE
*            MCOR(7)=PLOT IR1 CORF SCIP INCROM
```

```
*       MCOR( 8 )=PLOT GRAIN SKIP INCROM
*
*       MCOR( 9 )=NOT USED
*
*       MCOR( 10 )=SEARCH START TIME
*       MCOR( 11 )=SEARCH END TIME
*       MCOR( 12 )=SEL MAX OR MIN  0=MIN  1=MAX
*
*       MCOR( 13 )=PLOT IR1 X SCAL FACTOR
*       MCOR( 14 )=PLOT IR1 STACK INCROM
*       MCOR( 15 )=PLOT IR1  HORIZ START
*
*
700     CALL DECIN( L )
        IF( L. GT. 15 )GO TO 6
        IF( L. LE. 0 )GO TO 6
        CALL DECIN( MCOR( L ) )
        GO TO 700
*
*       P=PLOT A
*
*
 15     CALL    ERAS
        NSTAR=1
        NEND=512
        CALL DECIN( NSTAR )
        CALL DECIN( NFND )
11      CALL PHEAD( INT( 1 ) )
        =MCOR( 9 )
        CALL FHEAD
16      =36
        CALL BLANKA
        CALL DECH4( IBLK, 2H T, INT( 2 ) )
        CALL DECH4( IBLK, IBLK, INT( 3 ) )
        CALL CHOU( 13 )
        CALL CHOU( 10 )
        =30
        CALL BLANKA
        CALL DECH4( IBLK, 2H N, IREC )
        CALL DECH4( IBLK, 2H R, ID( 2 ) )
        CALL ENPLOT( A, NSTAR, NEND, SAMP, IH( 1 ) )
        GO TO 5
*
*       CURSOR=MEASURS TIME AND FREQ FROM AVER PLOTS
*          T=TIME IN M. SEC  RUBOUT =RET TO 6  OTHERS=FREQ
*
 402    CALL CURSOR( ICHAR, NXP, NYP )
        NXO=FLOAT( NXP )*SAMP
        IF( ICHAR. EQ. 84 )NXO=FLOAT( NXP )*SAMP*1000.
        IF( ICHAR. EQ. 127 )GO TO 5
```

PAGE 5

```
            =NXO
            CALL DECINA
            GO TO 402
*
*
*           INPUT DATA ACORDING TO INT TABLE
*
*           INT( 1 )=DATA TYPE 1. . . 4
*           INT( 2 )=START TIME
*           INT( 3 )=END TIME IN M. SEC
*           INT( 4 )=SEMP   0=SUM    1=DEFOLD
*           INT( 5 )=# RECS IN ANAL.
*
*
*
 39         IZS=0
            CALL INIBUF( 32, MCUT )
            ICUT=0
            GO TO 35
*
*
 49         NRECNT=NRECNT+1
            GO TO 42
*
  40        CALL INIBUF( 1024, A )
            CALL INIBUF( 10, HAD )
*
            IZSA=IZS/ICUT
*
            IREC=0
 35         NRECNT=0
*
 37         SAMT=SAM( 1 )
            IF( INT( 1 ). GE. 3 )SAMT=SAM( 2 )
            X=SAMT*1000.
            ISTART=FLOAT( INT( 2 ) )/X
            IEND=FLOAT( INT( 3 ) )/X
            RMSV=RMS( 1 )
            IF( INT( 1 ). EQ. 2 )RMSV=RMS( 2 )
            IF( INT( 4 ). GE. 1 )SAMT=SAMT/2.
            SAMF=1. /( 1024. *SAMT )
*
 44         MXSTR=MCOR( 15 )
*
  42        IWC=IEND-ISTART+1
            CALL INIBUF( 2048, IPW )
            CALL IODATA( INT( 1 ), 2051, LUNO, ID( 1 ), IOFS )
            IF( IOFS. EQ. 0 )GO TO 10
            NRECNT=NRECNT+1
            IF( ID( 2 ). EQ. MCOR( 3 ). OR. ID( 2 ). EQ. MCOR( 4 ) )GO TO 42
```

PAGE 6

```
 41   IF( ID( 1 ). LT. MCOR( 1 ). OR. ID( 1 ). GT. MCOR( 2 ))GO TO 42
      J=ID( 1 )-ISTART-3
      IF( IWC. GT. J )IWC=J
      IF( IWC. GT. 1024 )IWC=1024
      CALL SHIFTB( 2048, ISTART, IPW )
      LWCO=2048-IWC
      CALL INIBUF( LWCO, IPW( IWC+1 ))
*
*     DEFOLD
*
      IF( INT( 4 ). EQ. 0 )GO TO 43
      CALL DEFOLD( IWC, IR1 )
      IWC=2*IWC
      HAD( 2 )=AT( 5 )
      GO TO 48
*
*     SUM
*
 43   CALL SUMBUF( IWC, IR1 )
      HAD( 2 )=AT( 4 )
*
 48   IF( INT( 1 ). EQ. 1 )ID( 3 )=IL( 1 )
      IH( 1 )=ID( 3 )
      IH( 2 )=IL( 2 )
*
      IF( ICOM. EQ. 90 )GO TO 800
*
*
*     TEST COMMAND CHAR
*
*     V=AVERAGE=86
*     T=TIME REMAVER=84
*     S=POWER SPECTRUM=83
*     R=REMOVE AVERAGE =82
*     P=80=PLOT IR1 ARRAY
*     M=MAGNETUD =77
*     I=INV FFT =73
*     F=FFT=70
*     E=69=ERAS AND PLOT IR1 ARRAY
*     D=ANALITIC SIGNAL=68
*     C=CALIBRATIAN=67
*     A=ANALYZ=65
*
*     Z=90=SLIDE REC TO ALINE
*
*
 50   IC=0
      IAV=2
      FSCAL=1.
*
```

PAGE 7

```
 51     IC=IC+1
 52     ICOM=MAT( IC )
*
        IF( ICOM-90 )53,850,6
53      IF( ICOM-84 )54,84,86
54      IF( ICOM-82 )55,82,83
55      IF( ICOM-77 )56,83,80
56      IF( ICOM-70 )58,70,73
 58     IF( ICOM-68 )60,68,69
 60     IF( ICOM-65 )6,59,67
*
59      IREC=IREC+1
        SAMF=SAMF*FLOAT( IAV )
        IF( IREC. GE. INT( 5 ) )GO TO 10
        CALL CSTOP( 127, J )
        IF( J. EQ. 0 )GO TO 6
        GO TO 42
*
*       Z=90=SCAN TAPE TO ALINE RECORDS
*
800     GO TO 42
*
*       Z=90=SLID EACH REC TO LEFT
*
850     GO TO 51
*
*
*       FFT
*
 70     NSHFT=-1
        CALL FFTM( IR1, IM1, NSHFT )
        FSCAL=FLOAT( 2**NSHFT )/1024.
        SAMF=SAMF
        GO TO 51
*
*       POWER PECTRUM OR MAGN
*
 83     CALL ISHUF( 1024, IPW )
        X=FSCAL/RMSV
        Z=X*X
        IAV=1
        IF( ICOM. EQ. 77 )IAV=2
        DO 100 N=1,512
        J=IAV*N
        X=IPW( 2*J-1 )
        Y=IPW( 2*J )
  100   PW( J )=( X*X+Y*Y )*Z
        IF( ICOM. EQ. 77 )GO TO 105
        HAD( 1 )=AT( 3 )
        GO TO 51
```

```
*
 105    DO 106 N=1,512
        J=IAV*N
  106   PW(J)=SQRT(PW(J))
        GO TO 51
*
*       TIME FLOATS ARRAY IR1 AND NORMAL BY RMSV AND FSCAL
*
  84    DO 180 J=1,1024
        JNUM=1025-J
        PW(JNUM)=IR1(JNUM)
  180   PW(JNUM)=PW(JNUM)*FSCAL/RMSV
        HAD(1)=AT(1)
        GO TO 51
*
*
*
*       REMMOVES AVERAGE VALUE
*
  82    SUMA=0.
        DO 90 J=1,IWC
        XR=IR1(J)
  90    SUMA=SUMA+XR
        SUMA=SUMA/FLOAT(IWC)
        ISUM=SUMA
        DO 91 J=1,IWC
  91    IR1(J)=IR1(J)-ISUM
        SAMP=SAMT
        IF(IWC.LE.512)IAV=1
        GO TO 51
*
*       CALIBRATION=C
*
  67    RMSC=0.
        DO 96 J=1,IWC
        XR=IR1(J)
  96    RMSC=RMSC+XR*XR
        RMSC=RMSC/FLOAT(IWC)
        RMSC=SQRT(RMSC)
        IF(INT(1).EQ.1)RMS(1)=RMSC
        IF(INT(1).EQ.2)RMS(2)=RMSC
        IDA(4)=0
        SAMP=SAMT
        GO TO 51
*
*       AVERAGE=V  FLOATING POINT ONLY
*
*       IAV=1=AVER EVERY POINT
*       IAV=2=AVER EVERY 2ND POINT
*
```

PAGE 9

```
      *
 86         DO 110 J=1,512
            JDAM=IAV*J
  110       A(J)=A(J)+PW(JDAM)
            IDA(2)=IDA(2)+1
            GO TO 51
      *
      *     E=69=ERAS AND PLOT IR1 ARRAY
      *     P=80=PLOT IR1 ARRAY
      *     PLOT RANGE -128,+128
      *
 69         CALL ERAS
 80         K=0
            GO TO 51
      *
      *
      *     D=68=ANALYTIC SIGNAL
      *
  68        IR1(1)=IR1(1)/2
            IM1(1)=IM1(1)/2
            FSCAL=2.0*FSCAL
            DO 140 J=513,1024
            IR1(J)=0
 140        IM1(J)=0
            HAD(1)=AT(2)
            GO TO 51
      *
      *     INV FFT
      *
  73        ISHFT=-1
            SAMP=SAMT
            DO 500 J=1,1024
  500       IM1(J)=-IM1(J)
            CALL FFTM(IR1,IM1,ISHFT)
            DO 520 J=1,1024
  520       IM1(J)=-IM1(J)
            FSCAL=FLOAT(2**ISHFT)*FSCAL
            GO TO 51
      *
      *     FUNCTION AT END OF FILE
      *
 10         IF(MANAL.EQ.90)GO TO 451
            IF(MOUT.EQ.0)GO TO 900
            IDA(1)=INT(1)
            IDA(2)=IREC
            IDA(3)=INT(2)
            IDA(4)=INT(3)
            DA(1)=SAMP
            DA(2)=HAD(1)
      *
```

PAGE 10

```
              CALL IODATA( 0, 1032, 1, IDA( 1 ), J )
              CALL ADELAY( IDEAL )
      901     CALL CONTAP( 1, ZHWE, 1, 1 )
      902     CALL ADELAY( LDEAL )
      900     RETURN
      *
      *       GO BACK ON MT00
      *
      451     J=NRECNT-1
              IF( IOFS. EQ. 0 )J=J+1
              J=4*J+1
              CALL CONTAP( 1, ZHRB, 0, 1 )
              GO TO 900
      *
      *
              END
```

```
ENTRY/COMMON BLOCK NAMES
003517 R   FANAL
006013 C  COMMON
000021 C  IBLOCK
EXTERNAL  NAMES
000002 E     $SE
000156 E   ICSTB
000000 E   NAMBF
000155 E   INFFT
000455 E  HOLLER
000463 E     BEL
000465 E    CHIN
000617 E   DECIN
002700 E    ERAS
000622 E   PHEAD
000630 E   FHEAD
000663 E  BLANKA
000700 E   DECH4
000656 E    CHOU
000705 E  ENPLOT
000716 E  CURSOR
003074 E   FLOAT
003077 E     $QM
002413 E     $IC
000777 E  DECINA
001426 E  INIBUF
002723 E     $HN
002534 E     $QN
003205 E  IODATA
001412 E  SHIFTB
001447 E  DEFOLD
001470 E  SUMBUF
001730 E   CSTOP
003034 E    FFTM

003067 E     $HE
002013 E   ISHUF
002631 E     $HM
002475 E     $PC
002652 E     $QK
003057 E     $DO
002542 E    SQRT
003230 E  ADELAY
003265 E  CONTAP
```

DESCRIPTION OF THE SECOND-PASS SEVERITY ANALYSIS PROGRAM, PPAVER

PPAVER = Prints, plots, and averages analyzed data files.

Prior to program execution, the following command parameters must be entered through teletype as unsigned integers less than 5 digit length.

NFILE = Number of files to average

NPRINT = List the $\bar{f}$ and %F on the printer

If NPRINT = 0 = No print

If NPRINT = 1 = Print

IPLOT = Plot averaged data on the graphics terminal

If IPLOT = 0 = No plot

If IPLOT = 1 = Plot

MAXL = Maximum number of lines per page for printing

NOP = Number of tables per page

NSKIP(I) = Skip the I^{th} file (in the modulo 6 file format) from the analysis

I = 1, 2, ..., 6

If NSKIP(I) = 0 = Do not skip I^{th} file

If NSKIP(I) = 1 = Skip I^{th} file

Input Data:

Magnetic tape unit: MTOO

Format: PASS 1 severity analysis output format

Output Data:

Plots on graphics terminal or tables on printer

PAGE 1

```
***     PPAVER  FORTRAN   8-17-74 A. SARKADY
*
*       PPAVER=PRINTS AND PLOTS AVERAGED FILES
*
*       DATA INPUT FORMET   OUT PUT OF ALINEFREQ
*
*       INPUT DATA IDS
*
*       IDA( 1 )=DATA TYPE 1,..4
*       IDA( 2 )=# OF CARDIO CYCLES/FILE
*       IDA( 3 )=START TIME IN M.SEC.
*       IDA( 4 )=END TIME IN M.SEC.
*       DA( 1 )=SAMP  PLOT SEMPLE INCROMENT
*       DA( 2 )=4 CAR OF ANAL. ID
*
*
*
*
*
*       INPUT COMMEND PARAMETERS
*
*       NFILE=# OF FILES TO AVER
*       NPRINT=PRINT ?  0=NO,1=YES
*       IPLOT=PLOT ? 0=NO,1=YES
*       MAXL=MAX PRINT LINE NUM /PAGE
*       NOP=# OF PLOTS OR PRINT BLOCKS
*
*
*
*       NSKIP( I )= SIP FILE IN GROUP AND NO AVERAGE
*       NSKIP( I )=0,1   1=SKIP  0=NO SKIP  OF I TH FILE
*
*
*
*       ICOM=INPUT COMMEND
*
*       A=65=INIT AND START ANALYSIS
*       C=67=CHANGE PARAMETERS
*       J=74=CONTINUE WITH ANAL DONT INIT
*
*
*
        COMMON/TABLE/LINE( 50 )
*
        COMMON IDA( 8 ),A( 512 ),IAV( 8 )
        COMMON DB( 1 ),AV( 512 ),DE( 1 )
*
        DIMENSION BW( 10 )
        DIMENSION BL2( 11 ),BL3( 8 ),BL4( 18 )
        DIMENSION IBLK( 4 ),AFM( 4 ),AT( 4 )
```

```
              DIMENSION NSKIP(6),DA(2),BMAS(5),ITEM(5)
*
              EXTERNAL NAMBF
              EXTERNAL IP2BF
*
              EQUIVALENCE(IDA(5),DA(1))
*
              DATA BLK/4H    /
*
              DATA IBLK/2H  ,2H  ,2H  ,2H  /
              DATA BMAS/4HNFL=,4HNPR=,4HIPL=,4HMXL=,4HNOP=/
*
              DATA BL2/4H  N.,4HREC=,4H  S.,4HTIM=,
           A4H  E.,4HTIM=,4H  SA,4HMP.=,
           A4H  AN,4HAL.=,4H    /
*
              DATA BL3/4HAVE.,4HFRQ=,4HF.M.,4HMAG=,
           A4HAREA,4H100=,4HM.M*,4H10K=/
*
              DATA BL4/4H  10,4H%F  ,4H  20,4H%F  ,4H  30,4H%F  ,
           A4H  40,4H%F  ,4H  50,4H%F  ,4H  60,4H%F  ,
           A4H  70,4H%F  ,4H  80,4H%F  ,4H  90,4H%F  /
*
*
*
 2            CALL ERAS
              CALL BEL
              ITEM(1)=1
              ITEM(2)=1
              ITEM(3)=1
              ITEM(4)=50
              ITEM(5)=1
 3            =0
              CALL HOLLER(4HPAR=,4)
              DO 5 J=1,5
 4            CALL DECIN(ITEM(J))
              =ITEM(J)
              CALL DECINA
 5            CALL CHOU(10)
*
              NFILF=ITEM(1)
              NPRINT=ITEM(2)
              IPLOT=ITEM(3)
              MAXLIN=ITEM(4)
              NOP=ITEM(5)
*
*
              CALL INIBUF(6,NSKIP)
              =0
              CALL HOLLER(6HNSKIP=,6)
```

PAGE 3

```
        CALL BEL
        DO 7 J=1,6
        CALL DECIN(I)
        IF(I.GT.7)GO TO 8
        NSKIP(J)=I
7       CONTINUE
*
*       A=65=INIT AND ANALIZ
*       C=67=CHANGE PAR
*       J=74=CONTINUE WITH ANAL
*
8       NOFF=0
9       =0
        CALL HOLLER(6H ICOM=,6)
11      CALL BEL
        CALL BEL
        CALL CHIN(ICOM)
*
        IF(ICOM.EQ.65)GO TO 10
        IF(ICOM.EQ.67)GO TO 2
        IF(ICOM.EQ.74)GO TO 12
        GO TO 9
*
10      MODE=0
15      IF(NPRINT.EQ.0)GO TO 12
        NLINE=0
        CALL PRTLNE(100)
*
*
12      CALL INIBUF(1028,DB(1))
        NAV=0
        NOFF=NOFF+1
        IF(NOFF.GT.NOF)GO TO 9
*
        DO 60 I=1,NFILE
        CALL ERAS
        CALL CONTAP(MODE,2HRH,0,1)
        IF(MODE.EQ.1)GO TO 14
        CALL BEL
        CALL CHIN(J)
        IF(J.EQ.127)GO TO 8
14      MODE=1
        CALL INIBUF(1032,IDA(1))
        CALL IODATA(10,1032,0,IDA(1),J)
        CALL CONTAP(1,2HFF,0,1)
*
*       FLOAT PAR
*
        AT(1)=IDA(2)
        AT(2)=IDA(3)
```

```
            AT(3)=IDA(4)
            AT(4)=DA(1)
            BL2(11)=DA(2)
            SAMP=DA(1)
*
            IF(NSKIP(I).NE.0)GO TO 60
  18        IF(NPRINT.EQ.0)GO TO 40
*
*
*           PRINT 1ST LINE
*
            CALL INIBUF(50,LINE)
            IF(IDA(1).EQ.2)GO TO 20
            CALL ADDR(0,NAMBF,-64,0)
            GO TO 25
*
  20        CALL ADDR(0,NAMBF,-44,0)
            CALL ADDR(1,IBLK,-2,0)
            CALL ADDR(2,IP2BF,-16,0)
*
  25        CALL PRTLNE(35)
            CALL PRTLNE(200)
*
*           2ND LINE
*
            CALL INIBUF(50,LINE)
            N=0
            K=1
            DO 30 J=1,4
            CALL ADDR(N,BL2(K),-8,0)
            N=N+1
            CALL ADDR(N,AT(J),6,2)
            N=N+1
            K=K+2
  30        CONTINUE
*
            CALL ADDR(N,BL2(K),-12,0)
            CALL PRTLNE(35)
            CALL PRTLNE(200)
            NLINE=NLINE+4
*
  40        DO 50 J=1,512
  50        AV(J)=AV(J)+A(J)
            NAV=NAV+IDA(2)
  60        CONTINUE
*
*
*           ANALYSIS
*
*
```

```
PAGE     5

 65     CONTINUE
 70     PROD=0.
        SUM=0.
        X=FLOAT( NAV )
        DO 75 J=1,512
        AV( J )=AV( J )/X
        SUM=SUM+AV( J )
        PROD=AV( J )*FLOAT( J )+PROD
 75     CONTINUE
*
        IF( NPRINT. EQ. 0 )GO TO 120
*
 77     X=PROD/SUM
        JAVER=X
        AVF=X*SAMP
        AREA=SUM*100.
        K=-1
 78     AMAX=-10000.
        DO 80 J=1,512
        IF( AV( J ). GT. AMAX )K=J
        IF( AV( J ). GT. AMAX )AMAX=AV( J )
 80     CONTINUE
*
        FMAX=FLOAT( K )*SAMP
        AFM( 1 )=AVF
        AFM( 2 )=FMAX
        AFM( 3 )=AREA
        AFM( 4 )=AMAX*10000.
*
*
*       FIND BAND WIDTH
*
 82     DB( 1 )=0.
        DE( 1 )=0.
        LUP=512-JAVER
        LLOW=JAVER-1
        LIM=LUP
        IF( LLOW. GT. LUP )LIM=LLOW
*
        SINC=. 1*SUM
        K=JAVER
        I=JAVER+1
        TOTAL=AV( JAVER )
        N=1
 84     Y=SINC
        DO 90 J=1,LIM
        IF( K. LE. 512 )K=K+1
        IF( I. GE. 1 )I=I-1
        TOTAL=TOTAL+AV( K )+DB( I )
        IF( TOTAL. LT. Y )GO TO 90
```

PAGE 6

```
             X=K-I+1
             BW(N)=X*SAMP
             N=N+1
             IF(N.GT.9)GO TO 95
             Y=Y+SINC
      90     CONTINUE
      *
      *
      *      PRINT LINE #3
      *
      95     CALL INIBUF(50,LINE)
             K=1
             N=0
             DO 100 J=1,4
             CALL ADDR(N,BLK,-2,0)
             N=N+1
             CALL ADDR(N,BL3(K),-8,0)
             N=N+1
             K=K+2
             CALL ADDR(N,AFM(J),7,2)
             N=N+1
      100    CONTINUE
      102    CALL PRTLNE(35)
             CALL PRTLNE(200)
      *
      *      PRINT LINE# 4
      *
      103    CALL INIBUF(50,LINE)
             CALL ADDR(0,BL4(1),-64,0)
             CALL PRTLNE(35)
             CALL PRTLNE(200)
      *
      *      LINE# 5
      *
      105    CALL INIBUF(50,LINE)
      *
      200    CALL ADDR(0,BLK,-2,0)
      201    CALL ADDR(1,BW(1),5,1)
             CALL ADDR(2,BLK,-3,0)
      202    CALL ADDR(3,BW(2),5,1)
             CALL ADDR(4,BLK,-3,0)
      203    CALL ADDR(5,BW(3),5,1)
             CALL ADDR(6,BLK,-3,0)
      204    CALL ADDR(7,BW(4),5,1)
             CALL ADDR(8,BLK,-3,0)
      205    CALL ADDR(9,BW(5),5,1)
             CALL ADDR(10,BLK,-3,0)
      206    CALL ADDR(11,BW(6),5,1)
             CALL ADDR(12,BLK,-3,0)
      207    CALL ADDR(13,BW(7),5,1)
```

PAGE 7

```
          CALL ADDR( 14, BLK, -3, 0 )
  208     CALL ADDR( 15, BW( 8 ), 5, 1 )
  *
  111     CALL PRTLNE( 35 )
          CALL PRTLNE( 200 )
          CALL PRTLNE( 200 )
  112     NLINE=NLINE+7
          IF( NLINE. LE. MAXLIN )GO TO 120
  115     NLINE=0
          CALL PRTLNE( 100 )
  *
  120     IF( IPLOT. EQ. 0 )GO TO 150
  *
  *       PLOT AV( ) ARRAY  NSTAR=START CORE
  *               NEND=END CORE  FOR PLOT ARRAY
  *
  130     CALL ERAS
          CALL BEL
          NSTAR=1
          NEND=512
          CALL DECIN( NSTAR )
          CALL DECIN( NEND )
          CALL PHEAD( IDA( 1 ) )
          =NFILE-1
          CALl. FHEAD
          =36
          CALL BLANKA
          I=IDA( 3 )
          J=IDA( 4 )
          CALL DECH4( IBLK, 2H T, I )
          CALL DECH4( IBLK, IBLK, J )
          CALL CHOU( 13 )
          CALL CHOU( 10 )
          =30
          CALL BLANKA
          CALL DECH4( IBl K, 2H N, NAV )
          CALL DECH4( IBLK, 2H F, NFILE )
          CALL ENPLOT( AV, NSTAR, NEND, SAMP, DA( 2 ) )
  *
  *       CURSOR
  *       P=80=RE PLOT  RUBOUT=GO127= GO TO 9
  *       J=74=RETURN TO ANAL    OTHERS=LABOL PLOT
  *
  140     CALL DAMCUR( ICHAR, I, J )
          CALL CHOU( 31 )
          X=SAMP
          IF( SAMP. LE. . 1 )X=X*1000.
          IF( ICHAR. EQ. 80 )GO TO 130
          IF( ICHAR. EQ. 127 )GO TO 11
          IF( ICHAR. EQ. 74 )GO TO 12
```

```
PAGE     8

              I=FLOAT( I )*X
              =I
              CALL DECINA
              GO TO 140
      *
      *
      150     CALL CSTOP( 127, J )
              IF( J. EQ. 0 )GO TO 9
              GO TO 12
              END
ENTRY/COMMON BLOCK NAMES
003031 R
004024 C COMMON
000062 C  TABLE
EXTERNAL NAMES
001021 E  NAMBF
001035 E  IP2BF
002342 E   ERAS
002344 E    BEL
000426 E HOLLER
002356 E  DECIN
002577 E DECINA
002471 E   CHOU
002074 E    $DO
002130 E INIBUF
000606 E   CHIN
002374 E PRTLNE
000645 E CONTAP
000633 E IODATA
001732 E    $PC
002266 E   ADDR
001774 E    $QK
002564 E  FLOAT
001347 E    $QN
002567 E    $QM
002572 E    $IC
002503 E    $QL
002361 E  PHEAD
002367 E  FHEAD
002433 E BLANKA
002450 E  DECH4
002455 E ENPLOT
002464 E DAMCUR
002603 E  CSTOP
SYMBOL TABLE
002623 R 000001
002704 R 000002
002633 R 000004
000002 R     BW
002637 R 000012
```

ERROR ANALYSIS OF $\bar{f}$

The J^{th} spectral component of the mean murmur spectrum is defined as

$$\bar{P}(J\Omega) = \bar{P}_J = \frac{1}{L} \sum_{i=1}^{L} P_i(J\Omega)$$

and the first moment of this spectrum $\bar{f}$ as

$$\bar{f} = \frac{\sum_{J=0}^{N} (J\Omega)\ \bar{P}_j}{\sum_{J=0}^{N} \bar{P}_J} = \frac{\Omega M}{S}$$

where $M = \sum_{J=0}^{N} J\bar{P}(J\Omega)$

$$S = \sum_{J=0}^{N} \bar{P}(J\Omega)$$

$N = 511$ and $L = N.REC$

and $\Omega = \frac{1.250K\ Hz}{1024} = 1.2207\ Hz$

Assuming that the random errors of $\bar{P}_1$, $\bar{P}_2$, ..., $\bar{P}_J$ are independent and uncorrelated, the standard deviation of $\bar{f}$ is found from the equation given below [78].

$\sigma_{\bar{f}}$ = standard deviation of $\bar{f}$

$$\sigma_{\bar{f}} = \sqrt{\left(\frac{\partial \bar{f}}{\partial \bar{P}_0}\right)^2 \left(\sigma_{\bar{P}_0}\right)^2 + \left(\frac{\partial \bar{f}}{\partial \bar{P}_1}\right)^2 \left(\sigma_{\bar{P}_1}\right)^2 + \dots \left(\frac{\partial \bar{f}}{\partial \bar{P}_N}\right)^2 \left(\sigma_{\bar{P}_N}\right)^2}$$

where the J^{th} partial derivative is

$$\frac{\partial \bar{f}}{\partial \bar{P}_J} = \Omega \frac{[JS - M]}{S^2}$$

$$\left(\frac{\partial \bar{f}}{\partial \bar{P}_J}\right)^2 = \frac{\Omega^2}{S^4} [J^2 S^2 - 2JSM + M^2]$$

$$\left(\frac{\partial \bar{f}}{\partial \bar{P}_J}\right)^2 = \frac{1}{S^2} \left[\Omega^2 J^2 - 2J\Omega \left(\frac{\Omega M}{S}\right) + \left(\frac{\Omega M}{S}\right)^2\right]$$

$$\left(\frac{\partial \bar{f}}{\partial \bar{P}_J}\right)^2 = \frac{1}{S^2} [\Omega^2 J^2 - 2J\Omega \bar{f} + \bar{f}^2]$$

Assuming that the spectrum is white and that

$$\sigma_{\bar{P}_0} = \sigma_{\bar{P}_1} = \dots . \sigma_{\bar{P}_N} = \sigma_{\bar{P}} = \frac{\sigma_P}{\sqrt{N.REC.}}$$

$$S = N\mu_P$$

and $\sigma_P \simeq \mu_P$, [71]

where σ_P = standard deviation of spectral estimates

μ_P = mean value of power spectrum

and N.REC. = Number of records averaged yields the following equation.

$$\sigma_{\bar{f}} = \frac{\sigma_{\bar{P}}}{S} \sqrt{\Omega^2 \sum_{J=1}^{N} J^2 - (2\Omega\bar{f}) \sum_{J=1}^{N} J + N(\bar{f})^2}$$

Expressing the sums in closed forms,

$$\sum_{J=1}^{N} J^2 = \frac{N(N+1)(2N+1)}{6} = \frac{N}{6}\,[2N^2 + 3N + 1]$$

$$\sum_{J=1}^{N} J = \frac{N(N+1)}{2}$$

Substituting these values in the previous equation,

$$\sigma_{\bar{f}} = \frac{\sqrt{\frac{1}{N^2}\left[N(\bar{f})^2 + \Omega^2 \frac{N}{6}\,(2N^2+3N+1) - (2\Omega\bar{f})\,\frac{N(N+1)}{2}\right]}}{\sqrt{N.REC.}}$$

$$\sigma_{\bar{f}} = \frac{\sqrt{\frac{\bar{f}^2}{N} + \Omega^2 \left(\frac{2N^2+3N+1}{6N}\right) - \Omega\bar{f}\,\frac{(N+1)}{N}}}{\sqrt{N.REC.}}$$

$$\sigma_{\bar{f}} = \frac{\sqrt{\frac{\bar{f}^2}{511} + 254.56 - 1.223\,\bar{f}}}{\sqrt{N.REC.}}$$

The calculated values for $\sigma_{\bar{f}}$ are summarized in Table 2, Chapter 5.

LEAST SQUARE REGRESSION LINE AND CORRELATION COEFFICIENT CALCULATIONS

The correlation coefficient and linear least square estimate of P.S.E.G. from $\bar{f}$ are calculated from the short formula [79] as given below where

N = number of patients

X = independent variable ($\bar{f}$ or 50%F)

Y = dependent variable (P.S.E.G.)

r = correlation coefficient

and Y_{est} = linear least square estimate of Y from X

$$D_1 = N \sum_{i=1}^{N} X_i^2 - \left[\sum_{i=1}^{N} X_i\right]^2$$

$$a_0 = \frac{\left[\sum_{i=1}^{N} Y_i\right]\left[\sum_{i=1}^{N} X_i^2\right] - \left[\sum_{i=1}^{N} X_i\right]\left[\sum_{i=1}^{N} X_i Y_i\right]}{D_1}$$

$$K_1 = N\left(\sum_{i=1}^{N} X_i Y_i\right) - \left(\sum_{i=1}^{N} X_i\right)\left(\sum_{i=1}^{N} Y_i\right)$$

$$a_1 = \frac{K_1}{D_1}$$

$$Y_{est} = a_0 + a_1 X$$

$$D_2 = N\left(\sum_{i=1}^{N} Y_i^2\right) - \left(\sum_{i=1}^{N} Y_i\right)^2$$

$$r = \frac{K_1}{\sqrt{D_1 D_2}}$$

TABLE 1,AII

CORRELATION STUDY BETWEEN P.S.E.G. AND 50%F AT THE 2ND. R.I. ON INSPIRATION, EXPIRATION AND CAROTID DATA FOR THE TWELVE CATHETERIZED VALVAR AORTIC STENOSIS PATIENTS

Catheterization and Personal Data				Phono. Data
Name	Hosp. #	Chest Wall	Y=P.S.E.G. mm Hg	50%F In Hz
Tommy K.	63-77-80	Thin	9-18	78.1
Donald G.	62-12-80	Thin	16	61.0
Natalie K.	70-89-65	Med.	23	95.2
Bryan K.	60-91-88	Thin	39	73.2
Robert M.	53-91-59	Med.	42-45	90.3
Elizabeth R.	55-01-61	Thin	45	80.6
Rudolph B.	68-97-78	Thin-Med.	45	97.7
Richard F.	57-53-27	Med.	61-68	78.1
Jean S.	58-79-24	Med.	70-90	68.4
Mark M.	68-95-48	Thin	6-8	78.1
Jonathan F.	64-87-14	Thin	5-9	36.6
Barry F.	60-50-48	Med.	16-24	56.2

$\Sigma Y = 403.5$ $\Sigma Y^2 = 19{,}488.75$ $\Sigma 50\%F = 893.5$

$\Sigma Y(50\%F) = 31{,}462.65$ $\Sigma(50\%F)^2 = 69{,}813.41$

Correlation Coefficient between P.S.E.G. and 50%F = .3217

TABLE 2,AII

CORRELATION STUDY BETWEEN P.S.E.G. AND $\bar{f}$ AT THE 2ND. R.I. ON INSPIRATION, EXPIRATION AND CAROTID DATA FOR THE TWELVE CATHETERIZED VALVAR AORTIC STENOSIS PATIENTS

Catheterization and Personal Data				Phono. Data
Name	Hosp. #	Chest Wall	Y=P.S.E.G. mm Hg	$\bar{f}$ In Hz
Tommy K.	63-77-80	Thin	9-18	85.79
Donald G.	62-12-80	Thin	16	89.70
Natalie K.	70-89-05	Med.	23	124.53
Bryan K.	60-91-88	Thin	39	127.97
Robert M.	53-91-59	Med.	42-45	124.53
Elizabeth R.	55-01-61	Thin	45	147.77
Rudolph B.	68-97-78	Thin-Med.	45	142.86
Richard F.	57-53-27	Med.	61-68	168.56
Jean S.	58-79-24	Med.	70-90	201.84
Mark M.	68-95-48	Thin	6-8	95.89
Jonathan F.	64-87-14	Thin	5-9	93.12
Barry F.	60-50-48	Med.	16-24	104.15

$\Sigma Y = 403.5$ $\quad \Sigma Y^2 = 19{,}488.75$ $\quad \Sigma \bar{f} = 1{,}506.71$

$\Sigma \bar{f}Y = 59{,}369.19$ $\quad \Sigma \bar{f}^2 = 202{,}908.02$

Correlation Coefficient between P.S.E.G. and $\bar{f}$ = .9657

Least Square Line = $(\text{P.S.E.G.})_{\text{est.}} = -46.0 + .634\,\bar{f}$

TABLE 3,AII

CORRELATION STUDY BETWEEN P.S.E.G. AND $\bar{f}$ AT THE 2ND. R.I. ON INSPIRATION DATA FOR THE TWELVE CATHETERIZED VALVAR AORTIC STENOSIS PATIENTS

Catheterization and Personal Data				Phono. Data
Name	Hosp. #	Chest Wall	Y=P.S.E.G. mm Hg	$\bar{f}$ In Hz
Tommy K.	63-77-80	Thin	9-18	89.66
Donald G.	62-12-80	Thin	16	94.52
Natalie K.	70-89-05	Med.	23	126.7
Bryan K.	60-91-88	Thin	39	122.29
Robert M.	53-91-59	Med.	42-45	125.49
Elizabeth R.	55-01-61	Thin	45	149.32
Rudolph B.	68-97-78	Thin-Med.	45	143.91
Richard F.	57-53-27	Med.	61-68	168.81
Jean S.	58-79-24	Med.	70-90	203.8
Mark M.	68-95-48	Thin	6-8	99.98
Jonathan F.	64-87-14	Thin	5-9	96.66
Barry F.	60-50-48	Med.	16-24	106.66

$\Sigma Y = 403.5$ $\Sigma Y^2 = 19{,}488.75$ $\Sigma \bar{f} = 1{,}527.8$

$\Sigma \bar{f} Y = 59{,}762.24$ $\Sigma \bar{f}^2 = 207{,}481.75$

Correlation Coefficient between P.S.E.G. and $\bar{f}$ = .9575

Least Square Line = $(\text{P.S.E.G.})_{est.} = -48.74 + .647\,\bar{f}$

TABLE 4,AII

CORRELATION STUDY BETWEEN P.S.E.G. AND $\bar{f}$ AT THE 2ND. R.I. ON EXPIRATION DATA FOR THE TWELVE CATHETERIZED VALVAR AORTIC STENOSIS PATIENTS

Catheterization and Personal Data				Phono. Data
Name	Hosp. #	Chest Wall	Y=P.S.E.G. mm Hg	$\bar{f}$ In Hz
Tommy K.	63-77-80	Thin	9-18	82.55
Donald G.	62-12-80	Thin	16	87.93
Natalie K.	70-89-05	Med.	23	122.06
Bryan K.	60-91-88	Thin	39	129.2
Robert M.	53-91-59	Med.	42-45	125.89
Elizabeth R.	55-01-61	Thin	45	145.67
Rudolph B.	68-97-78	Thin-Med.	45	138.25
Richard F.	57-53-27	Med.	61-68	163.9
Jean S.	58-79-24	Med.	70-90	199.03
Mark M.	68-95-48	Thin	6-8	95.02
Jonathan F.	64-87-14	Thin	5-9	91-94
Barry F.	60-50-48	Med.	16-24	99.73

$\Sigma Y = 403.5$ $\Sigma Y^2 = 19,488.75$ $\Sigma \bar{f} = 1,481.17$

$\Sigma \bar{f} Y = 58,417.38$ $\Sigma \bar{f}^2 = 196,222.54$

Correlation Coefficient between P.S.E.G. and $\bar{f}$ = .9669

Least Square Line = $(P.S.E.G.)_{est.} = - 45.70 + .6427\ \bar{f}$